Article

Cell Host & Microbe

Bacterial Adaptation to the Host's Diet Is a Key Evolutionary Force Shaping *Drosophila-Lactobacillus* Symbiosis

Graphical Abstract

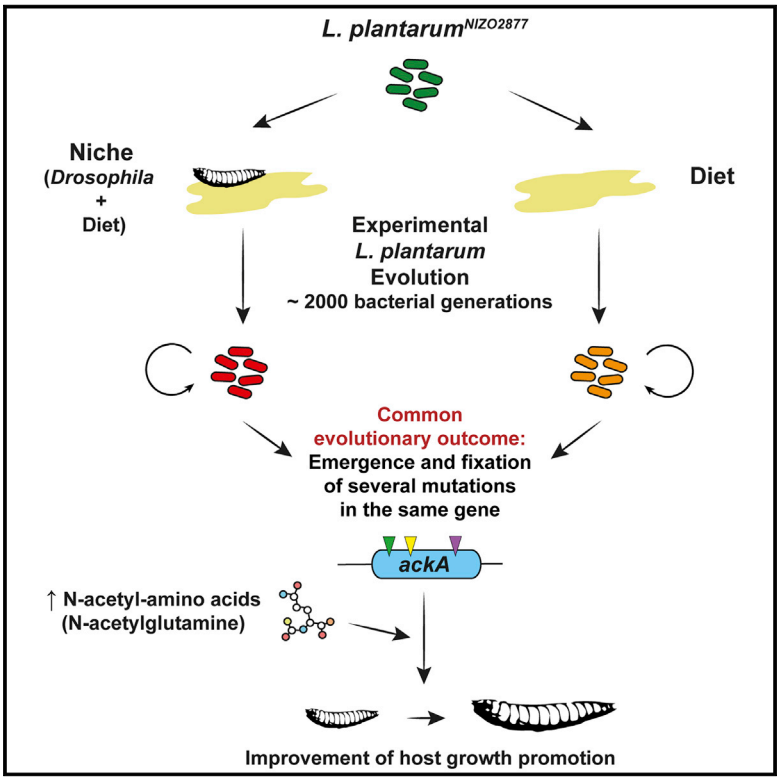

Highlights

- *L. plantarum* experimental evolution leads to the improvement of its symbiotic benefit
- *L. plantarum* increases its growth-promotion ability by adapting to *Drosophila* diet
- Mutation of *ackA* gene enhances both *L. plantarum* fitness and benefit to the host
- N-acetyl-glutamine production is sufficient to improve *L. plantarum* growth promotion

Authors

Maria Elena Martino, Pauline Joncour, Ryan Leenay, ..., Benjamin Gillet, Chase Beisel, François Leulier

Correspondence

maria-elena.martino@ens-lyon.fr (M.E.M.),
francois.leulier@ens-lyon.fr (F.L.)

In Brief

Martino et al. demonstrate that, in the symbiosis between *Drosophila* and *Lactobacillus plantarum*, the host diet represents the driving force in the evolution of *L. plantarum* symbiotic effect. This is a clear example of by-product mutualism, where the host capitalizes on the by-products of the self-serving traits of their symbionts.

Martino et al., 2018, Cell Host & Microbe *24*, 109–119
July 11, 2018
https://doi.org/10.1016/j.chom.2018.06.001

CellPress

Cell Host & Microbe
Article

Bacterial Adaptation to the Host's Diet Is a Key Evolutionary Force Shaping *Drosophila-Lactobacillus* Symbiosis

Maria Elena Martino,[1,*] Pauline Joncour,[1] Ryan Leenay,[2] Hugo Gervais,[1] Malay Shah,[2] Sandrine Hughes,[1] Benjamin Gillet,[1] Chase Beisel,[2,3] and François Leulier[1,4,*]
[1]Institut de Génomique Fonctionnelle de Lyon, Université de Lyon, Ecole Normale Supérieure de Lyon, Centre National de la Recherche Scientifique, Université Claude Bernard Lyon 1, Unité Mixte de Recherche 5242, 69364 Lyon Cedex 07, France
[2]North Carolina State University, Department of Chemical and Biomolecular Engineering, Raleigh, NC 27695, USA
[3]Helmholtz Institute for RNA-based Infection Research, Josef-Schneider-Straße 2/D15, 97080 Würzburg, Germany
[4]Lead Contact
*Correspondence: maria-elena.martino@ens-lyon.fr (M.E.M.), francois.leulier@ens-lyon.fr (F.L.)
https://doi.org/10.1016/j.chom.2018.06.001

SUMMARY

Animal-microbe facultative symbioses play a fundamental role in ecosystem and organismal health. Yet, due to the flexible nature of their association, the selection pressures that act on animals and their facultative symbionts remain elusive. Here we apply experimental evolution to *Drosophila melanogaster* associated with its growth-promoting symbiont *Lactobacillus plantarum*, representing a well-established model of facultative symbiosis. We find that the diet of the host, rather than the host itself, is a predominant driving force in the evolution of this symbiosis. Furthermore, we identify a mechanism resulting from the bacterium's adaptation to the diet, which confers growth benefits to the colonized host. Our study reveals that bacterial adaptation to the host's diet may be the foremost step in determining the evolutionary course of a facultative animal-microbe symbiosis.

INTRODUCTION

Animal-microbe symbioses are ubiquitous and their nature can be extremely diverse. Mutualistic relationships are those symbioses whereby both partners benefit from each other (Bronstein, 1994). They can differ in the number of species involved, the duration of the symbiotic relationship, and how dependent the partners are on the interaction for their development, survival, and reproduction (Douglas, 2011). In obligate mutualism, the organisms depend on each other for their survival. In many cases, this co-dependency has occurred over time as each organism adapts to the reciprocal benefits (Holland and Bronstein, 2008). In facultative symbioses, microbes and their hosts are not fully dependent on each other: the host can survive without its bacterial symbionts, which, in turn, can live in different ecosystems regardless of the host presence (Gilbert and Neufeld, 2014). Nevertheless, facultative microbial symbionts confer crucial benefits to their animal partners (Feldhaar, 2011; Ferrari and Vavre, 2011). The flexible nature of facultative mutualism suggests that there are both costs and benefits associated with maintaining such symbiosis (Bronstein, 1994; Douglas, 2011; Engel and Moran, 2013; Fisher et al., 2017). However, the ecological and evolutionary forces that drive the emergence and evolution of the benefits conferred by facultative symbionts to their animal hosts remain largely elusive.

To address this question, we experimentally tested microbial evolution using *Drosophila melanogaster* associated with one of its most abundant facultative symbionts, *Lactobacillus plantarum*, with whom it establishes nutritional mutualism (Douglas, 2011; Erkosar et al., 2015; Ma et al., 2015; Matos et al., 2017; Storelli et al., 2011, 2018). *L. plantarum* positively affects juvenile growth rate and maturation when *Drosophila* faces chronic undernutrition (Storelli et al., 2011). Such benefit results, at least in part, from the capacity of *L. plantarum* to promote the expression of larval intestinal peptidases and the consequent increase of dietary protein digestion and amino acid intake by the host (Erkosar et al., 2015; Matos et al., 2017). Conversely, *L. plantarum* benefits from its animal partner. Although *L. plantarum* encounters a strong cost during transit through larval gut, larvae secrete bacterial maintenance factors that counteract this cost and improve microbial fitness, thus perpetuating symbiosis (Storelli et al., 2018). *Drosophila*/*L. plantarum* association also represents a prototypical case of facultative symbiosis. Indeed, *L. plantarum*, as well as most *Drosophila* facultative symbionts, does not colonize the host intestine, but remains associated with *Drosophila* during its entire life cycle by constant reassociation through cycles of ingestion and excretion (Blum et al., 2013; Broderick et al., 2014; Storelli et al., 2011, 2018). In addition, it is vertically transmitted to progenies via the deposition of contaminated mother's feces on the surface of the embryo during egg laying and on the surrounding substratum (Matos and Leulier, 2014).

Here we show that the host nutritional environment, instead of the host, is a predominant driving force in the emergence and evolution of symbiotic benefits that *L. plantarum* confers to its animal partner. By applying experimental evolution to a moderate *Drosophila* growth-promoting strain *L. plantarum*^{NIZO2877} (Schwarzer et al., 2016), we found that the *de novo* mutations

in the same acetate kinase (*ackA*) locus invariably emerge first and rapidly become fixed, and such evolution occurs with or without the host. Furthermore, we demonstrate that *ackA* mutations trigger the increased production of N-acetylated amino acids by the evolved strain, including N-acetyl-glutamine, a compound that is sufficient to confer improved *Drosophila* growth capabilities when provided together with the ancestral bacterial strain. Our study therefore identifies a specific mechanism by which a symbiotic bacterial strain increases its benefit to its animal host, and reveals that adaptation to the host diet is a foremost step in the emergence and perpetuation of facultative animal-microbe symbioses.

RESULTS

Experimental Evolution of *L. plantarum* with *D. melanogaster* Improves Its Growth-Promoting Effect

As growth promotion during chronic undernutrition is one of the major advantages conferred by *L. plantarum* to its animal host (Schwarzer et al., 2016; Storelli et al., 2011), we asked if and how this bacterium can increase its potential to support animal growth while both partners face chronic undernutrition.

To this end, we performed experimental evolution of NIZO2877 ($Lp^{NIZO2877}$), a strain of *L. plantarum* isolated from processed human food (Martino et al., 2015a), which was previously shown to moderately promote growth both in *Drosophila* and mice (Schwarzer et al., 2016). We mono-associated germ-free (GF) *Drosophila* eggs with a fully sequenced clonal population of $Lp^{NIZO2877}$ on a low-nutritional diet and studied the partners for 20 *Drosophila* generations (i.e., 313 days, corresponding to about 2,000 bacterial generations; see STAR Methods and Figure S1). At each generation, we selected the first emerging pupae carrying a subpopulation of *L. plantarum* strains and transferred them to a new sterile diet (STAR Methods and Figure S1A). The adults rapidly emerged from the pupae and deposited the new embryos and their associated *L. plantarum* strains that subsequently colonized and propagated in the new environment. We then isolated the $Lp^{NIZO2877}$-evolved strains associated with the adult flies that emerged from the transferred pupae, selected a representative set of isolates, and measured individually their growth-promoting capacity on an independent set of naive GF fly larvae. After only two fly generations (i.e., after about 124 bacterial generations, Figures 1A and 1B), we identified a few evolved $Lp^{NIZO2877}$ strains that significantly improved larval growth and accelerated pupariation timing compared with the ancestor strain. Specifically, the evolved strains exhibited the same effect as Lp^{WJL}, a potent *L. plantarum* growth-promoting strain (Martino et al., 2015b; Storelli et al., 2011) (Figures 1A and 1B). These results show that the evolution of $Lp^{NIZO2877}$ in the context of its symbiosis with *Drosophila* leads to the rapid improvement of *L. plantarum* animal growth promotion (Figures 1C and 1D).

Genome Sequencing Reveals the Appearance and Fixation of a Single Mutation in *L. plantarum ackA* Gene

To identify the genetic changes underlying the rapid microbial adaptation responsible for the improved growth of the host, we sequenced the genomes of 11 evolved $Lp^{NIZO2877}$ strains (Table S1, replicate 1) with increased host growth-promoting potential sampled across the 20 *Drosophila* generations. We identified a total of 11 mutations, including nine SNPs and two small deletions (Figure 1E and Table S2). In particular, in the strain isolated from the second fly generation (FlyG2.1.8), we found a single change in the genome within one of the three acetate kinase genes (*ackA*). Remarkably, this first mutation was subsequently fixed and strictly correlated with the improved animal growth phenotype (Figure 1E). Following *ackA* mutation, additional variants appeared along *L. plantarum* experimental evolution, which seem to correlate with further improvement of symbiotic benefit (Figure 1A).

Independent Replicate of Experimental Evolution Confirms that *L. plantarum*^{NIZO2877} Improves Its Growth-Promoting Effect through Mutation of the *ackA* Gene

To test the repeatability of our findings, we conducted an independent replicate of *L. plantarum* experimental evolution while in symbiosis with *Drosophila*. Both the phenotypic and genomic evolution of *L. plantarum* were again obtained: $Lp^{NIZO2877}$ improved its animal growth-promoting potential by rapidly acquiring and fixing mutations, including variants in the *ackA* gene (Figure 2 and Table S2). In the first experiment, the evolved $Lp^{NIZO2877}$ strains with improved animal growth potential all carried a three-nucleotide deletion in the *ackA* gene that removed one proline residue. From the second replicate, the evolved strains carried a SNP that resulted in a premature stop codon leading to protein truncation (Figure S2). These independently isolated mutations likely generate an inactive *ackA* protein. Although both replicates of *L. plantarum* experimental evolution show additional mutations besides the *ackA* variant (Figures 1E and 2E), the two evolved strains each bearing only one mutation in *ackA* (FlyG2.1.8 and FlyG3.1.8) already showed a statistically significant *Drosophila* growth improvement compared with their ancestor (Figures 1A and 1B). This suggests that acquiring an *ackA* mutation is sufficient to confer an increased *Drosophila* growth-promotion potential. Therefore, we propose that the *de novo* appearance of the *ackA* mutation is the first fundamental step in shaping the evolutionary trajectory in the $Lp^{NIZO2877}$/*Drosophila* symbiosis model.

ackA Mutation Is Necessary to Improve *L. plantarum*^{NIZO2877} Growth-Promoting Effect

To fully establish that *ackA* mutation is responsible for the evolution of $Lp^{NIZO2877}$/*Drosophila* symbiosis, we employed CRISPR/Cas9-based bacterial genetic engineering (Jiang et al., 2013) to reinsert the deleted CCT triplet in the FlyG2.1.8 *ackA* locus (Figure S3), so that we genetically reverted the *ackA* allele in the FlyG2.1.8 isolate back to its ancestral form. The reverted strain (FlyG2.1.8^{Rev}) bearing the ancestral *ackA* allele lost its increased capacity to promote animal growth when compared with the ancestor strain (Figure 3). These results therefore demonstrate that the *ackA* mutation in $Lp^{NIZO2877}$ is a causative change resulting in faster and increased *Drosophila* growth.

ackA Confers Competitive Advantage to *L. plantarum* Evolved Strains in Both Presence and Absence of the Host

To investigate the complete *L. plantarum* population dynamics while in symbiosis with *Drosophila*, we sequenced the

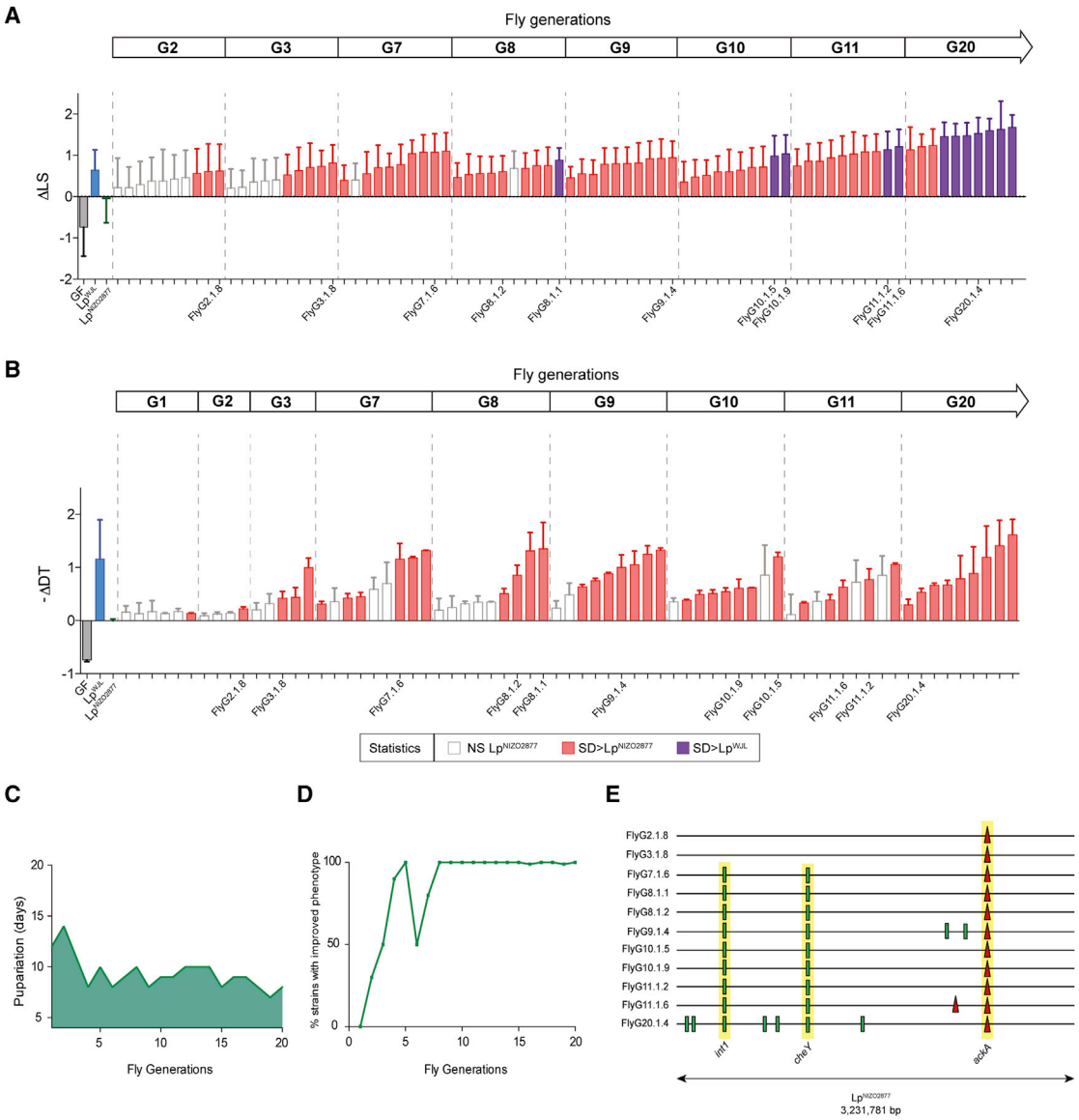

Figure 1. Experimental Evolution of *L. plantarum* with *D. melanogaster* Improves Its Growth-Promoting Effect

(A) Longitudinal size of larvae (LS) measured 7 days after egg deposition (AED) on poor-nutrient diet. Larvae were kept germ-free (GF) or associated with $Lp^{NIZO2877}$ (ancestor), Lp^{WJL} (growth-promoting *L. plantarum* strain), or $Lp^{NIZO2877}$-evolved strains. The Delta in larval size (ΔLS) shows the difference between the size of larvae associated with the respective condition and the size of larvae associated with $Lp^{NIZO2877}$ from *Drosophila* generation 2 (G2) to generation 20 (G20). Each bar refers to an $Lp^{NIZO2877}$-evolved strain isolated from the first replicate of experimental evolution from G2 to G20. $Lp^{NIZO2877}$-evolved strains that exhibited a significant difference (improved) at promoting larval growth compared with the ancestor strain (Student's t test: $p < 0.05$) are shown in red. $Lp^{NIZO2877}$-evolved strains that exhibited a significant difference (improved) at promoting larval growth compared with the beneficial *L. plantarum* Lp^{WJL} strain are shown in purple.

(B) Developmental timing (DT) of individuals that were kept GF or associated with $Lp^{NIZO2877}$, Lp^{WJL}, or $Lp^{NIZO2877}$-evolved strains isolated from *Drosophila* G1 to G20. The minus Delta in developmental timing (−ΔDT) is calculated from the mean time of emergence of 50% of the pupae associated with the respective condition and the mean time of emergence of 50% of the pupae associated with $Lp^{NIZO2877}$, and shown in the graph. $Lp^{NIZO2877}$-evolved strains that exhibited a significant difference at accelerating DT compared with the ancestor strain (Student's t test: $p < 0.05$) are shown in red. The evolved strains that have been selected for further analyses are labeled on the x axis.

(C) Difference in maturation time of individuals associated with $Lp^{NIZO2877}$-evolved strains along the first replicate of $Lp^{NIZO2877}$ adaptive evolution. The mean pupariation time of the first 15 individuals at each fly generation is shown on the y axis.

(D) Percentage of $Lp^{NIZO2877}$-evolved strains isolated at each fly generation that were found to be significantly better than the $Lp^{NIZO2877}$ at increasing larval size. Ten bacterial isolates were randomly isolated at the end of each fly generation from newly emerged adult *Drosophila* (see Figure S1A) and reassociated with new GF *Drosophila* embryos to quantify their ability to promote larval growth (see A).

(E) Mutations identified in $Lp^{NIZO2877}$-evolved strains from *Drosophila* generation 2 (G2) to generation 20 (G20) represented along the $Lp^{NIZO2877}$ genome. The genome of each evolved strain is represented as a horizontal line. Red triangles indicate deletions and small green bars show SNPs. Mutations occurring in the same gene of different strains and fixed along the experimental evolution are highlighted in yellow (*int1*, *cheY*, *ackA*).

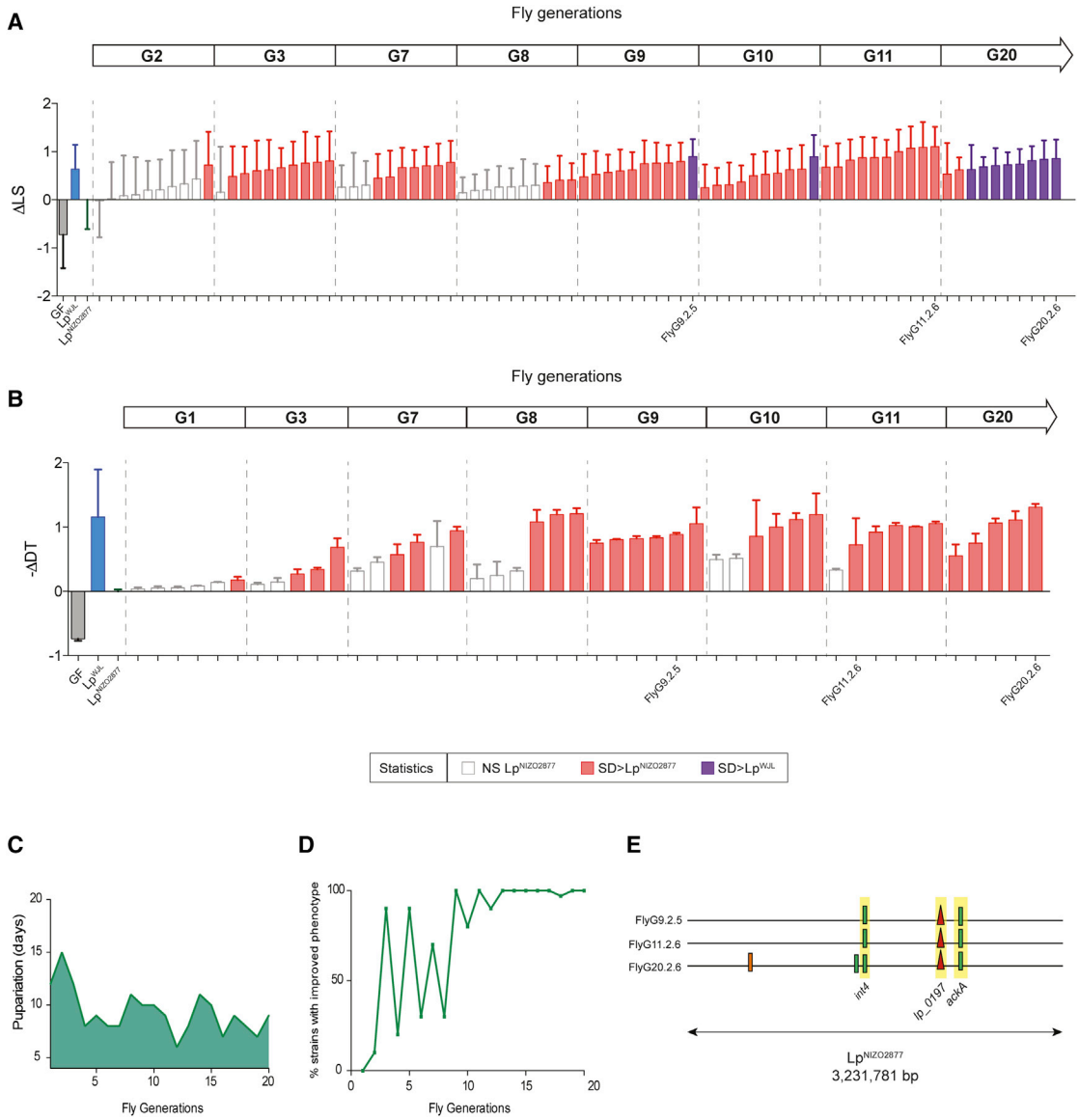

Figure 2. Second Replicate of *Lp*^{NIZO2877} Adaptive Evolution Confirms the Ability of *L. plantarum* Evolved Strains to Improve Fly Growth

(A) Difference in longitudinal size of larvae (LS) measured 7 days AED on poor-nutrient diet. Larvae were kept GF or associated with *Lp*^{NIZO2877}, *Lp*^{WJL}, or *Lp*^{NIZO2877}-evolved strains. The Delta in larval size (ΔLS) shows the difference between the size of larvae associated with the respective condition and the size of larvae associated with the ancestor from *Drosophila* generation 2 (G2) to generation 20 (G20). Each bar refers to an *Lp*^{NIZO2877}-evolved strain isolated from the second replicate of experimental evolution from G2 to G20. *Lp*^{NIZO2877}-evolved strains that exhibited a significant difference (improved) at promoting larval growth compared with the ancestor strain (Student's t test: $p < 0.05$) are shown in red. *Lp*^{NIZO2877}-evolved strains that exhibited a significant difference (improved) at promoting larval growth compared with the beneficial *L. plantarum Lp*^{WJL} strain are shown in purple.

(B) Developmental timing (DT) of individuals that were kept GF or associated with *Lp*^{NIZO2877}, *Lp*^{WJL}, or *Lp*^{NIZO2877}-evolved strains isolated from *Drosophila* G1 to G20. The minus Delta in developmental timing (−ΔDT) is calculated from the mean time of emergence of 50% of the whole adult population associated with the respective condition and the mean time of emergence of 50% of the whole adult population associated with *Lp*^{NIZO2877}, and shown in the graph. *Lp*^{NIZO2877}-evolved strains that exhibited a significant difference at accelerating developmental timing compared with the ancestor strain (Student's t test: $p < 0.05$) are shown in red. The evolved strains that have been selected for further analyses are labeled on the x axis.

(C) Difference in maturation time of individuals associated with *Lp*^{NIZO2877}-evolved strains along the second replicate of *Lp*^{NIZO2877} adaptive evolution. The pupariation time of the first 15 individuals at each fly generation is shown on the y axis.

(D) Percentage of *Lp*^{NIZO2877} –evolved strains isolated at each fly generation that were found to be significantly better than the ancestor at increasing larval size during the second replicate of *L. plantarum* adaptive evolution. Ten bacterial isolates were randomly isolated at the end of each fly generation from newly emerged adult *Drosophila* (see Figure S1) and reassociated with new GF *Drosophila* embryos to quantify their ability to promote larval growth.

(E) Mutations identified in *Lp*^{NIZO2877}-evolved strains isolated from the second replicate of experimental evolution from *Drosophila* generation 9 (G9) to generation 20 (G20) represented along *Lp*^{NIZO2877} genome. The genome of each evolved strain is represented as a horizontal line. Red triangles indicate deletions and small green bars show SNPs. Mutations occurring in the same gene of different strains and fixed along the experimental evolution are highlighted in yellow (*int4*, *lp_0197*, *ackA*).

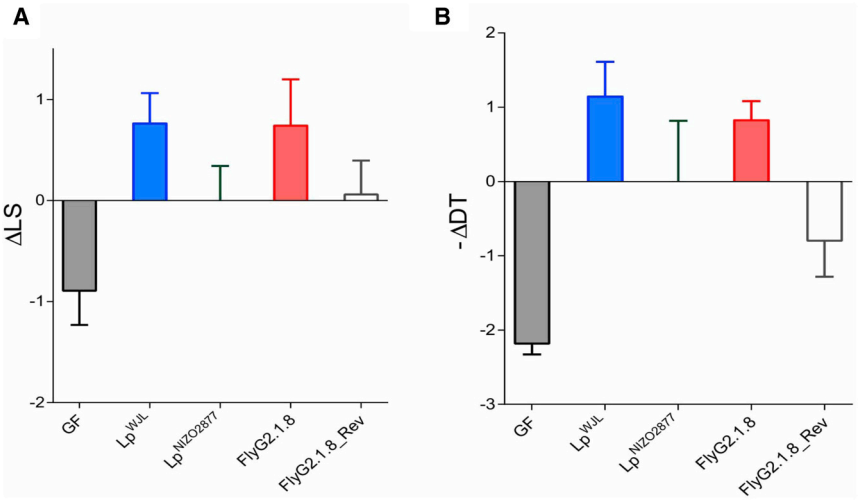

Figure 3. *ackA* Mutation Is Sufficient to Improve *L. plantarum*^{NIZO2877} Growth-Promoting Effect

(A) Longitudinal size of larvae measured 7 days AED on poor-nutrient diet. Larvae were kept germ-free (GF) or associated with *Lp*^{NIZO2877}, *Lp*^{WJL}, FlyG2.1.8, or with FlyG2.1.8-reverted strain (FlyG2.1.8^{Rev}). The Delta in larval size (ΔLS), the difference between the size of larvae associated with the respective *L. plantarum* strain and the size of larvae associated with *Lp*^{NIZO2877}, is shown. FlyG8.2.1 strain, exhibiting a significant difference (improved) at promoting larval growth compared with *Lp*^{NIZO2877} (Student's t test: $p < 0.05$), is shown in red. Strains that did not exhibit a significant difference (improved) at promoting larval growth compared with *Lp*^{NIZO2877} are shown in white.

(B) Developmental timing (DT) of individuals that were kept GF or associated with *Lp*^{NIZO2877}, *Lp*^{WJL}, FlyG2.1.8 or with FlyG2.1.8^{Rev} strain. The minus Delta in developmental timing (−ΔDT) between the mean time of emergence of 50% of the pupae associated with the respective condition and the mean time of emergence of 50% of the pupae associated with *Lp*^{NIZO2877} is shown in the graph. FlyG8.2.1 strain, exhibiting a significant difference (improved) at promoting larval growth compared with *Lp*^{NIZO2877} (Student's t test: $p < 0.05$), is shown in red. Strains that did not exhibit a significant difference (improved) at promoting larval growth compared with *Lp*^{NIZO2877} are shown in white.

metagenome of whole bacterial population samples across the 20 *Drosophila* generations of the first replicate experiment. We identified both segregating and fixed mutations and tracked their frequencies through time (STAR Methods). We found that the *ackA* mutation was the first variant to appear in the population. Remarkably, the *ackA* variant showed a rapid selective sweep and became fixed as early as after three *Drosophila* generations (Figure 4A). This observation suggests a competitive advantage of the evolved *Lp*^{NIZO2877} strains bearing this variant. To test this hypothesis, we performed a competition assay between the ancestral *Lp*^{NIZO2877} strain and the derived FlyG2.1.8 isolate in symbiosis with *Drosophila* (STAR Methods; Figures 4B and S4). We found that the evolved strain bearing only the *ackA* mutation started outcompeting the ancestor strain as early as after 1 day, demonstrating that the *ackA* mutation confers a strong competitive advantage in symbiosis with *Drosophila*. To test whether such advantage requires the host's presence, we performed the same competition assay by inoculating only the bacterial strains on the *Drosophila* nutritional environment (i.e., the diet). Surprisingly, we observed that FlyG2.1.8 outcompeted the ancestral strain even when the *Drosophila* host was absent (Figure 4C). To characterize the nature of such competitive advantage, we measured the growth rate of both strains on the *Drosophila* nutritional environment. We find that the evolved strain FlyG2.1.8 was able to replicate much faster than its ancestral strain *Lp*^{NIZO2877} in the *Drosophila* diet (Figure 4D), which contributes to establishing its competitive advantage. Taken together, these results show that *L. plantarum* evolved strains bearing the *ackA* variant shows higher fitness compared with their ancestor in our experimental settings, and that their competitive advantage is likely independent of the animal host.

L. plantarum Evolution and Improvement in Symbiotic Benefit Is Driven by the Adaptation to the Host Nutritional Environment Rather Than to Its Host

To determine whether the animal host has an influence on the evolution of its symbiotic bacteria, we experimentally evolved *Lp*^{NIZO2877} in the same low-yeast fly diet, but without *Drosophila* (STAR Methods and Figure S5) and tested the capacity of isolates sampled throughout the course of the experimental evolution to promote fly growth on a set of naive GF fly larvae. Strikingly, in two parallel experiments, the *Lp*^{NIZO2877} strains evolved in the absence of the host also show an increased ability to promote *Drosophila* growth when mono-associated with naive GF fly larvae (Figures 5A and 5B). Furthermore, genome sequencing of single evolved isolates from both experiments again revealed the acquisition of novel mutations in the *ackA* gene (Figures 5C and S5). Taken together, these findings show that the genomic evolution of *L. plantarum* is driven by the adaptation to the host nutritional environment, rather than to its host per se; the acquisition of the *ackA* variant is sufficient to drive the adaptive process to the fly diet, which ultimately results in the improvement of the *L. plantarum* symbiotic effect on *Drosophila*.

L. plantarum Improves *Drosophila* Growth through Secretion of N-Acetyl-Glutamine

We next investigated how *L. plantarum* adaptation to the nutritional environment enhances *Drosophila* growth. We postulated that *L. plantarum* adaptation to the specific nutritional environment of *Drosophila* would lead to the production of metabolites that are beneficial for *Drosophila* growth. To test this hypothesis, we analyzed the metabolome of *Drosophila* diets colonized with either *Lp*^{NIZO2877} or the evolved FlyG2.1.8 strain that bears only the *ackA* variant. Among all of the metabolites differentially detected in the substrate (Table S6), we observed a significant and robust increase in the levels of N-acetyl-amino acids in the diet processed by the evolved strain compared with the diet processed by the ancestral strain (Figure 6A). Specifically, N-acetyl-glutamine is one of the most differentially represented compounds between the two conditions. We therefore tested whether N-acetyl-glutamine is sufficient to improve the animal growth-promoting capacity of *Lp*^{NIZO2877}. Remarkably we find that, when N-acetyl-glutamine is added in a dose-dependent

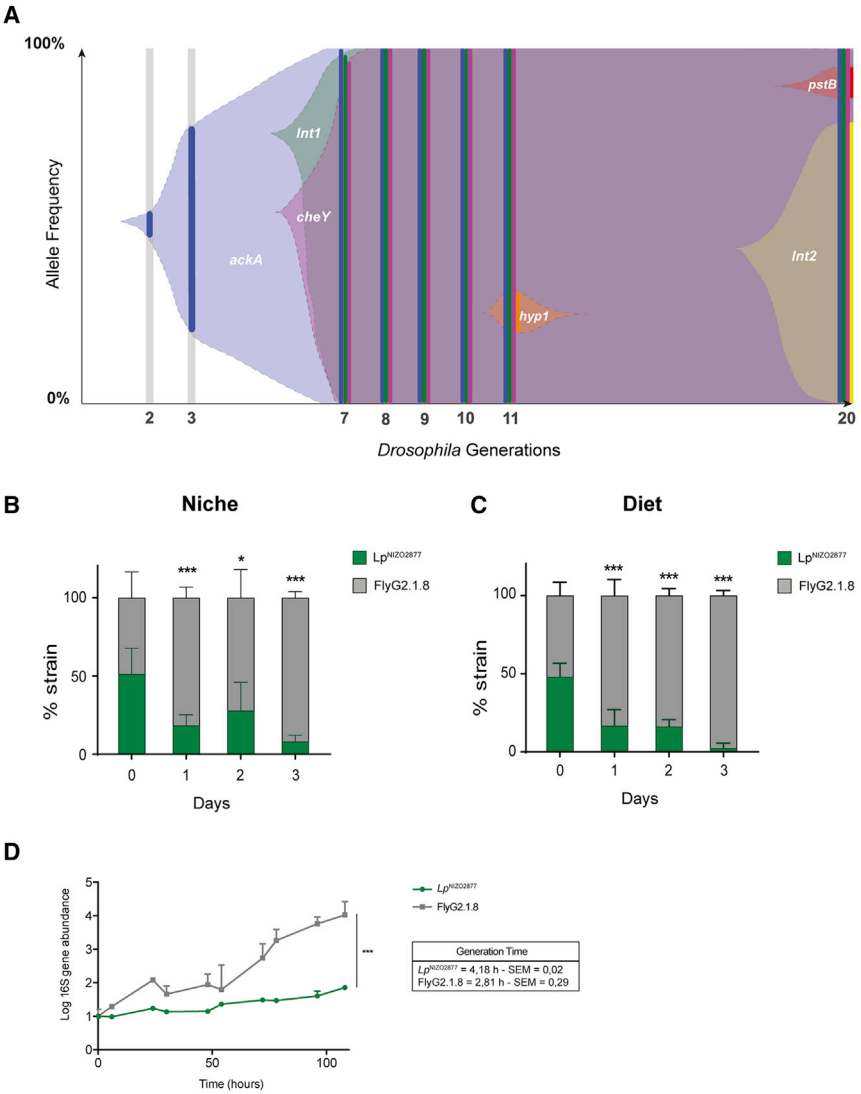

Figure 4. $Lp^{NIZO2877}$-Evolved Strain Shows Higher Fitness Compared with the Ancestor

(A) Muller diagram showing the genome evolutionary dynamics of $Lp^{NIZO2877}$ population (replicate I) along 20 *Drosophila* generations. The y axis shows the percentage of the detected frequencies of each mutation (plain colors). Shaded areas represent the inferred allele frequencies. Lower axis shows the fly generation where the sampling took place.

(B and C) 1:1 competitive assay between $Lp^{NIZO2877}$ and $Lp^{NIZO2877}$-evolved strain (FlyG2.1.8) in poor-nutrient diet with *Drosophila* larvae (B) and without *Drosophila* larvae (C). Error bars represent the percentage of each strain detected in each sample (Niche or Diet) by qPCR. $^{*}p < 0.05$, $^{***}p < 0.01$ obtained by Student's t-test.

(D) 16S rRNA kinetics of $Lp^{NIZO2877}$ and FlyG2.1.8 in the *Drosophila* nutritional environment. Absolute quantification of the 16rRNA gene (ng/μL) has been conducted for each time point. 16S rRNA gene quantification is shown in logarithmic scale. The values have been normalized by the mean of t0 (time 0). The mean generation time (h) of each strain ± SEM is reported on the graph (see STAR Methods). The result of the non-parametric analysis of covariance (*sm.ancova* function in R) between the curves is reported ($^{***}p < 0.005$).

manner in the diet, the ancestor strain $Lp^{NIZO2877}$ is now able to recapitulate the beneficial effect conferred by FlyG2.1.8 on *Drosophila* growth (Figure 6B). However, the molecule alone is not sufficient to improve the growth of GF flies at low concentrations, but benefits the larvae when added at the highest concentration (10g/L) (Figure 6B). We then asked whether N-acetyl-glutamine enhances fly growth by improving $Lp^{NIZO2877}$ fitness. To test this, we performed a competition assay between $Lp^{NIZO2877}$ and FlyG2.1.8 strains in the host diet supplemented with 0.1 g/L of N-acetyl-glutamine (a concentration sufficient to confer improved symbiotic benefit to the ancestral strain). We find that FlyG2.1.8 still outcompetes the ancestor strain even in presence of N-acetyl-glutamine (Figure 6C). This result indicates that N-acetyl-glutamine does not confer a competitive advantage to $Lp^{NIZO2877}$ over FlyG2.1.8 while growing on the diet; nevertheless, it benefits the host physiology. Taken together, these findings establish N-acetyl-amino acids, and in particular N-acetyl-glutamine, as molecules produced by the evolved *L. plantarum* strains during growth on the *Drosophila* diet, which enhance *Drosophila* growth but not $Lp^{NIZO2877}$ fitness.

DISCUSSION

Our results uncover the nature of the adaptive process of *L. plantarum* while in symbiosis with its fly host. We report direct experimental evidence showing that the host nutritional environment, and not the host per se, drives microbial adaptation and metabolic changes that alter the functional outputs of a facultative nutritional symbiosis. In our experimental context, the dietary substrate asserts the predominant selective pressure dictating the evolutionary change of facultative symbiotic bacteria and their consequent benefits to host physiology. Rapid adaptation of the *L. plantarum*^{NIZO2877} strain to the host nutritional environment occurred in multiple independent experimental lineages through the parallel fixations of different variants of a single gene, the acetate kinase *ackA*. This is a spectacular case of parallel evolution, indicating that the *ackA* mutation is the preferred or possibly the unique means for *L. plantarum*^{NIZO2877} to adapt to its host nutritional environment. Our experimental settings represent a harsh nutritional condition, which only allows *L. plantarum* slow growth (calculated generation time: 3.2 hr; Figure S1B). It was shown that the expression of *L. plantarum ackA* (*ack2* in the *L. plantarum* reference strain WCFS1) is downregulated at low growth rates, suggesting that silencing *ackA* would be required to cope with poor growth condition (Goffin et al., 2010). This observation may explain the observed strong selection pressure on *ackA* in our experimental settings, which led to the rapid *de novo* emergence of variants in the population (Figures 1 and 2). *ackA* mutation significantly improved *L. plantarum* fitness on

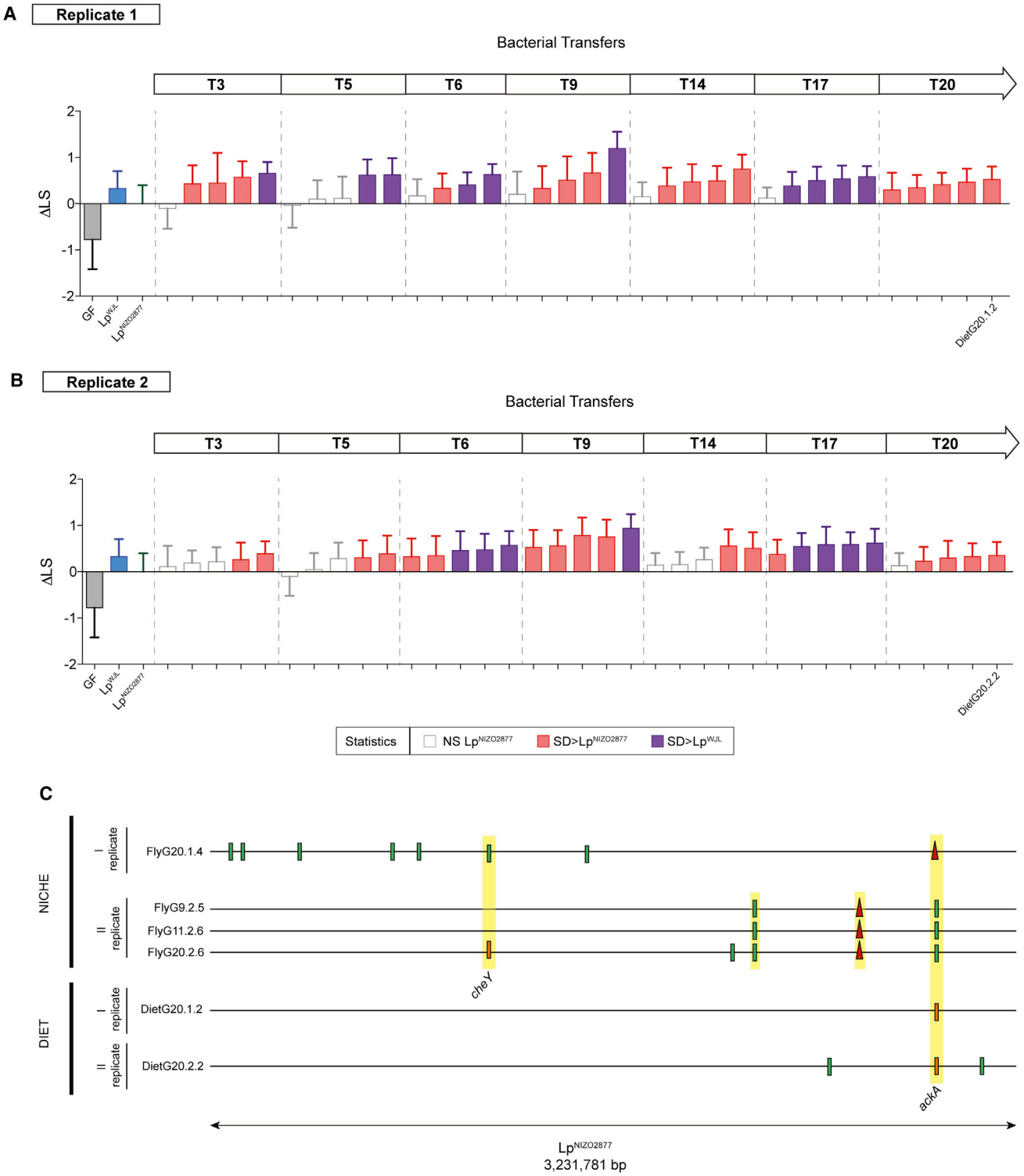

Figure 5. *Lp*^{NIZO2877} Adaptation to the Diet Increases Its Host's Growth

(A and B) Longitudinal size of larvae (LS) measured 7 days AED on poor-nutrient diet. Larvae were kept germ-free (GF) or associated with *Lp*^{NIZO2877}, *Lp*^{WJL} and with *Lp*^{NIZO2877}-evolved strains evolved in poor-nutrient diet in the absence of *Drosophila*. The Delta in larval size (ΔLS) shows the difference between the size of larvae associated with *Lp*^{NIZO2877}-evolved strains and the size of larvae associated with *Lp*^{NIZO2877} from transfer 3 (T3) to transfer 20 (T20) for the first replicate (A) and the second replicate (B) of evolution. *Lp*^{NIZO2877}-evolved strains that exhibited a significant difference (improved) at promoting larval growth compared with the ancestor strain (Student's t test: $p < 0.05$) are shown in red. *Lp*^{NIZO2877}-evolved strains that exhibited a significant difference (improved) at promoting larval growth compared with the beneficial *L. plantarum* *Lp*^{WJL} strain are shown in purple. The evolved strains that have been selected for further analyses are labeled on the x axis.

(legend continued on next page)

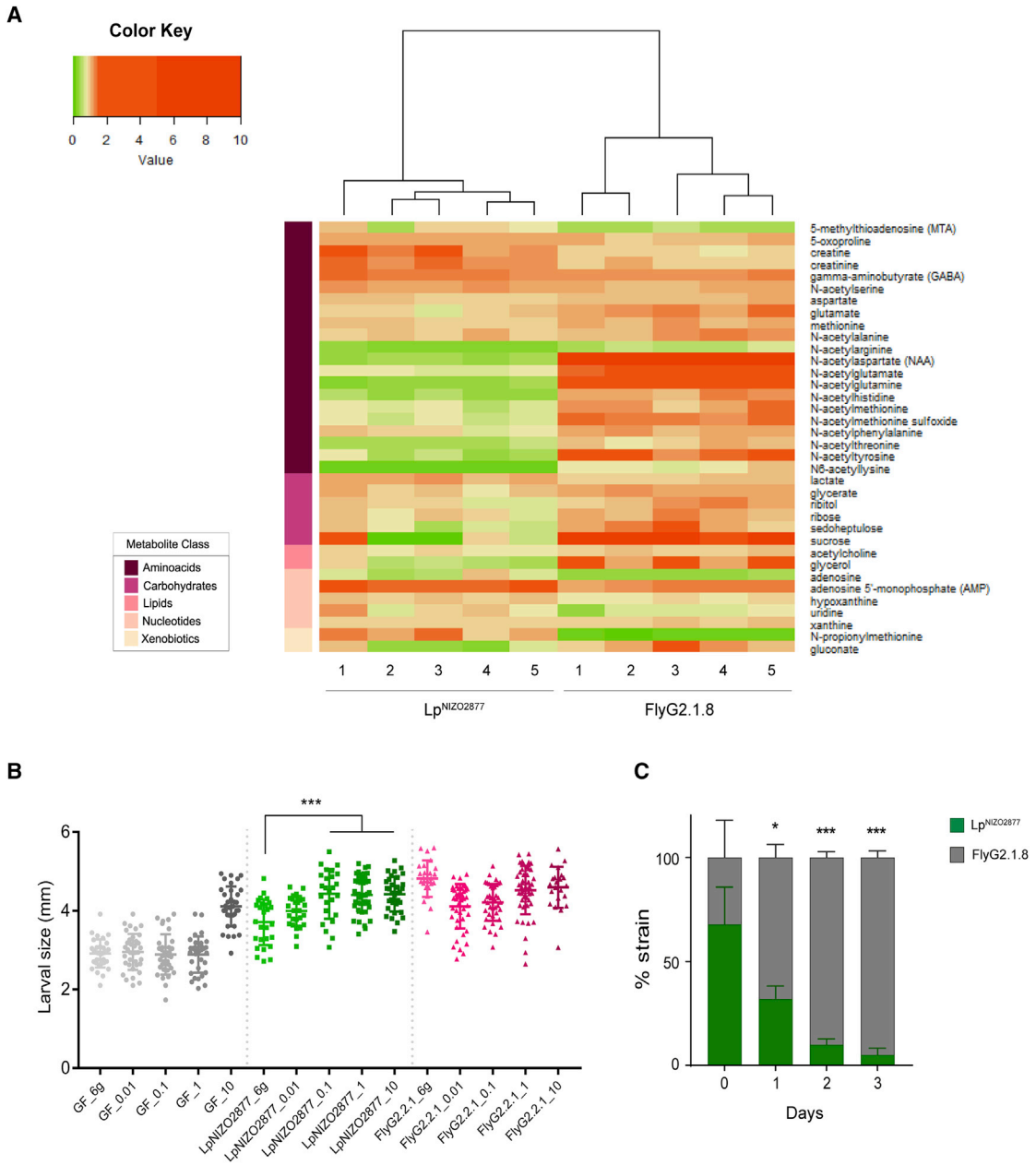

Figure 6. N-Acetyl-Glutamine Recapitulates the Beneficial Effect of FlyG2.1.8 on *Lp*^{NIZO2877}-Associated Larvae

(A) Heatmap showing the metabolites that differ significantly between experimental groups (*Lp*^{NIZO2877} and FlyG2.1.8) (two-sided t tests, $p < 0.05$). The heatmap was generated with *heatmap.2* function in R. The compounds are ordered by the metabolite class given by the left scale.

(B) Longitudinal size of larvae ($n > 60$ larvae/group) measured 7 days AED on poor-nutrient diet supplemented with different concentrations (g/L) of N-acetyl-glutamine (x axis). Larvae were kept germ-free (GF) or associated with *Lp*^{NIZO2877} (ancestor) and with Fly.G2.1.8 (evolved strain). Larval size is shown as mean ± SEM. ***$p < 0.01$.

(C) 1:1 competitive assay between *Lp*^{NIZO2877} and *Lp*^{NIZO2877}-evolved strain (FlyG2.1.8) in poor-nutrient diet supplemented with 0.1 g/L of N-acetyl-glutamine. Error bars represent the percentage of each strain detected by qPCR. *$p < 0.05$, ***$p < 0.01$, obtained by Student's t test.

the fly diet (Figure 4D); this conferred a strong competitive advantage to the evolved strains bearing these mutations and led to their fixation (Figure 4). The appearance of the *ackA* variants provoked a significant modification of *L. plantarum* metabolite production, leading to the accumulation of N-acetyl-glutamine. This molecule does not per se improve bacterial fitness, so it

(C) Mutations identified in *Lp*^{NIZO2877}-derived strains of all replicates evolved in poor-nutrient diet with *Drosophila* larvae (Niche) and in poor-nutrient diet without *Drosophila* larvae (Diet). Each evolved strain genome is represented as a horizontal line. Red triangles indicate deletions and small bars show SNPs. Different colors indicate different variants. Mutations occurring in the same gene and fixed along the experimental evolution are highlighted in yellow. The genes mutated in independent replicates of experimental evolution are labeled (*cheY*, *ackA*).

remains elusive how *ackA* variants confers competitive advantage to *L. plantarum* cells on the fly diet. Nevertheless, N-acetyl-glutamine is directly involved in *L. plantarum*/*Drosophila* symbiosis, as it is sufficient to improve *L. plantarum* benefit on fly growth (Figure 6B). Our results indicate that *ackA* mutations possibly cause a shift in the metabolism of *L. plantarum* by modifying the usage of cellular acetyl groups, which would confer benefits to *L. plantarum* growth on the fly diet, thus improving its symbiotic effect. *ackA* participates in the reversible conversion of acetate to acetyl-phosphate; *ackA* variants might impede this reaction, and therefore shunt the pools of cellular acetyl groups into different metabolic routes leading to the accumulation of other acetylated compounds, such as N-acetyl-amino acids, which, once secreted, are consumed and beneficial to the host. These interpretations stem from the hypothesis that all the *ackA* variants obtained along *L. plantarum* experimental evolution likely generate inactive proteins (Figures S2 and S5B). Nevertheless, further work is needed to establish that all the variants lead to strict loss of function of *ackA*. Generating an *ackA* knockout in the ancestral $Lp^{NIZO2877}$ strain, measuring the activity of *ackA* protein variants, and probing the metabolic consequences of *ackA* variants in all the ancestral and evolved strains will likely provide insights into the specific molecular mechanisms underlying our findings.

Our results identify *ackA* as the first target of selection exerted by the nutritional environment on $Lp^{NIZO2877}$. Of note, Lp^{WJL}, a potent growth-promoting strain isolated from *D. melanogaster* gut (Martino et al., 2015b; Ryu et al., 2008; Storelli et al., 2011), shows two nucleotide substitutions in the *ackA* gene, compared with $Lp^{NIZO2877}$ (Figure S6), which might concur with its high beneficial effect in our experimental settings. Yet, due to the high genetic diversity of *L. plantarum* strains (Martino et al., 2016), we posit that such a genetic target hinges upon the genomic background of $Lp^{NIZO2877}$. According to their specific network of genetic polymorphisms, other non-beneficial isolates might fix mutations affecting other genes in order to adapt to the host environment and improve their fitness.

Understanding how evolutionary forces shape host-microbe symbiosis is essential to comprehend the mechanisms of their functional influence. Using the facultative nutritional mutualism between *Drosophila* and *L. plantarum* as a model, our results reveal that the primary selection pressure acting on *L. plantarum* originates from the nutritional substrate alone, which is strong enough to drive the rapid fixation of a *de novo* mutation. The resulting genetic changes confer a fitness advantage to the evolved bacteria and trigger a metabolic adaptation in bacterial cells, which is quickly capitalized by *Drosophila* as a physiological growth advantage, hence symbiosis can be perpetuated. This is a clear example of by-product mutualism, whereby animal hosts enjoy benefits from the by-products of the self-serving traits of their microbial symbionts (Bronstein, 1994; Connor, 1995; Holland and Bronstein, 2008). By showing that bacterial adaptation to the host nutritional medium results in a higher microbial competitive advantage and improvement of symbiotic benefit, we posit that such a process represents the first step in the emergence and evolution of facultative mutualism. Our results do not rule out the possibility that the animal host might exert additional selection pressure on its bacterial partners. Indeed, *Drosophila* is also known to directly affect the fitness of its own microbiota through the activity of innate immune effectors (Guo et al., 2014; Ryu et al., 2008) or the secretion of bacterial maintenance factors (Storelli et al., 2018). Nevertheless, our findings demonstrate the utmost importance of the shared nutritional substrate in the evolution of *Drosophila*-*L. plantarum* symbiosis.

Symbiosis is an evolutionary imperative and facultative symbioses are widespread in nature. Despite their unequivocal diversity, animal-microbe symbioses share striking similarities (Foster et al., 2017) and nutrition often plays a major role in shaping the composition of symbiotic microbial communities (Conlon and Bird, 2015; David et al., 2015; Groussin et al., 2017; Hacquard et al., 2015; Lozupone et al., 2012; Muegge et al., 2011). Our results provide direct experimental evidence that nutrition drives the evolution of a bacterial symbiont and, given that other animal and microbe partners have likely faced nutritional challenges over time, common evolutionary trajectories might have occurred. We therefore posit that bacterial adaptation to the diet can be the first step in the emergence and perpetuation of facultative animal-microbe symbioses. Our work provides another angle from which to help unravel the complex adaptive processes in the context of evolving symbiosis.

STAR★METHODS

Detailed methods are provided in the online version of this paper and include the following:

- KEY RESOURCES TABLE
- CONTACT FOR REAGENT AND RESOURCE SHARING
- EXPERIMENTAL MODEL AND SUBJECT DETAILS
  - Bacterial Strains and Culture Conditions
  - *Drosophila* Stocks and Breeding
  - Fly Diets Used in This Study
  - Colonization and Infection of Larvae
- METHOD DETAILS
  - Experimental Evolution Design
  - Generation Time of *L. plantarum*
  - Larval Size Measurements
  - Developmental Timing
  - Genome Sequencing
  - *L. plantarum* Genomic Editing with CRISPR-Cas9
  - Bacterial Competitions Tests
  - Metabolite Profiling
  - Information Related to Experimental Design
- QUANTIFICATION AND STATISTICAL ANALYSIS
- DATA AND SOFTWARE AVAILABILITY

SUPPLEMENTAL INFORMATION

Supplemental Information includes six figures and six tables and can be found with this article online at https://doi.org/10.1016/j.chom.2018.06.001.

ACKNOWLEDGMENTS

We thank B. Prud'homme and colleagues at the Institut de Génomique Fonctionnelle de Lyon for critical reading of the manuscript. We gratefully acknowledge support from the PSMN (Pôle Scientifique de Modélisation Numérique) of the ENS de Lyon for the computing resources. This work was funded by an ERC starting grant (FP7/2007-2013-N° 309704). M.E.M. was funded by the European Union's Horizon 2020 research and innovation

program under the Marie Sklodowska-Curie grant agreement N° 659510. The lab of F.L. is supported by the FINOVI foundation and the EMBO Young Investigator Program. The CRISPR/Cas9 work was supported through funding from the National Science Foundation (MCB-1452902 to C.B.). WCFS1 was a kind gift from Dr. Nikhil U. Nair. EC135 was provided to us by Tingyi Wen. We thank the University of Padua and Dr. Barbara Cardazzo for hosting M.E.M. during the last stages of this work.

AUTHOR CONTRIBUTIONS

M.E.M. and F.L. designed the project; M.E.M. and H.G. conducted the experiments; M.E.M. and P.J. conducted the bioinformatics analyses; R.L., M.S., and C.B. designed and performed the CRISPR/Cas9 engineering experiments; S.H. and B.G. generated the sequencing data; M.E.M. and F.L. analyzed the data and wrote the paper.

DECLARATION OF INTERESTS

M.E.M. and F.L. are inventors of a pending patent application (INPI-n° FR1757717) which applies to bacterial strains presented in this article.

Received: March 29, 2018
Revised: April 27, 2018
Accepted: May 11, 2018
Published: June 28, 2018

REFERENCES

Blum, J.E., Fischer, C.N., Miles, J., and Handelsman, J. (2013). Frequent replenishment sustains the beneficial microbiome of *Drosophila melanogaster*. MBio *4*, e00860–13.

Broderick, N.A., Buchon, N., and Lemaitre, B. (2014). Microbiota-induced changes in *Drosophila melanogaster* host gene expression and gut morphology microbiota-induced changes in *Drosophila melanogaster* host gene. MBio *5*, 1–13.

Bronstein, J.L. (1994). Our current understanding of mutualism. Q. Rev. Biol. *69*, 31–51.

Choi, Y., Sims, G.E., Murphy, S., Miller, J.R., and Chan, A.P. (2012). Predicting the functional effect of amino acid substitutions and indels. PLoS One *7*, e46688.

Conlon, M.A., and Bird, A.R. (2015). The impact of diet and lifestyle on gut microbiota and human health. Nutrients *7*, 17–44.

Connor, R.C. (1995). The benefits of mutualism: a conceptual framework. Biol. Rev. *70*, 427–457.

David, L.A., Materna, A.C., Friedman, J., Campos-Baptista, M.I., Blackburn, M.C., Perrotta, A., Erdman, S.E., and Alm, E.J. (2015). Host lifestyle affects human microbiota on daily timescales. Genome Biol. *15*, R89.

Deatherage, D.E., and Barrick, J.E. (2014). Identification of mutations in laboratory-evolved microbes from next-generation sequencing data using breseq. Methods Mol. Biol. *1151*, 165–188.

Douglas, A.E. (2011). Lessons from studying insect symbioses. Cell Host Microbe *10*, 359–367.

Duong, T., Miller, M.J., Barrangou, R., Azcarate-Peril, M.A., and Klaenhammer, T.R. (2011). Construction of vectors for inducible and constitutive gene expression in *Lactobacillus*. Microb. Biotechnol. *4*, 357–367.

Engel, P., and Moran, N.A. (2013). The gut microbiota of insects—diversity in structure and function. FEMS Microbiol. Rev. *37*, 699–735.

Erkosar, B., Storelli, G., Mitchell, M., Bozonnet, L., Bozonnet, N., and Leulier, F. (2015). Pathogen virulence impedes mutualist-mediated enhancement of host juvenile growth via inhibition of protein digestion. Cell Host Microbe *18*, 445–455.

Feldhaar, H. (2011). Bacterial symbionts as mediators of ecologically important traits of insect hosts. Ecol. Entomol. *36*, 533–543.

Ferrari, J., and Vavre, F. (2011). Bacterial symbionts in insects or the story of communities affecting communities. Philos. Trans. R. Soc. Lond. B Biol. Sci. *366*, 1389–1400.

Fisher, R.M., Henry, L.M., Cornwallis, C.K., Kiers, E.T., and West, S.A. (2017). The evolution of host-symbiont dependence. Nat. Commun. *8*, 15973.

Foster, K.R., Schluter, J., Coyte, K.Z., and Rakoff-Nahoum, S. (2017). The evolution of the host microbiome as an ecosystem on a leash. Nature *548*, 43–51.

Gibson, D.G., Young, L., Chuang, R.-Y., Venter, J.C., Hutchison, C.A., and Smith, H.O. (2009). Enzymatic assembly of DNA molecules up to several hundred kilobases. Nat. Methods *6*, 343–345.

Gilbert, J.A., and Neufeld, J.D. (2014). Life in a world without microbes. PLoS Biol. *12*, e1002020.

Goffin, P., van de Bunt, B., Giovane, M., Leveau, J.H.J., Höppener-Ogawa, S., Teusink, B., and Hugenholtz, J. (2010). Understanding the physiology of *Lactobacillus plantarum* at zero growth. Mol. Syst. Biol. *6*, 413.

Gomaa, A.A., Klumpe, H.E., Luo, M.L., Selle, K., Barrangou, R., and Beisel, L. (2014). Programmable removal of bacterial strains by use of genome-targeting CRISPR/Cas systems. MBio *5*, e00928–13.

Groussin, M., Mazel, F., Sanders, J.G., Smillie, C.S., Lavergne, S., Thuiller, W., and Alm, E.J. (2017). Unraveling the processes shaping mammalian gut microbiomes over evolutionary time. Nat. Commun. *8*, 14319.

Guo, L., Karpac, J., Tran, S.L., and Jasper, H. (2014). PGRP-SC2 promotes gut immune homeostasis to limit commensal dysbiosis and extend lifespan. Cell *156*, 109–122.

Hacquard, S., Garrido-Oter, R., González, A., Spaepen, S., Ackermann, G., Lebeis, S., McHardy, A.C., Dangl, J.L., Knight, R., Ley, R., et al. (2015). Microbiota and host nutrition across plant and animal kingdoms. Cell Host Microbe *17*, 603–616.

Holland, J.N., and Bronstein, J.L. (2008). Mutualism. In Encyclopedia of Ecology, S.E. Jorgensen and B.D. Fath, eds. (Elsevier), pp. 2485–2491.

Jiang, W., Bikard, D., Cox, D., Zhang, F., and Marraffini, L.A. (2013). RNA-guided editing of bacterial genomes using CRISPR-Cas systems. Nat. Biotechnol. *31*, 233–239.

Kearse, M., Moir, R., Wilson, A., Stones-Havas, S., Cheung, M., Sturrock, S., Buxton, S., Cooper, A., Markowitz, S., Duran, C., et al. (2012). Geneious Basic: an integrated and extendable desktop software platform for the organization and analysis of sequence data. Bioinformatics *28*, 1647–1649.

Lozupone, C.A., Stombaugh, J.I., Gordon, J.I., Jansson, J.K., and Knight, R. (2012). Diversity, stability and resilience of the human gut microbiota. Nature *489*, 220–230.

Ma, D., Storelli, G., Mitchell, M.L., and Leulier, F. (2015). Studying host-microbiota mutualism in *Drosophila*: harnessing the power of gnotobiotic flies. Biomed. J. *38*, 285–293.

Martino, M.E., Bayjanov, J.R., Joncour, P., Hughes, S., Gillet, B., Kleerebezem, M., Siezen, R., van Hijum, S.A.F.T., and Leulier, F. (2015a). Nearly complete genome sequence of *Lactobacillus plantarum* strain NIZO2877. Genome Announc. *3*, https://doi.org/10.1128/genomeA.01370-15.

Martino, M.E., Bayjanov, J.R., Joncour, P., Hughes, S., Gillet, B., Kleerebezem, M., Siezen, R., van Hijum, S.A.F.T., and Leulier, F. (2015b). Resequencing of the *Lactobacillus plantarum* strain WJL genome. Genome Announc. *3*, https://doi.org/10.1128/genomeA.01382-15.

Martino, M.E., Bayjanov, J.R., Caffrey, B.E., Wels, M., Joncour, P., Hughes, S., Gillet, B., Kleerebezem, M., van Hijum, S.A.F.T., and Leulier, F. (2016). Nomadic lifestyle of *Lactobacillus plantarum* revealed by comparative genomics of 54 strains isolated from different habitats. Environ. Microbiol. *18*, 4974–4989.

Matos, R.C., and Leulier, F. (2014). Lactobacilli-host mutualism: "learning on the fly". Microb. Cell Fact. *13*, S6.

Matos, R.C., Schwarzer, M., Gervais, H., Courtin, P., Joncour, P., Gillet, B., Ma, D., Bulteau, A.L., Martino, M.E., Hughes, S., et al. (2017). D-Alanylation of teichoic acids contributes to Lactobacillus plantarum-mediated *Drosophila* growth during chronic undernutrition. Nat. Microbiol. *2*, 1635–1647.

Muegge, B.D., Kuczynski, J., Knights, D., Clemente, J.C., González, A., Fontana, L., Henrissat, B., Knight, R., and Gordon, J.I. (2011). Diet drives convergence in gut microbiome functions across mammalian phylogeny and within humans. Science *332*, 970–974.

Packey, C.D., Shanahan, M.T., Manick, S., Bower, M.A., Ellermann, M., Tonkonogy, S.L., Carroll, I.M., and Sartor, R.B. (2013). Molecular detection of bacterial contamination in gnotobiotic rodent units. Gut Microbes *4*, 361–370.

Poulsen, L.K., Licht, T.R., Rang, C., Krogfelt, K.A., and Molin, S. (1995). Physiological state of *Escherichia coli* BJ4 growing in the large intestines of streptomycin-treated mice. J. Bacteriol. *177*, 5840–5845.

RStudio Team (2015). RStudio: Integrated Development for R (RStudio).

Ryu, J.H., Kim, S.H., Lee, H.Y., Jin, Y.B., Nam, Y.D., Bae, J.W., Dong, G.L., Seung, C.S., Ha, E.M., and Lee, W.J. (2008). Innate immune homeostasis by the homeobox gene Caudal and commensal-gut mutualism in *Drosophila*. Science *319*, 777–782.

Schneider, C.A., Rasband, W.S., and Eliceiri, K.W. (2012). NIH Image to ImageJ: 25 years of image analysis. Nat. Methods *9*, 671–675.

Schwarzer, M., Makki, K., Storelli, G., Machuca-Gayet, I., Srutkova, D., Hermanova, P., Martino, M.E., Balmand, S., Hudcovic, T., Heddi, A., et al. (2016). *Lactobacillus plantarum* strain maintains growth of infant mice during chronic undernutrition. Science *351*, 854–857.

Spath, K., Hein, S., and Grabherr, R. (2012). Direct cloning in *Lactobacillus plantarum*: electroporation with non-methylated plasmid DNA enhances transformation efficiency and makes shuttle vectors obsolete. Microb. Cell Fact. *11*, 141.

Storelli, G., Defaye, A., Erkosar, B., Hols, P., Royet, J., and Leulier, F. (2011). *Lactobacillus plantarum* promotes *Drosophila* systemic growth by modulating hormonal signals through TOR-dependent nutrient sensing. Cell Metab. *14*, 403–414.

Storelli, G., Strigini, M., Grenier, T., Bozonnet, L., Schwarzer, M., Daniel, C., Matos, R., and Leulier, F. (2018). *Drosophila* perpetuates nutritional mutualism by promoting the fitness of its intestinal symbiont *Lactobacillus plantarum*. Cell Metab. *27*, 362–377.

Teresa Alegre, M., Carmen Rodríguez, M., and Mesas, J.M. (2004). Transformation of *Lactobacillus plantarum* by electroporation with in vitro modified plasmid DNA. FEMS Microbiol. Lett. *241*, 73–77.

Thompson, K., and Collins, M.A. (1996). Methods Improvement in electroporation efficiency for *Lactobacillus plantarum* by the inclusion of high concentrations of glycine in the growth medium. J. Microbiol. Methods *26*, 73–79.

Widdel, F. (2007). Theory and Measurement of Bacterial Growth Grundpraktikum Mikrobiologie (Universität Bremen), p. 11.

Zhang, G., Wang, W., Deng, A., Sun, Z., Zhang, Y., Liang, Y., Che, Y., and Wen, T. (2012). A mimicking-of-DNA-methylation-patterns pipeline for overcoming the restriction barrier of bacteria. PLoS Genet. *8*, e1002987.

STAR★METHODS

KEY RESOURCES TABLE

REAGENT or RESOURCE	SOURCE	IDENTIFIER
Bacterial and Virus Strains		
L. plantarum: $Lp^{NIZO2877}$	Martino et al., 2015a	LKHZ01000000
L. plantarum: Lp^{WJL}	Martino et al., 2015a, 2015b	LKLZ00000000
L. plantarum: FlyG2.1.8	This paper	PEBE00000000
L. plantarum: FlyG3.1.8	This paper	PEGI00000000
L. plantarum: FlyG7.1.6	This paper	PEGJ00000000
L. plantarum: FlyG8.1.1	This paper	PEGK00000000
L. plantarum: FlyG8.1.2	This paper	PEGL00000000
L. plantarum: FlyG9.1.4	This paper	PEGM00000000
L. plantarum: FlyG10.1.5	This paper	PEGN00000000
L. plantarum: FlyG10.1.9	This paper	PEGO00000000
L. plantarum: FlyG11.1.2	This paper	PEGP00000000
L. plantarum: FlyG11.1.6	This paper	PEGQ00000000
L. plantarum: FlyG20.1.4	This paper	PEGR00000000
L. plantarum: FlyG2.1.8Rev	This paper	N/A
L. plantarum: FlyG9.2.5	This paper	PEGS00000000
L. plantarum: FlyG11.2.6	This paper	PEGT00000000
L. plantarum: FlyG20.2.6	This paper	PEGU00000000
L. plantarum: DietG20.1.2	This paper	PEGV00000000
L. plantarum: DietG20.2.2	This paper	PEGW00000000
E. coli E135	Zhang et al., 2012	N/A
Chemicals, Peptides, and Recombinant Proteins		
Inactivated Dried Yeast	Bio Springer	Springaline BA95/0-PW
Cornmeal	Westhove	Farigel maize H1
Agar	VWR	#20768.361
Methylparaben Sodium Salt	MERCK	#106756
Propionic Acid	Sigma-Aldrich	P1386
Man, Rogosa and Sharpe (MRS) Broth Medium	Difco	#288130
Man, Rogosa and Sharpe (MRS) Agar Medium	Difco	#288210
N-Acetyl Glutamine	Sigma-Aldrich	A9125-25G
PBS	Dutscher	NA.25
Glycerol	Sigma-Aldrich	G5516
SuperScript™ II Reverse Transcriptase	Invitrogen, Thermofisher Scientific	18064014
SYBR GreenER™ qPCR SuperMix Universal	Invitrogen, Thermofisher Scientific	1176202K
Rifampicin	Sigma-Aldrich	R3501
Chloramphenicol	Sigma-Aldrich	C0378
Erythromycin	Sigma-Aldrich	E1300000
Ampicillin	Sigma-Aldrich	A9393
Glycine	Sigma-Aldrich	67419
Sucrose	Sigma-Aldrich	S7903
Magnesium chloride	Sigma-Aldrich	M8266
Critical Commercial Assays		
NucleoSpin RNA Isolation Kit	Macherey-Nagel	740955.240C
UltraClean Microbial DNA Isolation Kit	MOBIO Laboratories, Inc.	12224-250

(*Continued on next page*)

Continued

REAGENT or RESOURCE	SOURCE	IDENTIFIER
Ion Xpress™ Plus Fragment Library Kit	Ion Torrent	4471269
Gibson Assembly Master Mix	NEB	E2611S
T4 Polynucleotide Kinase	NEB	M0201S
T4 DNA Ligase	NEB	M0202S
Deposited Data		
Metabolomic Dataset of Diet	This paper	Table S3
L. plantarum FlyG2.1.8 genome	This paper	PEBE00000000
L. plantarum FlyG3.1.8 genome	This paper	PEGI00000000
L. plantarum FlyG7.1.6 genome	This paper	PEGJ00000000
L. plantarum FlyG8.1.1 genome	This paper	PEGK00000000
L. plantarum FlyG8.1.2 genome	This paper	PEGL00000000
L. plantarum FlyG9.1.4 genome	This paper	PEGM00000000
L. plantarum FlyG10.1.5 genome	This paper	PEGN00000000
L. plantarum FlyG10.1.9 genome	This paper	PEGO00000000
L. plantarum FlyG11.1.2 genome	This paper	PEGP00000000
L. plantarum FlyG11.1.6 genome	This paper	PEGQ00000000
L. plantarum FlyG20.1.4 genome	This paper	PEGR00000000
L. plantarum FlyG9.2.5 genome	This paper	PEGS00000000
L. plantarum FlyG11.2.6 genome	This paper	PEGT00000000
L. plantarum FlyG20.2.6 genome	This paper	PEGU00000000
L. plantarum DietG20.1.2 genome	This paper	PEGV00000000
L. plantarum DietG20.2.2 genome	This paper	PEGW00000000
Experimental Models: Organisms/Strains		
D.melanogaster: y,w (reference strain for this work)		N/A
Oligonucleotides		
Primer: 16S_UniF: GTGSTGCAYGGYTGTCGTCA	Packey et al., 2013	N/A
Primer: 16S_UniR: ACGTCRTCCMCACCTTCCTC	Packey et al., 2013	N/A
Primers for SNP verification, see Table S4	This paper	N/A
Primers for competition tests, see Table S4	This paper	N/A
Primers for engineering *L. plantarum* with CRISPR-Cas9, see Table S6	This paper	N/A
Recombinant DNA		
Plasmids used to engineer *L. plantarum* with CRISPR-Cas9, see Table S5	This paper	N/A
pJP005		CB651
pMSP3545		Addgene 46888
pCas9	Jiang et al., 2013	Addgene 42876
Software and Algorithms		
ImageJ	NIH Image	https://imagej.net/ImageJ
Leica application suite (LAS)	Leica	N/A
Scan 1200 Automatic HD colony counter and Software	Intersciences	Ref. 437 000
Breseq	Deatherage and Barrick, 2014	http://barricklab.org/twiki/bin/view/Lab/ToolsBacterialGenomeResequencing
R Studio	RStudio Team, 2015	https://www.rstudio.com/
PROVEAN	Choi et al., 2012	http://provean.jcvi.org
Geneious	Kearse et al., 2012	https://www.geneious.com
Gibson assembly	Choi et al., 2012	http://provean.jcvi.org

CONTACT FOR REAGENT AND RESOURCE SHARING

Further information and requests for resources and reagents should be directed to and will be fulfilled by the Lead Contact, François Leulier (francois.leulier@ens-lyon.fr).

EXPERIMENTAL MODEL AND SUBJECT DETAILS

Bacterial Strains and Culture Conditions

The strains used in the present study are listed in Table S1. All experimentally evolved strains were derived from *L. plantarum*^{NIZO2877} (kind gift from Prof. Michiel Kleerebezem, NIZO Food Research BV, Netherlands) that was originally isolated from a sausage in Vietnam (Martino et al., 2015a). All strains were routinely grown overnight at 37°C in Man, Rogosa and Sharpe (MRS) medium (BD Bioscience) without agitation. Strains were stored at -80°C in MRS broth containing 20% glycerol.

Drosophila Stocks and Breeding

Drosophila yw flies were used as the reference strain in this work. *Drosophila* stocks were cultured at 25°C with 12/12 hour dark/light cycles on a yeast/cornmeal medium containing 50g/l inactivated yeast (rich diet) as described by Storelli et al. (2011). Poor-nutrient diet was obtained by reducing the amount of yeast extract to 8 g/l. Germ-free (GF) stocks were established and maintained as described in Storelli et al. (Storelli et al., 2011).

Fly Diets Used in This Study

Poor Yeast Diet: 8g inactivated dried yeast, 80g cornmeal, 7.2g Agar, 5.2g methylparaben sodium salt, 4 mL 99% propionic acid for 1 litre.

PYD + N-acetyl-Glutamine. Fly food is prepared by mixing 8g of inactive dried yeast, 80g of cornmeal, 7,2g of agar, 5,2g of methylparaben sodium salt, 4 mL of 99% propionic acid in 800 mL water. After cooking and before solidification, fly food is mixed with serial dilutions of N-acetyl-Glutamine solution (prepared from a stock solution at 1g N-acetyl-Glutamine/L sterile water). Fly food is then mixed vigorously by vortexing, and then poured in microtubes.

Fly food was poured in petri dishes (diameter=55mm; fly food volume ≈ 7ml) to grow larvae used for larval longitudinal length analysis. Fly food was poured in 50 ml tubes for Experimental Evolution setup. Fly food was poured in 1.5 ml microtubes (fly food volume=100µl) for metabolites profiling.

Colonization and Infection of Larvae

40 embryos collected from GF females were transferred to a fresh poor nutrient GF medium in a 55 mm petri dish. Bacterial strains were cultured to stationary phase (18h) in MRS broth at 37°C. The embryos and the fly medium were mono-associated with 300 µl (7 x10^7 CFU) of the respective bacteria. Emerging larvae were allowed to develop on the contaminated medium at 25°C.

METHOD DETAILS

Experimental Evolution Design

The experimental "Adaptive Evolution" (AE) model of *L. plantarum* in *Drosophila* Niche (*Drosophila* + Diet) was designed as follows: for the first generation of the AE model, GF female flies laid GF embryos on poor nutrient GF medium. Forty GF eggs were transferred on 10 ml of new poor nutrient GF medium. *L. plantarum*^{NIZO2877} (ancestor) was cultured in MRS broth to stationary phase (18h). The culture was washed in sterile PBS and 300 µl of PBS-washed culture containing 10^8 CFU of *L. plantarum*^{NIZO2877} were added directly on the embryos and the fly food (bacterial load = 10^7 CFU/ml) (Figure S1A). No further inoculation of the ancestor strain *L. plantarum*^{NIZO2877} has been performed after the beginning of the first generation until the end of the experimental evolution. Emerging larvae were allowed to develop on the medium inoculated with the bacterial culture at 25°C. The first 15 pupae were transferred to a new poor nutrient GF medium, and allowed to complete metamorphosis. Once the pupae were transferred, the bacterial community associated with them (on average 10^6 CFU/ml) was also indirectly transferred to the new medium by inoculation of the substratum from the surface of the transferred pupae and predominantly by defecation of the adults emerging from the transferred pupae. This allowed the propagation of an evolving bacterial subpopulation derived from the ancestor on the new medium. Once the emerging adults had laid eggs (a minimum of 40 and no more than 80 per tube), which were the founders for the next fly generation, they were collected and homogenized using the Precellys 24 tissue homogenizer (Bertin Technologies, France) and 0.75/1 mm glass beads in 800 µl of MRS broth and stored at -80°C by adding 20% glycerol. Single bacterial isolates were isolated at the end of each fly generation by plating the crushed adult flies on MRS agar plates at 37°C for 48h. Ten colonies were randomly selected from the plates and tested individually for *Drosophila* growth promotion (larval size and developmental timing assays) on new ancestral GF *yw* *Drosophila* embryos (see below). The AE model has been propagated for 20 fly generations.

The experimental evolution of *L. plantarum* in *Drosophila*'s nutritional medium (Diet) was designed as follows: *L. plantarum*^{NIZO2877} (ancestor) was cultured to stationary phase (18h). The culture was washed in sterile PBS and 3 µl (10^6 CFU) were added directly on 100 µl of poor nutrient GF diet (bacterial load = 10^7 CFU/ml) (Figure S5A) and kept at 25°C. After four days (time necessary for the microbial load to reach the same value found on the 15 pupae used for propagating the bacterial population in the Niche adaptive

evolution setup), the medium was crushed using the Precellys 24 tissue homogenizer (Bertin Technologies, France) and 0.75/1 mm glass beads in 500 μl of PBS using glass beads and 10 μl of the crushed medium (10^5 CFU) were used to inoculate 100 μl of new poor nutrient GF medium (10^6 CFU/ml). This protocol has been repeated 20 times.

Strain-specific PCR tests were performed to confirm the unique presence of *L. plantarum*^{NIZO2877} throughout both experimental evolution models as reported in Schwarzer et al. (Schwarzer et al., 2016).

Generation Time of *L. plantarum*

To determine the generation time of *L. plantarum* strains in the *Drosophila* Niche (*Drosophila* + Diet) and Diet, we used a modified version of a method that reported the correlation between bacterial growth rate and 16SrRNA content (Poulsen et al., 1995). *L. plantarum* strains were cultured to stationary phase (18h) and washed in sterile PBS. Serial dilutions have been prepared and 5 μl containing a total of 10^3 colony-forming units (CFUs) were added to 100 μl of GF poor nutrient diet with and without *Drosophila* larvae (Diet and Niche setup respectively) and kept at 25°C. Samples were snap-frozen in liquid nitrogen at different time points across five days of growth. Bacterial RNA was extracted using NucleoSpin RNA Isolation kit (Macherey-Nagel, Germany) following manufacturer's instructions. Reverse transcription of total extracted RNA into cDNA has been performed using Superscript II (Invitrogen, USA) according to manufacturer's instructions. Quantitative PCR was performed in a total of 20 μl on a Biorad CFX96 apparatus (Biorad) using SYBR GreenER qPCR Supermix (Invitrogen, USA). The reaction mixture consisted of 0.5 μl of each primer (10 μM each), 12,5 μl of SYBR GreenER mix, 10 μl of water and 1,5 μl of template cDNA. The PCR conditions included 1 cycle of initial denaturation at 95°C for 2 min, followed by 45 cycles of 95°C for 10 sec and 60°C for 40 sec. Absolute quantification of 16rRNA was conducted as follows: five 1:10 serial dilutions of the standard sample (100 ng/μl of cDNA extracted from *L. plantarum*^{NIZO2877} culture) were quantified by Real-time PCR using universal 16S primers (forward primer, UniF 5'-GTGSTGCAYGGYTGTCGTCA-3' and reverse primer, UniR 5'-ACGTCRTCCMCACCTTCCTC-3', Table S4) (Packey et al., 2013). Each dilution has been tested in triplicate. Melting curves of the detected amplicons were analysed to ensure specific and unique amplification. Standard curves were generated plotting threshold cycle (Ct) values against the log of the standard sample amount. Based on the data obtained from the standard curve, the Ct values of the Niche and Diet samples have been used to obtain the log of their 16SrRNA concentration at each time point. The 16S rRNA values during exponential phase have been used to infer the bacterial generation time following the equation reported by Widdel et al. (Widdel, 2007).

Larval Size Measurements

Larvae ($n \geq 120$) were collected 7 days after inoculation, washed in distilled water, transferred on a microscopy slide, killed with a short heat treatment (5s at 90°C) and mounted in 80% glycerol/PBS. The larvae were imaged under a Leica steromicroscope M205FA and larval longitudinal size (length) was measured using ImageJ software (Schneider et al., 2012).

Developmental Timing

Developmental timing of *Drosophila* associated with different bacteria was quantified by counting the number of pupae emerging over time. These results are represented as the day at which 50% of the whole population pupariated (D50). Each graph represents the mean of 3 biological replicates, including at least 30 individuals each.

Genome Sequencing

Genomic DNA of single bacterial strains was extracted from cultures grown to stationary phase in MRS broth using the UltraClean Microbial DNA isolation kit (Mo Bio, Qiagen, USA). For all single strain sequencing genomic libraries were prepared following Ion Xpress Plus gDNA Fragment Library construction protocol for 400bp reads. The strains were sequenced using the Ion Torrent PGM platform. The DNA library construction and sequencing was performed on the IGFL sequencing platform (Lyon, France). For community sequencing, the lysate obtained from the crushed adult flies was plated out on MRS agar and cultured at 37°C for 48h. A mixture of >1000 clones was used to extract the genomic DNA using the UltraClean Microbial DNA isolation kit (Mo Bio, Qiagen, USA). The DNA library construction and sequencing was carried out by the EMBL Genomics Core Facilities (Heidelberg, Germany). Each sample was pair-end sequenced on an Illumina MiSeq Benchtop Sequencer. Standard procedures produced data sets of Illumina paired-end 250 bp read pairs. The mean coverage per sample was 99x. Processed reads were aligned and analysed against their respective reference strain (ancestor) genome to identify mutations, using default settings in breseq (Deatherage and Barrick, 2014) for single isolate genomes and using the '-polymorphism' setting for libraries constructed for bacterial communities. In order to discard false positive mutations, we generated an R script (RStudio Team, 2015) which used the breseq file as input to derive the real percentage of reads affected by mutation. Candidate mutations were verified by targeted PCR amplification and Sanger sequencing. These data were used to build a decision tree in order to correlate the frequency of reads affected by a given mutation (%) and its real presence in the genome (obtained by Sanger sequencing). This allowed us to establish that the real mutation calls were those predicted by frequency values higher than 83,5%. All candidate mutations were subsequently confirmed by targeted PCR amplification and Sanger sequencing by using specific primers (Table S2). Non-synonymous mutations in genes belonging to pathway of interest were analysed with PROVEAN (Protein Variation Effect Analyzer) (Choi et al., 2012) to predict the functional impact of the genetic variant. The score threshold used was set to -2.5.

L. plantarum Genomic Editing with CRISPR-Cas9

Plasmid Generation

The Cas9 targeting plasmid was assembled by first amplifying the pMSP3545 plasmid backbone (Table S5) and the Cas9+tracrRNA from pCas9 with oligos oRL1-oRL4 (Table S6). These PCR fragments were stitched together using Gibson assembly (Gibson et al., 2009) (NEB CN#E2611S) and transformed into *E. coli* NovaBlue cells. This synthesized plasmid was named p3545Cas9 and served as the non-targeting control vector used for subsequent transformation assays (Figure S3A). The targeting sgRNA was synthesized as a repeat-spacer-repeat array under a constitutive *Lactobacillus* promoter (P_{pgm})(Duong et al., 2011). This array (gBlock 1) was amplified with oligos oRL5-oRL6. The p3545Cas9 plasmid was digested with XbaI and PstI and the two fragments were inserted by Gibson assembly. This step created the pCas9+RSR plasmid. To insert a spacer to specifically targeting the mutated *ackA* gene, oligos oRL13-14 were phosphorylated with T4 PNK (NEB CN#M0201S), annealed, and ligated into the pCas9+RSR plasmid after digestion with PvuI and NotI. The spacer was designed so the CCT triplet (absent in Fly.G2.1.8) was inserted within the seed portion of the target sequence (Figure S3B).

The repair template plasmid was assembled by amplifying the $Lp^{NIZO2877}$ *ackA* gene with oRL7-oRL8, digesting this PCR product and the pJP005 plasmid with SpeI and SacI, and ligating them together with T4 DNA ligase (NEB CN#M0202S). 300ng of backbone was ligated with 422 ng of insert, ethanol precipitated, and entirely transformed into *L. plantarum* WCFS1. The center of the amplified region contained the CCT triplet absent in Fly.G2.1.8 *ackA* gene (Table S5). Colony PCR was used to screen for successful clones using oligos oRL09-10. Colony PCR was performed by picking a single colony into 20 μL of 20 mM NaOH and incubating at 98°C for 20 minutes. These tubes were then microwaved for 1 minute with the cap open, and 5 μL of this mixture was added to the PCR mix and amplified with PFU polymerase isolated from *Pyrococcus furiosus* (gift from R.M. Kelly).

Growth Conditions and Electroporation

All *L. plantarum* strains were grown on MRS liquid broth and MRS agar and incubated at 37°C. Antibiotic concentrations for *L. plantarum* were as follows: rifampicin (25μg/mL), chloramphenicol (10μg/mL), and erythromycin (10μg/mL). All *E. coli* strains were cultured in LB medium (10 g/L NaCl, 5 g/L yeast extract, 10 g/L tryptone) while being shaken at 250 RPM at 37°C. Plasmids were maintained at the following antibiotic concentrations: erythromycin (50μg/mL), chloramphenicol (34μg/mL), and ampicillin (50μg/mL). Electroporation of *L. plantarum* was adapted from numerous protocols (Spath et al., 2012; Teresa Alegre et al., 2004; Thompson and Collins, 1996). To prepare cells for electroporation, 1 mL of overnight culture of *L. plantarum* was back-diluted into 25 mL of MRS liquid broth containing 0.41 M glycine and any necessary antibiotics. This was performed in sealed 50-mL falcon tubes to prevent aeration of the bacteria. These tubes were cultured at 37°C and 250 RPM for ~3 hours, or until the OD_{600} was approximately 0.85. Cells were centrifuged at 5,000 RPM for 10 minutes at 4°C. The pelleted cells were kept on ice, then washed twice with ice-cold 10 mM $MgCl_2$ followed by a wash in SacGly (10% glycerol with 0.5 M sucrose). The washed cell pellet was then re-suspended in 1mL of SacGly and centrifuged at 20,000 RPM for 1 minute and the final pellet was re-suspended in 500 μL of SacGly. For all transformations, 60μL of this suspension was added to a 1-mm gap cuvette and transformed at 1.8kV, 200Ω resistance, and 25 μF capacitance. Following electroporation, cells were resuspended in 1 mL of MRS broth and transferred to a sterile tube and incubated at 37°C without shaking for 3 hours. 250 μL of the recovered cells was then plated on MRS agar with appropriate antibiotics. Any dilutions prior to plating was done in MRS media.

CRISPR-Cas9 Repair-Template Editing

To perform the genomic edits, the *ackA*_pJP005 plasmid was transferred from WCFS1 into Fly.G2.1.8 and prepared for electroporation using the previously described conditions, selecting for the ackA_pJP005 plasmid with chloramphenicol. Electrocompetent cells were then transformed with 5μg of p3545_Cas9 or pCas+RSR isolated from a methylation-free *E. coli* strain (EC135) (Zhang et al., 2012). Transformation efficiencies of the Cas9 plasmid into Fly.G2.1.8 were vastly improved in the presence of the homologous-recombination template (Figure S3C). After transformation, cells were plated on solid MRS media supplemented with erythromycin to only select for the CRISPR-Cas9 plasmid. The *ackA* gene from the resultant colonies was amplified with oRL11-12 and subjected to Sanger sequencing (Figure S3D). Seven colonies harbored the inserted CCT triplet ($FlyG2.1.8^{Rev}$, Figure S3D), while two colonies were unedited and one colony did not yield an amplification product. The lack of editing in the two colonies may be due to mutation of Cas9 or the spacer as reported previously (Gomaa et al., 2014). To clear the plasmids from the edited strains, colonies were subjected to multiple rounds of non-selective outgrowths in liquid medium (Figure S3E). After each round of non-selective outgrowths, edited *Lactobacillus* cultures were struck out on non-selective plates and colonies were then struck out on selective chloramphenicol or erythromycin plates to determine if plasmids were successfully cleared. Once colonies were no longer able to grow on selective medium, antibiotic susceptibility was tested in liquid culture and strains were analyzed *in vivo*. Two isolates from separate colonies were subjected to whole-genome sequencing (using an Ion torrent PGM platform) to confirm the insertion of the CCT triplet in *ackA* and the absence of any mutations elsewhere in the genome (Table S1).

Bacterial Competitions Tests

Competition assays between $Lp^{NIZO2877}$ (ancestor) and FlyG2.1.8 (evolved beneficial strain) have been tested in *Drosophila* Niche and Diet. The competitions were performed at a ratio of 1:1, over 3 days of co-colonization, following the same inoculation procedure described for the Diet evolution experiment. A total of 10^4 CFUs has been used as inoculum. During the three days of co-colonization, the samples have been crushed using the Precellys 24 tissue homogenizer (Bertin Technologies, France) and 0.75/1 mm glass beads in 500 μl of PBS. The lysate has been plated out on MRS agar and cultured at 37°C for 48h. 10000 colonies have been collected and bacterial DNA was extracted using the UltraClean Microbial DNA isolation kit (Mo Bio, Qiagen, USA). A specific Real-time PCR assay

has been developed to distinguish and quantify the presence of *Lp*^{NIZO2877} (ancestor) and *FlyG2.1.8* (evolved beneficial strain). Specific primer pairs have been designed on the *ackA* gene sequence using Geneious 9 (Kearse et al., 2012). Quantitative PCR was performed in a total of 20 μl on a Biorad CFX96 apparatus (Biorad) using SYBR GreenER qPCR Supermix (Invitrogen, USA), bacterial DNA and the gene specific primer sets (forward primer *Lp*^{NIZO2877}-specific: ackA_NIZO2877_F_RT; forward primer FlyG2.1.8-specific: ackA_FlyG2_F_RT; and common reverse primer: ackA_R_RT; Table S4). The reaction mixture consisted of 0.5 μl of each primer (10 μM each), 12,5 μl of SYBR GreenER mix, 10 μl of water and 1,5 μl of template cDNA. Each sample has been tested in triplicate. The PCR conditions included 1 cycle of initial denaturation at 95°C for 2 min, followed by 45 cycles of 95°C for 10 sec and 60°C for 40 sec. Melting curves of the detected amplicons were analysed to ensure specific and unique amplification. PCR efficiency was calculated for each primer set using six serial dilutions of DNA starting from 2 ng/μl. Relative quantification of each bacterial strain has been performed using 16SrRNA as reference gene (UniF-UniR primers, Table S4).

Metabolite Profiling

Microtubes containing axenic poor nutrient diet were inoculated with bacterial suspension (10^3 CFU/ml) or with PBS and incubated for 3 days at 25°C. Microtubes were then snap-frozen in liquid nitrogen and stored at -80°C before sending to Metabolon Inc. (www.metabolon.com). Five biological replicates per condition were generated. Samples were then extracted and prepared for analysis using Metabolon's standard solvent extraction method. Each resulting extract was divided into five fractions: two for analysis by two separate reverse phase/Ultrahigh Performance Liquid Chromatography-Tandem Mass Spectroscopy (RP/UPLC-MS/MS) methods with positive ion mode electrospray ionization (ESI), one for analysis by RP/UPLC-MS/MS with negative ion mode ESI, one for analysis by HILIC/UPLC-MS/MS with negative ion mode ESI, and one sample was reserved for backup. Compounds were identified by comparison to library entries of purified standards or recurrent unknown entities.

Information Related to Experimental Design

Blinding was not used in the course of our study. No data or subjects were excluded from our analyses.

QUANTIFICATION AND STATISTICAL ANALYSIS

Data representation and statistical analysis were performed using Graphpad PRISM 6 software (www.graphpad.com). For metabolite profiling, we performed Student's t test with Welch correction to determine if differences in metabolites levels between two conditions are statistically significant. For all the other pairwise comparisons throughout our study, we performed Mann Whitney's test. We applied Kruskal Wallis test to perform statistical analyses of multiple (n>2) conditions. No particular method was used to determine whether the data met assumptions of the statistical approach.

DATA AND SOFTWARE AVAILABILITY

The accession number for FlyG2.1.8 genome reported in this paper is NCBI: PEBE00000000. The accession number for FlyG3.1.8 genome reported in this paper is NCBI: PEGI00000000. The accession number for FlyG7.1.6 genome reported in this paper is NCBI: PEGJ00000000. The accession number for FlyG8.1.1 genome reported in this paper is NCBI: PEGK00000000. The accession number for FlyG8.1.2 genome reported in this paper is NCBI: PEGL00000000. The accession number for FlyG9.1.4 genome reported in this paper is NCBI: PEGM00000000. The accession number for FlyG10.1.5 genome reported in this paper is NCBI: PEGN00000000. The accession number for FlyG10.1.9 genome reported in this paper is NCBI: PEGO00000000. The accession number for FlyG11.1.2 genome reported in this paper is NCBI: PEGP00000000. The accession number for FlyG11.1.6 genome reported in this paper is NCBI: PEGQ00000000. The accession number for FlyG20.1.4 genome reported in this paper is NCBI: PEGR00000000. The accession number for FlyG9.2.5 genome reported in this paper is NCBI: PEGS00000000. The accession number for FlyG11.2.6 genome reported in this paper is NCBI: PEGT00000000. The accession number for FlyG20.2.6 genome reported in this paper is NCBI: PEGU00000000. The accession number for DietG20.1.2 genome reported in this paper is NCBI: PEGV00000000. The accession number for DietG20.2.2 genome reported in this paper is NCBI: PEGW00000000.

Cell Host & Microbe, Volume *24*

Supplemental Information

Bacterial Adaptation to the Host's Diet Is a Key Evolutionary Force Shaping *Drosophila-Lactobacillus* Symbiosis

Maria Elena Martino, Pauline Joncour, Ryan Leenay, Hugo Gervais, Malay Shah, Sandrine Hughes, Benjamin Gillet, Chase Beisel, and François Leulier

Supplemental figure titles and legends

-

Bacterial adaptation to diet is a key evolutionary force shaping *Drosophila-Lactobacillus* symbiosis

Maria Elena Martino,[1*] Pauline Joncour,[1] Ryan Leenay,[2] Hugo Gervais,[1] Malay Shah,[2] Sandrine Hughes,[1] Benjamin Gillet,[1] Chase Beisel,[2,3] and François Leulier [1,4*]

[1]Institut de Génomique Fonctionnelle de Lyon, Université de Lyon, Ecole Normale Supérieure de Lyon, Centre National de la Recherche Scientifique, Université Claude Bernard Lyon 1, Unité Mixte de Recherche 5242, 69364 Lyon, Cedex 07, France

[2]North Carolina State University, Department of Chemical and Biomolecular Engineering, Raleigh, NC 27695, United States

[3]Helmholtz Institute for RNA-based Infection Research, Josef-Schneider-Str. 2 / D15, D-97080 Würzburg, Germany

[4]Lead Contact

*Correspondence: maria-elena.martino@ens-lyon.fr, francois.leulier@ens-lyon.fr

A

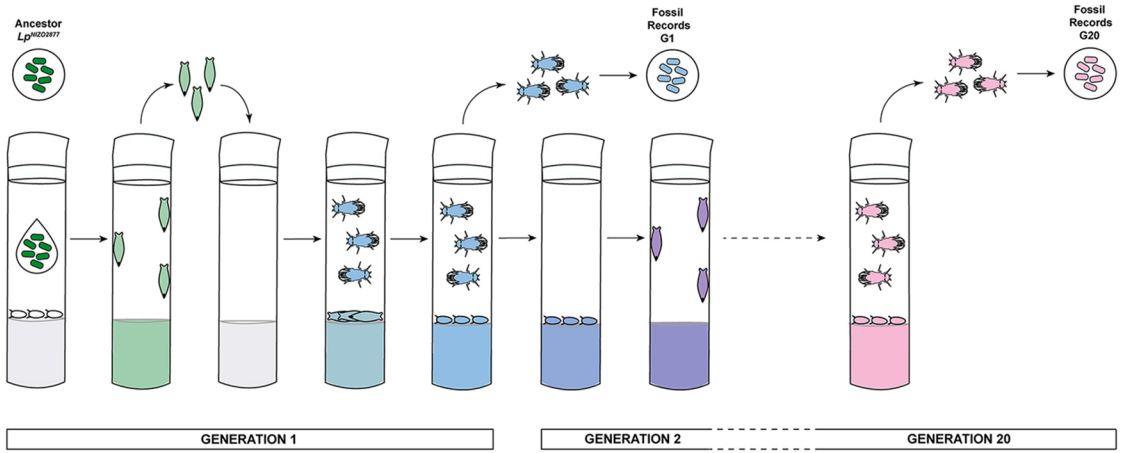
Ancestor
Lp NIZO2877
Fossil Records G1
Fossil Records G20
GENERATION 1
GENERATION 2
GENERATION 20

B

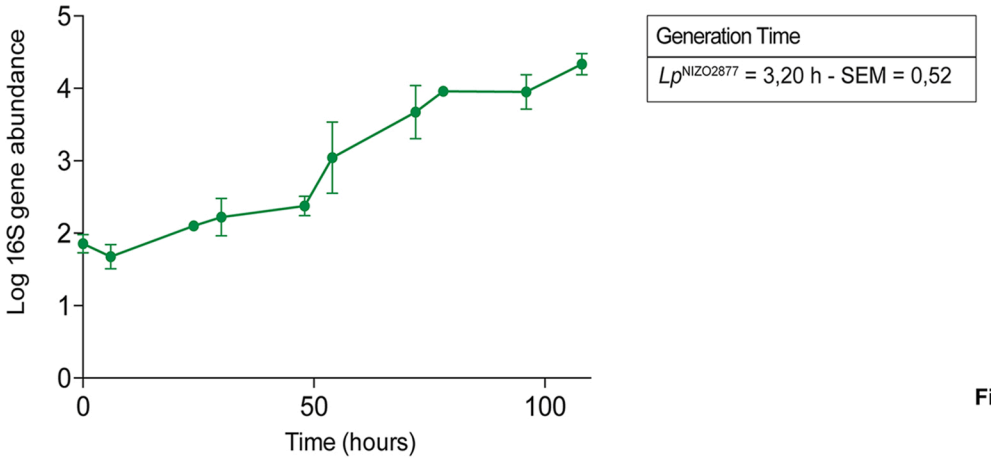
Log 16S gene abundance
Time (hours)
0
1
2
3
4
5
0
50
100
Generation Time
Lp NIZO2877 = 3,20 h - SEM = 0,52

Figure S1

Supplemental Figure 1 (related to Fig. 1): Rationale and schematic representation of the experimental setup for studying *L. plantarum* adaptive evolution (AE) with *Drosophila melanogaster*.

(A) The ancestor strain (*Lp*^{NIZO2877}) was added to 40 germ-free (GF) *Drosophila* embryos at the beginning of the first *Drosophila* generation (Generation 1). The first 15 emerging pupae were transferred to a new sterile poor nutrient diet. This allowed the bacteria associated with the pupae to propagate and colonize the new environment. The 15 adults emerged from the 15 transferred pupae, mated and females laid eggs that became the founders of the following fly generation (Generation 2). Once the eggs were laid, the adults were collected and homogenized to isolate the evolved bacteria they carry (fossil records from generation 1). Generation 2 followed the same experimental cycle as Generation 1, with the exception that no further inoculation of the ancestor strain *L. plantarum*^{NIZO2877} has been performed. Evolving bacteria were propagated through the transfer of the pupae during each generation. The experimental evolution lasted 20 *Drosophila* generations (313 days). Colour shading represents the evolution of the bacterial population during the experiment.

(B) 16S rRNA kinetics of *Lp*^{NIZO2877} in *Drosophila* Niche (*Drosophila* + Diet). The 16S rRNA gene quantification is shown in logarithmic scale. The mean generation time (h, hours) of *Lp*^{NIZO2877} in *Drosophila* niche ± the standard error of the mean (SEM) are reported on the graph (see Methods).

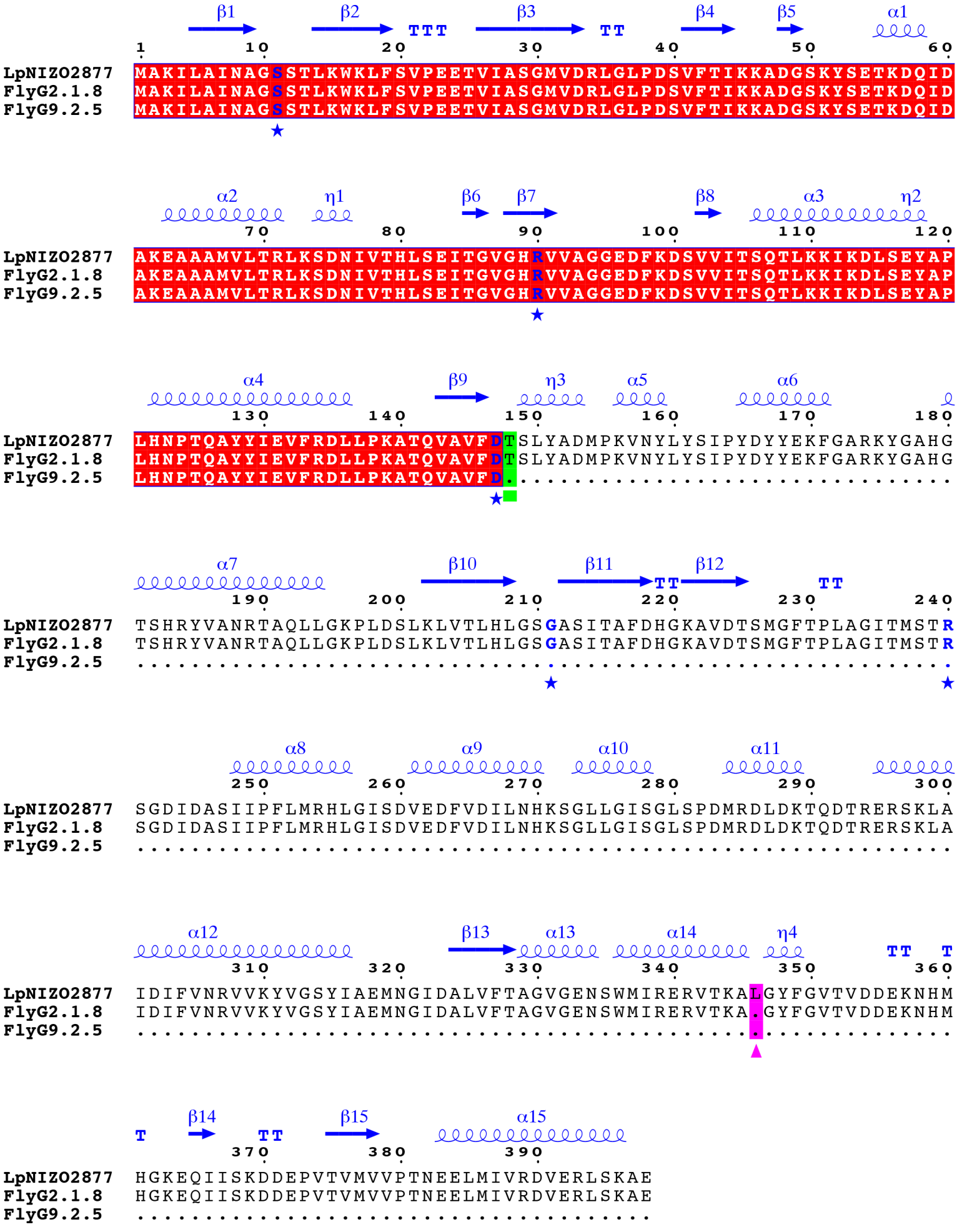
β1 β2 TTT β3 TT β4 β5 α1
1 10 20 30 40 50 60
LpNIZO2877 MAKILAINAGSSTLKWKLFSVPEETVIASGMVDRLGLPDSVFTIKKADGSKYSETKDQID
FlyG2.1.8 MAKILAINAGSSTLKWKLFSVPEETVIASGMVDRLGLPDSVFTIKKADGSKYSETKDQID
FlyG9.2.5 MAKILAINAGSSTLKWKLFSVPEETVIASGMVDRLGLPDSVFTIKKADGSKYSETKDQID
α2 η1 β6 β7 β8 α3 η2
70 80 90 100 110 120
LpNIZO2877 AKEAAAMVLTRLKSDNIVTHLSEITGVGHRVVAGGEDFKDSVVITSQTLKKIKDLSEYAP
FlyG2.1.8 AKEAAAMVLTRLKSDNIVTHLSEITGVGHRVVAGGEDFKDSVVITSQTLKKIKDLSEYAP
FlyG9.2.5 AKEAAAMVLTRLKSDNIVTHLSEITGVGHRVVAGGEDFKDSVVITSQTLKKIKDLSEYAP
α4 β9 η3 α5 α6
130 140 150 160 170 180
LpNIZO2877 LHNPTQAYYIEVFRDLLPKATQVAVFDTSLYADMPKVNYLYSIPYDYYEKFGARKYGAHG
FlyG2.1.8 LHNPTQAYYIEVFRDLLPKATQVAVFDTSLYADMPKVNYLYSIPYDYYEKFGARKYGAHG
FlyG9.2.5 LHNPTQAYYIEVFRDLLPKATQVAVFD.
α7 β10 β11 TT β12 TT
190 200 210 220 230 240
LpNIZO2877 TSHRYVANRTAQLLGKPLDSLKLVTLHLGSGASITAFDHGKAVDTSMGFTPLAGITMSTR
FlyG2.1.8 TSHRYVANRTAQLLGKPLDSLKLVTLHLGSGASITAFDHGKAVDTSMGFTPLAGITMSTR
FlyG9.2.5 .
α8 α9 α10 α11
250 260 270 280 290 300
LpNIZO2877 SGDIDASIIPFLMRHLGISDVEDFVDILNHKSGLLGISGLSPDMRDLDKTQDTRERSKLA
FlyG2.1.8 SGDIDASIIPFLMRHLGISDVEDFVDILNHKSGLLGISGLSPDMRDLDKTQDTRERSKLA
FlyG9.2.5 .
α12 β13 α13 α14 η4 TT T
310 320 330 340 350 360
LpNIZO2877 IDIFVNRVVKYVGSYIAEMNGIDALVFTAGVGENSWMIRERVTKALGYFGVTVDDEKNHM
FlyG2.1.8 IDIFVNRVVKYVGSYIAEMNGIDALVFTAGVGENSWMIRERVTKA.GYFGVTVDDEKNHM
FlyG9.2.5 .
T β14 TT β15 α15
370 380 390
LpNIZO2877 HGKEQIISKDDEPVTVMVVPTNEELMIVRDVERLSKAE
FlyG2.1.8 HGKEQIISKDDEPVTVMVVPTNEELMIVRDVERLSKAE
FlyG9.2.5 .

Figure S2

Supplemental Figure 2 (related to Fig. 2): Sequence/structural analysis of *Lp*^{NIZO2877} Acetate kinase A (AckA) protein aligned against the AckA of *Lp*^{NIZO2877}-derived strains (FlyG2.1.8, FlyG9.2.5) evolved in *Drosophila* niche. The secondary structure of the protein is indicated in blue above the sequence alignment. Catalytic residues of the predicted active site are shown in bold blue characters. The mutation sites are highlighted in pink and green for FlyG2.1.8 and FlyG9.2.5 strains respectively. The alignment was performed using Clustal Omega and drawn with ESPript.

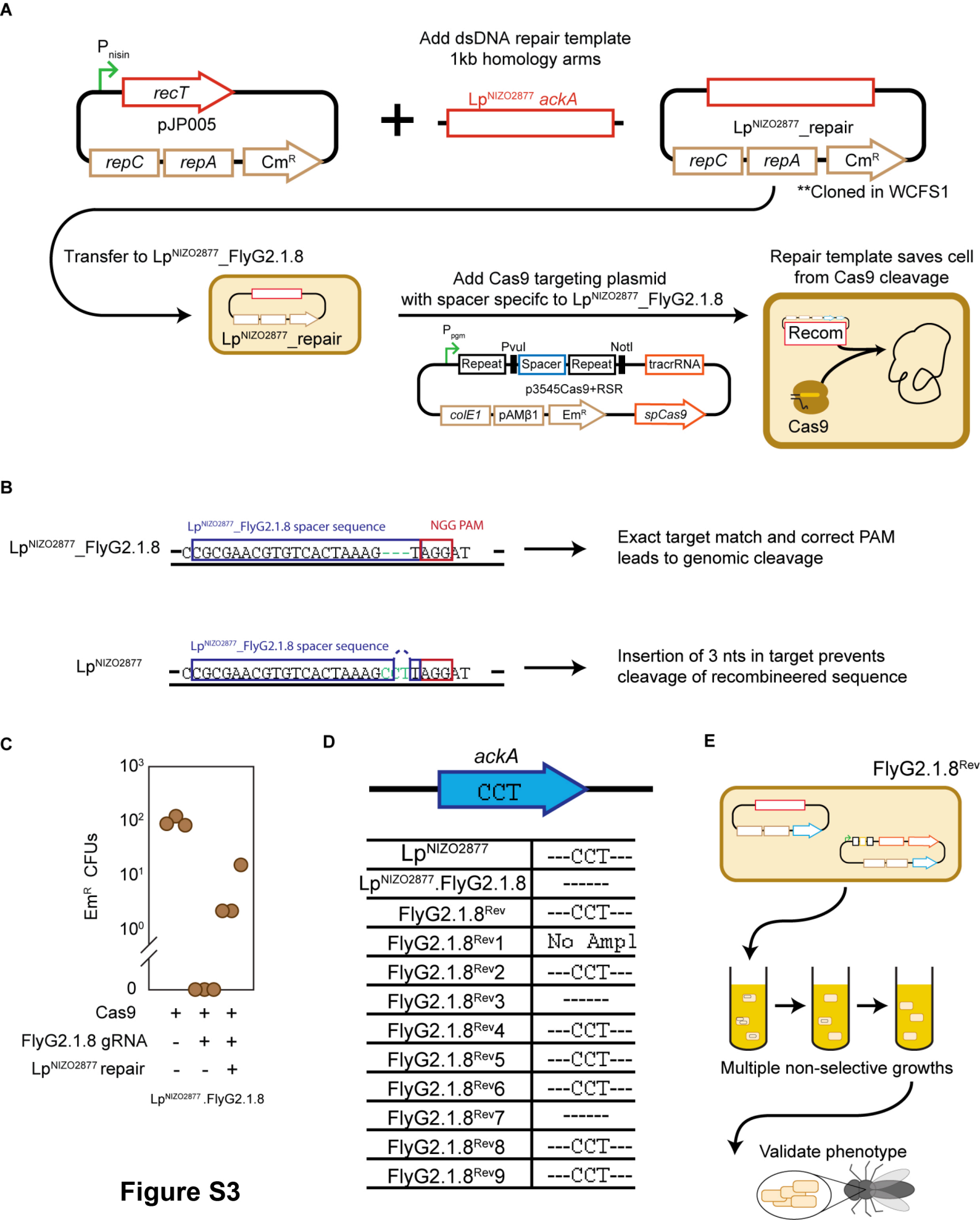
A
P nisin
recT
pJP005
repC
repA
Cm R
Add dsDNA repair template
1kb homology arms
Lp NIZO2877 ackA
Lp NIZO2877 _repair
repC
repA
Cm R
**Cloned in WCFS1
Transfer to Lp NIZO2877 _FlyG2.1.8
Lp NIZO2877 _repair
Add Cas9 targeting plasmid
with spacer specifc to Lp NIZO2877 _FlyG2.1.8
P pgm
PvuI
NotI
Repeat
Spacer
Repeat
tracrRNA
p3545Cas9+RSR
colE1
pAMβ1
Em R
spCas9
Repair template saves cell
from Cas9 cleavage
Recom
Cas9
B
Lp NIZO2877 _FlyG2.1.8
Lp NIZO2877 _FlyG2.1.8 spacer sequence
NGG PAM
CCGCGAACGTGTCACTAAAG---TAGGAT
Exact target match and correct PAM
leads to genomic cleavage
Lp NIZO2877
Lp NIZO2877 _FlyG2.1.8 spacer sequence
CCGCGAACGTGTCACTAAAGCCTTAGGAT
Insertion of 3 nts in target prevents
cleavage of recombineered sequence
C
Em R CFUs
10 3
10 2
10 1
10 0
0
Cas9 + + +
FlyG2.1.8 gRNA - + +
Lp NIZO2877 repair - - +
Lp NIZO2877 .FlyG2.1.8
D
ackA
CCT
Lp NIZO2877 ---CCT---
Lp NIZO2877 .FlyG2.1.8 ------
FlyG2.1.8 Rev ---CCT---
FlyG2.1.8 Rev 1 No Ampl
FlyG2.1.8 Rev 2 ---CCT---
FlyG2.1.8 Rev 3 ------
FlyG2.1.8 Rev 4 ---CCT---
FlyG2.1.8 Rev 5 ---CCT---
FlyG2.1.8 Rev 6 ---CCT---
FlyG2.1.8 Rev 7 ------
FlyG2.1.8 Rev 8 ---CCT---
FlyG2.1.8 Rev 9 ---CCT---
E
FlyG2.1.8 Rev
Multiple non-selective growths
Validate phenotype

Figure S3

Supplemental Figure 3 (related to Fig. 3): CRISPR/Cas9 genome editing in *Lactobacillus plantarum* with a dsDNA repair template.

(A) Construction of the repair template plasmid containing the dsDNA template. Following successful construct generation, cells containing the repair plasmid were transformed with the self-targeting Cas9 plasmid, thereby killing any cells that did not incorporate the repair template into the genome.

(B) Spacer design for targeting *ackA* in *Lp*^{NIZO2877}_FlyG2.1.8. The spacer will only successfully cleave *Lp*^{NIZO2877}_FlyG2.1.8, while allowing any edited survivors to evade cleavage due to a spacer mis-match and presence of a non-PAM.

(C) Transformation results after Cas9 self-targeting with the repair template plasmid. Presence of the repair template allowed for a total of 15 survivors clones to Cas9 killing.

(D) *ackA* locus sequencing results for 10 of the survivors. Two survivors contained the un-edited *ackA* gene in *Lp*^{NIZO2877}.FlyG2.1.8, and one did not yield a PCR product (No Ampl.). Seven colonies contained the edited *ackA* sequence.

(E) Plasmid removal after editing. Successfully edited cells were passaged multiple times through non-selective media to remove the genome editing plasmids. After validation of plasmid removal, strains had their genomes sequenced and were analyzed for *in vivo* validation.

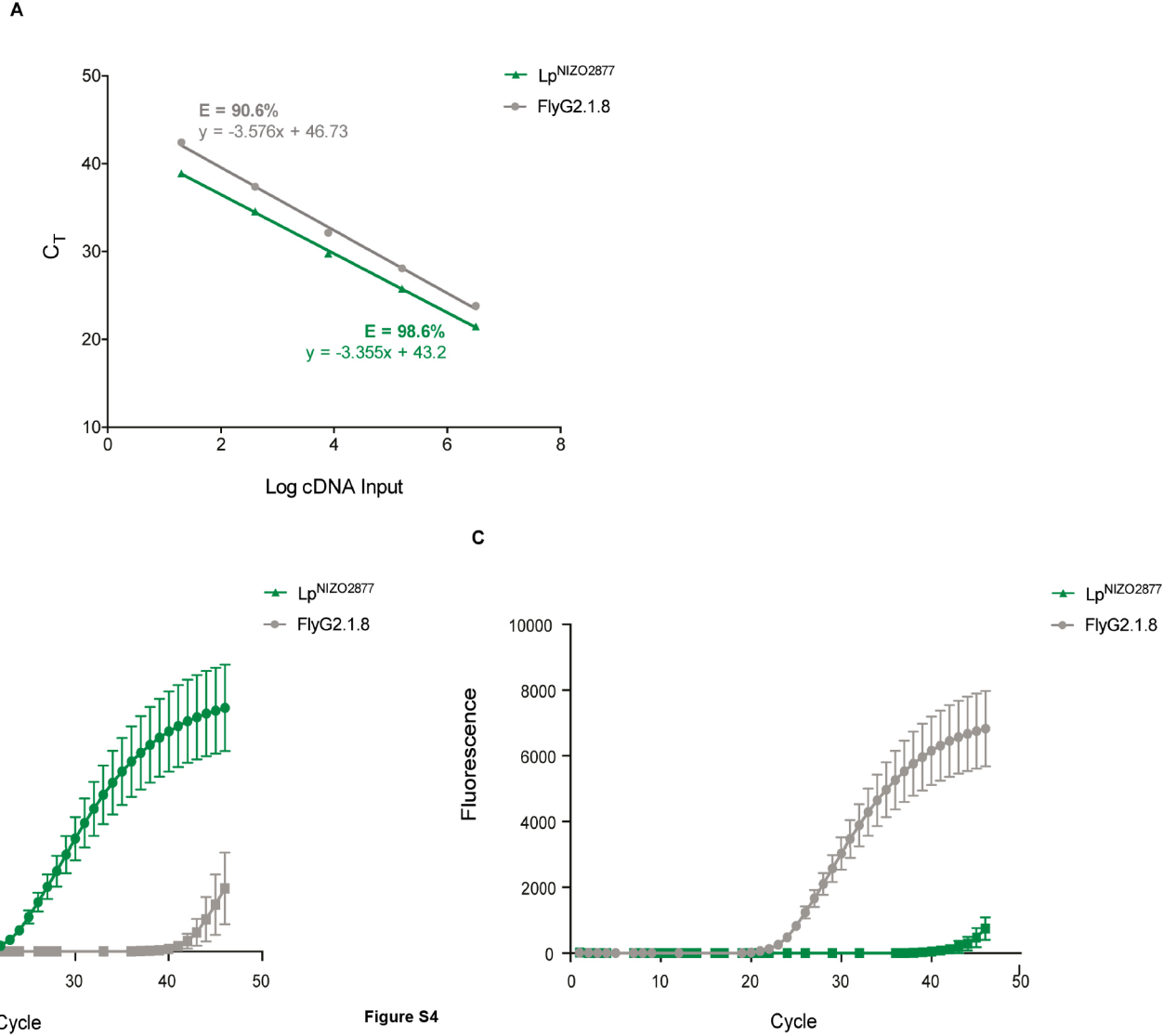
A
E = 90.6%
y = -3.576x + 46.73
E = 98.6%
y = -3.355x + 43.2
LpNIZO2877
FlyG2.1.8
CT
Log cDNA Input
B
Fluorescence
Cycle
C
Fluorescence
Cycle

Figure S4

Supplemental Figure 4 (related to Fig. 4): Development of two Real-Time PCR assays for the discrimination and quantification of *Lp*^{NIZO2877} and *Lp*^{NIZO2877}–evolved strain FlyG2.1.8.

(A) Real-time PCR standard curves obtained from the amplification of *Lp*^{NIZO2877} (green) and FlyG2.1.8 (grey) strains. The graph shows the interpolated standard curves using determined threshold cycles (C_T) values and known template numbers for five standard samples. All points represent the mean of triplicate PCR amplifications. The respective efficiency values and curve equations are reported on the graph.

(B, C) Fluorescence amplification plots obtained from the amplification of *Lp*^{NIZO2877} and FlyG2.1.8 strains using *Lp*^{NIZO2877}-specific (B) and FlyG2.1.8 specific (C) Real-time assays.

A

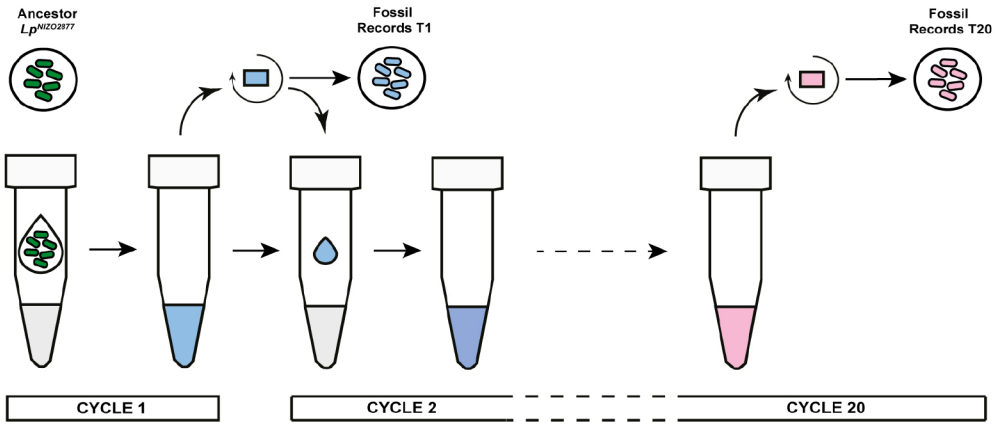
Ancestor
Lp^NIZO2877
Fossil
Records T1
Fossil
Records T20
CYCLE 1
CYCLE 2
CYCLE 20

B

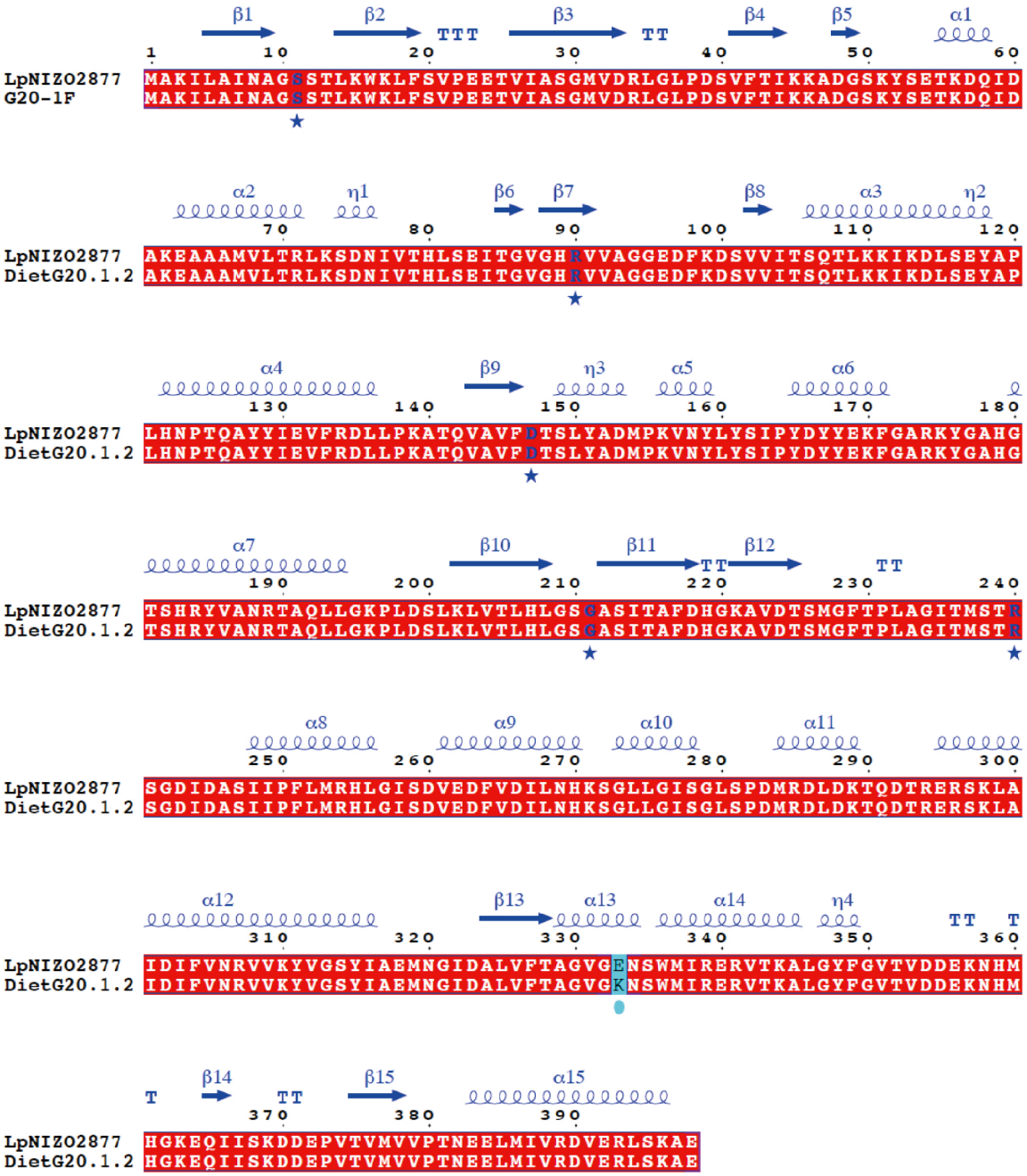
LpNIZO2877
G20-1F
LpNIZO2877
DietG20.1.2
LpNIZO2877
DietG20.1.2
LpNIZO2877
DietG20.1.2
LpNIZO2877
DietG20.1.2
LpNIZO2877
DietG20.1.2
LpNIZO2877
DietG20.1.2

Figure S5

Supplemental Figure 5 (related to Fig. 5): *L. plantarum* adaptive evolution (AE) in *Drosophila* diet without *Drosophila melanogaster*.

(A) Rationale and schematic representation of the experimental setup. The ancestor ($Lp^{NIZO2877}$) was added to sterile poor nutrient diet (Cycle 1). As soon as the microbial load reached the same value found on the 15 pupae used for propagating the bacterial population in the Niche adaptive evolution setup (10^7 CFU/mL of diet; Figure S1A), part of the medium was crushed and transferred to a new sterile poor nutrient diet. Fossil records were isolated from the crushed medium at the end of each cycle. Cycle 2 followed the same experimental course as Cycle 1. *L. plantarum* experimental evolution on *Drosophila* diet lasted 20 cycles. Colour shading represents the evolution of the bacterial population during the experiment.

(B) Sequence/structural analysis of $Lp^{NIZO2877}$ AckA protein aligned against AckA from $Lp^{NIZO2877}$-derived strain (DietG20.1.2) evolved in Drosophila diet. The secondary structure of the acetate kinase A protein is indicated in blue above the sequence alignment. The key catalytic residues of the predicted active sites are shown in bold blue characters. The mutation site is highlighted in cyan. The alignment was performed using Clustal Omega and drawn with ESPript.

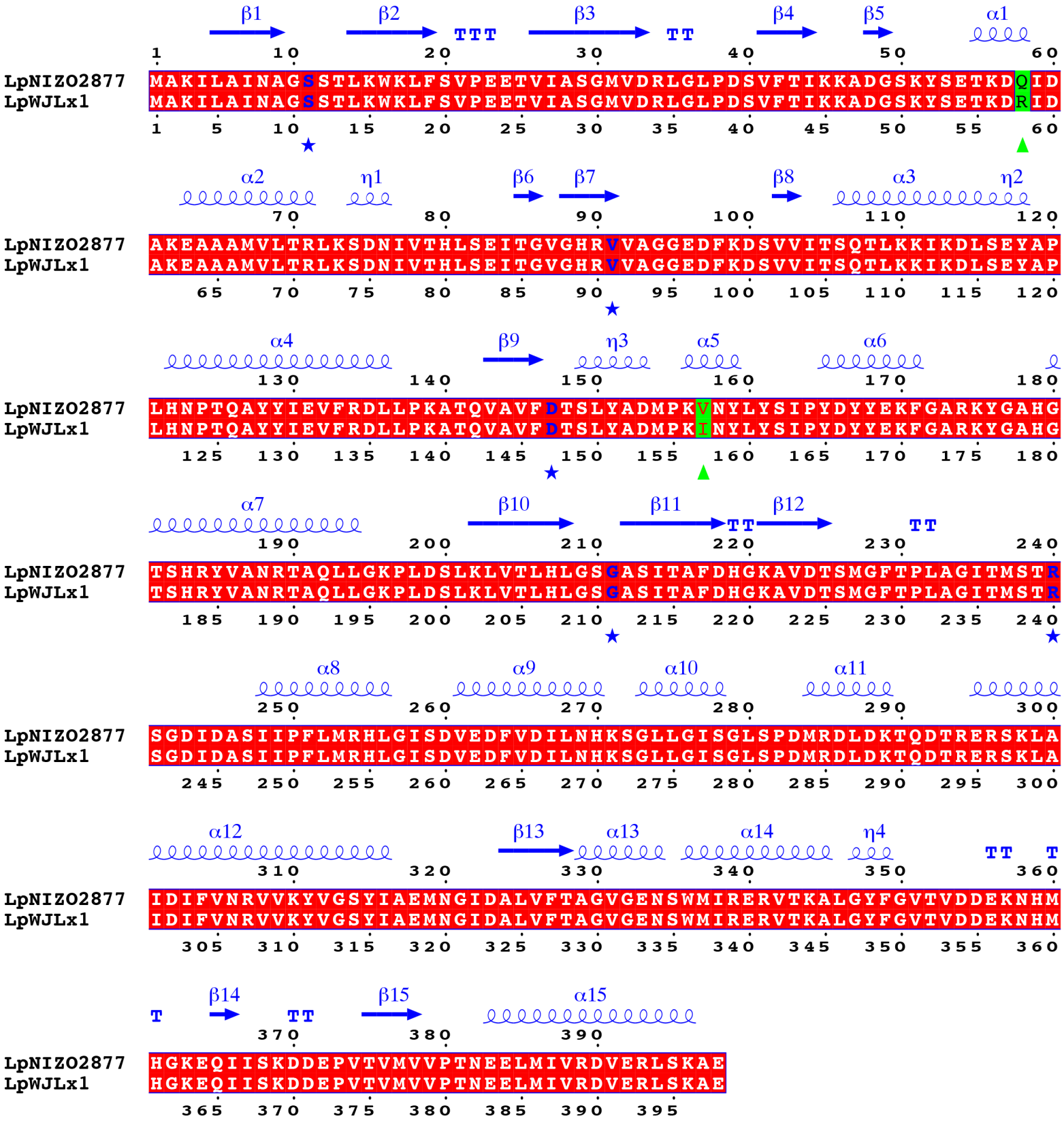
β1 β2 TTT β3 TT β4 β5 α1
1 10 20 30 40 50 60
LpNIZO2877 MAKILAINAGSSTLKWKLFSVPEETVIASGMVDRLGLPDSVFTIKKADGSKYSETKDQID
LpWJLx1 MAKILAINAGSSTLKWKLFSVPEETVIASGMVDRLGLPDSVFTIKKADGSKYSETKDRID
1 5 10 15 20 25 30 35 40 45 50 55 60
α2 η1 β6 β7 β8 α3 η2
70 80 90 100 110 120
LpNIZO2877 AKEAAAMVLTRLKSDNIVTHLSEITGVGHRVVAGGEDFKDSVVITSQTLKKIKDLSEYAP
LpWJLx1 AKEAAAMVLTRLKSDNIVTHLSEITGVGHRVVAGGEDFKDSVVITSQTLKKIKDLSEYAP
65 70 75 80 85 90 95 100 105 110 115 120
α4 β9 η3 α5 α6
130 140 150 160 170 180
LpNIZO2877 LHNPTQAYYIEVFRDLLPKATQVAVFDTSLYADMPKVNYLYSIPYDYYEKFGARKYGAHG
LpWJLx1 LHNPTQAYYIEVFRDLLPKATQVAVFDTSLYADMPKINYLYSIPYDYYEKFGARKYGAHG
125 130 135 140 145 150 155 160 165 170 175 180
α7 β10 β11 TT β12 TT
190 200 210 220 230 240
LpNIZO2877 TSHRYVANRTAQLLGKPLDSLKLVTLHLGSGASITAFDHGKAVDTSMGFTPLAGITMSTR
LpWJLx1 TSHRYVANRTAQLLGKPLDSLKLVTLHLGSGASITAFDHGKAVDTSMGFTPLAGITMSTR
185 190 195 200 205 210 215 220 225 230 235 240
α8 α9 α10 α11
250 260 270 280 290 300
LpNIZO2877 SGDIDASIIPFLMRHLGISDVEDFVDILNHKSGLLGISGLSPDMRDLDKTQDTRERSKLA
LpWJLx1 SGDIDASIIPFLMRHLGISDVEDFVDILNHKSGLLGISGLSPDMRDLDKTQDTRERSKLA
245 250 255 260 265 270 275 280 285 290 295 300
α12 β13 α13 α14 η4 TT T
310 320 330 340 350 360
LpNIZO2877 IDIFVNRVVKYVGSYIAEMNGIDALVFTAGVGENSWMIRERVTKALGYFGVTVDDEKNHM
LpWJLx1 IDIFVNRVVKYVGSYIAEMNGIDALVFTAGVGENSWMIRERVTKALGYFGVTVDDEKNHM
305 310 315 320 325 330 335 340 345 350 355 360
T β14 TT β15 α15
370 380 390
LpNIZO2877 HGKEQIISKDDEPVTVMVVPTNEELMIVRDVERLSKAE
LpWJLx1 HGKEQIISKDDEPVTVMVVPTNEELMIVRDVERLSKAE
365 370 375 380 385 390 395

Figure S6

Supplemental Figure 6 (related to Fig. 6): Sequence/structural analysis of *Lp*^{NIZO2877} AckA protein aligned against AckA from *Lp*^{WJL}. The secondary structure of the acetate kinase A protein is indicated in blue above the sequence alignment. The key catalytic residues of the predicted active sites are shown in bold blue characters. The mutation sites are highlighted in green. The alignment was performed using Clustal Omega and drawn with ESPript.

Supplemental tables Titles and Legends

Table S1. Bacterial strains, Related to Figures 1, 2, 3, 5. List of all *L. plantarum* strains used and sequenced in this study.

L. plantarum Strains	Description	Fly/Diet generation of isolation	Replicate	Accession Number	Reference
NIZO2877	Isolated from Vietnamese hotdog	-	-	LKHZ01000000	(Martino et al., 2015a)
WJL	Isolated from Drosophila melanogaster intestine	-	-	LKLZ00000000	(Martino et al., 2015b)
FlyG2.1.8	NIZO2877-evolved strain	2	1	PEBE00000000	This study
FlyG3.1.8	NIZO2877-evolved strain	3	1	PEGI00000000	This study
FlyG7.1.6	NIZO2877-evolved strain	7	1	PEGJ00000000	This study
FlyG8.1.1	NIZO2877-evolved strain	8	1	PEGK00000000	This study
FlyG8.1.2	NIZO2877-evolved strain	8	1	PEGL00000000	This study
FlyG9.1.4	NIZO2877-evolved strain	9	1	PEGM00000000	This study
FlyG10.1.5	NIZO2877-evolved strain	10	1	PEGN00000000	This study
FlyG10.1.9	NIZO2877-evolved strain	10	1	PEGO00000000	This study
FlyG11.1.2	NIZO2877-evolved strain	11	1	PEGP00000000	This study
FlyG11.1.6	NIZO2877-evolved strain	11	1	PEGQ00000000	This study
FlyG20.1.4	NIZO2877-evolved strain	20	1	PEGR00000000	This study
FlyG2.1.8Rev	NIZO2877-evolved strain	-	-	-	This study
FlyG9.2.5	NIZO2877-evolved strain	9	2	PEGS00000000	This study
FlyG11.2.6	NIZO2877-evolved strain	11	2	PEGT00000000	This study
FlyG20.2.6	NIZO2877-evolved strain	20	2	PEGU00000000	This study
DietG20.1.2	NIZO2877-evolved strain	20	1	PEGV00000000	This study
DietG20.2.2	NIZO2877-evolved strain	20	2	PEGW00000000	This study

Table S1

Table S2. Summary of mutations detected across the experimental evolution of *L. plantarum*, related to Figures 1, 2, 3, 5. List of all mutations detected in the *L. plantarum* experimental evolution replicates. §Locus tag refers to *L. plantarum* reference strain WCFS1 (Kleerebezem et al., 2003). nt: nucleotide; WGS: whole genome sequencing; SS: Sanger sequencing. Mutations identified by Sanger sequencing were confirmed from alignments of both forward and reverse reads.

Strain	Evolution Setup	Replicate	Generation/ Transfer	Detected mutation					
				Gene/ Region	Locus Tag[§]	Annotation	Mutation	Position in *Lp*^{NIZO2877}	Method
FlyG2.1.8	Niche	1	2	*ackA*	*lp_03010*	*acetate kinase*	deletion (Δ3)	2571613-5	WGS/SS
FlyG3.1.8	Niche	1	3	*ackA*	*lp_03010*	*acetate kinase*	deletion (Δ3)	2571613-5	WGS/SS
FlyG7.1.6	Niche	1	7	*int1*	-	*intergenic region*	1 nt substitution	504874	WGS/SS
				cheY	*lp_1544*	*two-component system response regulator*	1 nt substitution	1348923	WGS/SS
				ackA	*lp_03010*	*acetate kinase*	deletion (Δ3)	2571613-5	WGS
FlyG8.1.1	Niche	1	8	*int1*	-	*intergenic region*	1 nt substitution	504874	WGS
				cheY	*lp_1544*	*two-component system response regulator*	1 nt substitution	1348923	WGS
				ackA	*lp_03010*	*acetate kinase*	deletion (Δ3)	2571613-5	WGS
FlyG8.1.2	Niche	1	8	*int1*	-	*intergenic region*	1 nt substitution	504874	WGS
				cheY	*lp_1544*	*two-component system response regulator*	1 nt substitution	1348923	WGS
				ackA	*lp_03010*	*acetate kinase*	deletion (Δ3)	2571613-5	WGS
FlyG9.1.4	Niche	1	9	*int1*	-	*intergenic region*	1 nt substitution	504874	WGS
				cheY	*lp_1544*	*two-component system response regulator*	1 nt substitution	1348923	WGS
				adhE	*lp_3662*	*alcohol dehydrogenase/ acetaldehyde dehydrogenase*	1 nt substitution	2268660	WGS/SS
				int2	-	*intergenic region*	1 nt substitution	2456364	WGS/SS
				ackA	*lp_03010*	*acetate kinase*	deletion (Δ3)	2571613-5	WGS
FlyG10.1.5	Niche	1	10	*int1*	-	*intergenic region*	1 nt substitution	504874	WGS
				cheY	*lp_1544*	*two-component system response regulator*	1 nt substitution	1348923	WGS
				ackA	*lp_03010*	*acetate kinase*	deletion (Δ3)	2571613-5	WGS
FlyG10.1.9	Niche	1	10	*int1*	-	*intergenic region*	1 nt substitution	504874	WGS
				cheY	*lp_1544*	*two-component system response regulator*	1 nt substitution	1348923	WGS
				ackA	*lp_03010*	*acetate kinase*	deletion (Δ3)	2571613-5	WGS
FlyG11.1.2	Niche	1	11	*int1*	-	*intergenic region*	1 nt substitution	504874	WGS
				cheY	*lp_1544*	*two-component system response regulator*	1 nt substitution	1348923	WGS
				ackA	*lp_03010*	*acetate kinase*	deletion (Δ3)	2571613-5	WGS
FlyG11.1.6	Niche	1	11	*int1*	-	*intergenic region*	1 nt substitution	504874	WGS
				cheY	*lp_1544*	*two-component system response regulator*	1 nt substitution	1348923	WGS

				-	*lp_0055*	*fumarate reductase, flavoprotein subunit*	1 nt substitution	2347322	WGS/SS
				ackA	*lp_03010*	*acetate kinase*	deletion (Δ3)	2571613-5	WGS
FlyG20.1.4	Niche	1	20	*pstB*	*lp_0749*	*phosphate ABC transporter ATP-binding protein*	1 nt substitution	120791	WGS/SS
				-	*lp_0797*	*exoribonuclease II*	1 nt substitution	177140	WGS/SS
				int1	-	*intergenic region*	1 nt substitution	504874	WGS
				-	*lp_2499*	*ABC transporter ATP-binding protein/permease*	1 nt substitution	947607	WGS
				-	*lp_1258*	*LysR family transcriptional regulator*	1 nt substitution	1105664	WGS/SS
				cheY	*lp_1544*	*two-component system response regulator*	1 nt substitution	1348923	WGS
				int3	-	*intergenic region*	1 nt substitution	1736935	WGS/SS
				ackA	*lp_03010*	*acetate kinase*	deletion (Δ3)	2571613-5	WGS
FlyG9.2.5	Niche	2	9	*int4*	-	*intergenic region*	1 nt substitution	1982853	WGS/SS
				-	*lp_0197*	*cell surface protein precursor, LPXTG-motif cell wall anchor*	deletion (Δ6)	2471707-12	WGS/SS
				ackA	*lp_03010*	*acetate kinase*	1 nt substitution	2571025	WGS/SS
FlyG11.2.6	Niche	2	11	*int4*	-	*intergenic region*	1 nt substitution	1982853	WGS
				-	*lp_0197*	*cell surface protein precursor, LPXTG-motif cell wall anchor*	deletion (Δ6)	2471707-12	WGS
				ackA	*lp_03010*	*acetate kinase*	1 nt substitution	2571025	WGS
FlyG20.2.6	Niche	2	20	*cheY*	*lp_1544*	*two-component system response regulator*	1 nt substitution	1348886	WGS/SS
				-	*lp_2212*	*NADH-flavin reductase*	1 nt substitution	1937136	WGS
				int4	-	*intergenic region*	1 nt substitution	1982853	WGS
				-	*lp_0197*	*cell surface protein precursor, LPXTG-motif cell wall anchor*	deletion (Δ6)	2471707-12	WGS
				ackA	*lp_03010*	*acetate kinase*	1 nt substitution	2571025	WGS
DietG20.1.2	Diet	1	20	*ackA*	*lp_03010*	*acetate kinase*	1 nt substitution	2571576	WGS/SS
DietG20.2.2	Diet	2	20	*int5*	-	*intergenic region*	1 nt substitution	2313069	WGS/SS
				ackA	*lp_03010*	*acetate kinase*	1 nt substitution	2571576	WGS/SS
				int6	-	*intergenic region*	1 nt substitution	1736935	WGS/SS

Table S2

Table S3. Metabolomic dataset of *Drosophila* diet inoculated with *Lp*^{NIZO2877} and FlyG2.1.8 separately, Related to Figure 6. Table of metabolites resulted to be significantly different between Lp^{NIZO2877}- and FlyG2.1.8-associated *Drosophila* diets based on two-sided t-tests ($p<0.05$). Fold-changes (FC) are calculated with the ratio between means of Lp^{NIZO2877} and FlyG2.1.8 replicates for each metabolite. Metabolites with a positive FC are overrepresented in FlyG2.1.8-associated samples and those with a negative FC are underrepresented in FlyG2.1.8-associated samples. FC detail: If mean(FlyG2.1.8) > mean(Lp^{NIZO2877}), FC = mean(FlyG2.1.8)/mean(Lp^{NIZO2877}); If mean(Lp^{NIZO2877})>mean(FlyG2.1.8), FC = - mean(Lp^{NIZO2877})/mean(FlyG2.1.8)

Metabolite	Metabolite Class	$Lp^{NZO2877}$					FlyG2.1.8					Mean $Lp^{NZO2877}$	Mean FlyG2.1.8	FC	pvalue
		rep1	rep2	rep3	rep4	rep5	rep1	rep2	rep3	rep4	rep5				
2-aminoadipate	Amino Acid	1,1721	1,1259	0,7634	0,8569	1,0883	0,8108	1,1361	1,0611	1,0009	0,8761	1,00132	0,977	-1,0248925	0,81470234
2-hydroxy-3-methylvalerate	Amino Acid	1,4581	0,8634	1	0,9063	0,9814	1,1203	0,7945	0,925	1,243	0,7041	1,04184	0,95738	-1,0882199	0,57997116
3-(4-hydroxyphenyl) lactate	Amino Acid	1,1226	0,8179	1,1635	1,0026	0,976	0,9974	0,8097	0,8599	0,9336	0,7513	1,01652	0,87038	-1,1679037	0,09062559
4-guanidinobutanoate	Amino Acid	1,1821	1,0982	1,0856	0,9744	1,0666	0,9725	1,0347	0,9945	1,1894	1,0055	1,08138	1,03932	-1,0404688	0,43505117
4-hydroxyglutamate	Amino Acid	1,3091	0,6103	1,0206	1,1252	1,2235	0,6629	1,0585	1	1,0868	1,0593	1,05774	0,9735	-1,0865331	0,58024375
5-methylthioadenosine (MTA)	Amino Acid	1,0959	0,96	0,9639	0,8034	0,4754	0,4754	0,4754	0,4754	0,4754	0,6718	0,85972	0,51468	-1,6703971	0,02842545
5-oxoproline	Amino Acid	1,1954	1,1233	1,1947	1,195	1,1724	1,1093	0,9843	1,0254	1,1625	1,0666	1,17616	1,06962	-1,0996055	0,02291602
6-oxopiperidine-2-carboxylate	Amino Acid	1,7192	1,1342	0,993	1,0274	1,0631	1,2966	0,9756	0,9154	1,4487	1,0887	1,18738	1,145	-1,0370131	0,80769515
alpha-hydroxyisovalerate	Amino Acid	0,9352	1,0628	1,1737	1,0008	1,0235	1,028	0,8645	0,8496	0,9836	0,9314	1,0392	0,93142	-1,1157158	0,07337653
arginината*	Amino Acid	1,3557	1,1047	0,7951	0,6393	1	0,772	0,9297	0,6393	1,033	0,6393	0,97896	0,80266	-1,2196447	0,27003911
arginine	Amino Acid	1,0947	0,9995	1,0005	1,0144	1,0708	0,9955	1,0086	1,0046	1,0507	1,0452	1,03598	1,02092	-1,0147514	0,52933797
asparagine	Amino Acid	1,023	1,0109	1,0073	1,013	1,0218	0,9646	1,0003	0,9997	1,0675	1,0168	1,0152	1,00978	-1,0053675	0,76531216
beta-hydroxyisovalerate	Amino Acid	1,3585	1,3189	0,9354	0,6319	1,0873	1,3522	0,8014	1,1622	0,8728	1,0345	1,0664	1,04462	-1,0208497	0,89925383
betaine	Amino Acid	1,2	1,0632	1,1486	1,0452	1,0465	1,075	1,0252	1,0504	1,0965	1,1119	1,1007	1,0718	-1,026964	0,44066802
citrulline	Amino Acid	1,0994	1,0817	0,9968	1,0455	1,0638	0,9616	1,0032	0,8602	1,0719	0,9144	1,05744	0,96226	-1,098913	0,05809564
creatine	Amino Acid	1,607	1,1351	1,8726	1,2971	1,357	0,9386	1	0,898	0,997	0,9853	1,45376	0,96378	-1,508394	0,01843314
creatinine	Amino Acid	1,4011	1,2281	1,403	1,215	1,2862	0,9904	1,1115	0,997	0,9231	0,9789	1,30668	1,00018	-1,3064448	0,00042655
dimethylarginine	Amino Acid	1,1531	1,019	1,0559	1,0064	1,027	0,9517	1,0302	0,9957	1,052	1,1195	1,05228	1,02982	-1,0218096	0,57693576
gamma-aminobutyrate (GABA)	Amino Acid	1,4687	1,3374	1,3868	1,2807	1,3695	1,2188	1,2427	1,2288	1,3226	1,26	1,36862	1,25458	-1,0908989	0,01715585
gentisate	Amino Acid	1,4126	0,9723	1,3161	0,9425	1,3548	0,8668	0,99	0,9786	1,4068	1,181	1,19966	1,08464	-1,1060444	0,42919421
glutamine	Amino Acid	0,5846	0,362	0,0466	0,2916	0,16	0,128	0,1668	0,1731	0,1463	0,1323	0,28896	0,1493	-1,935432	0,20278362
histidine	Amino Acid	1,1493	0,7539	0,9959	0,7983	1,1392	0,8751	0,7085	0,7689	1,0211	1,015	0,96732	0,87772	-1,1020827	0,41691477
indole-3-carboxylic acid	Amino Acid	1,114	0,9486	1,2276	0,7704	1,2031	1,6359	0,5815	1,0634	0,5231	0,5231	1,05274	0,8654	-1,2164779	0,45830394
indoleacetate	Amino Acid	1,0697	1,052	0,967	1,0036	1,0486	0,9501	0,9964	0,9542	1,0818	1,0607	1,02818	1,00864	-1,0193726	0,57100065
indolelactate	Amino Acid	0,8525	0,841	1,0403	0,9854	1	0,8236	0,7344	0,8038	0,9121	0,9773	0,94384	0,85024	-1,1100866	0,15071114
leucine	Amino Acid	1,3723	1,2004	1,2288	1,2033	1,2548	1,2262	1,2101	1,1887	1,2538	1,2823	1,25192	1,23222	-1,0159874	0,6006747
lysine	Amino Acid	1,1143	0,9688	1,0113	0,9833	1,0953	0,9537	1,0109	1,0061	0,9906	1,0164	1,0346	0,99554	-1,039235	0,27123957
methionine sulfone	Amino Acid	1,0857	0,9206	0,8164	1,1381	1,0641	0,9823	1,2286	0,7304	0,7755	1,0756	1,00498	0,95848	-1,0485143	0,68625228
methionine sulfoxide	Amino Acid	1,1949	0,9476	1,0587	1,0264	1,0986	0,9607	0,9026	0,8874	1,0652	1,0445	1,06524	0,97208	-1,0958357	0,12619746
N-acetylglycine	Amino Acid	1,0657	0,5705	0,7542	0,9382	1,0038	0,6169	0,6166	0,6125	0,656	1,0228	0,86648	0,70496	-1,2291194	0,21821526
N-acetylhistamine	Amino Acid	0,2434	0,2434	0,2434	0,2434	0,2434	0,2434	0,2434	0,2434	0,2434	0,2434	0,2434	0,2434	-1	2
N-acetylserine	Amino Acid	1,238	1,2984	1,1698	1,1508	1,1555	1,1003	1,0157	1,1015	1,1172	1,0745	1,2025	1,08184	-1,1115322	0,00973102
N-acetyltaurine	Amino Acid	1,2099	0,9271	1,2037	0,9991	1,1427	1,1264	1,1501	0,8918	1,1832	0,8804	1,0965	1,04638	-1,0478985	0,58148706
N-formylmethionine	Amino Acid	1,1822	0,7999	1,1264	0,9315	1,0032	0,9266	0,9	0,8725	1,0437	0,7389	1,00864	0,89634	-1,1252873	0,22230373
N-formylphenylalanine	Amino Acid	1,7097	1,0462	1,4664	1,1893	1,0951	1,3092	0,7854	1	1,3644	0,7635	1,30134	1,0445	-1,2458976	0,18733804
N-methylproline	Amino Acid	0,916	1,416	1,248	2,0332	0,8394	0,9949	1,2046	0,9992	1,0587	1,3041	1,29052	1,1123	-1,1602266	0,46155114
N6,N6,N6-trimethyllysine	Amino Acid	1,1459	1,0173	0,965	1,0685	1,0693	0,9764	1,0009	1,017	1,0883	1,0979	1,0532	1,0361	-1,0165042	0,67037617
phenyllactate (PLA)	Amino Acid	1,1256	0,7493	1,1427	0,9547	0,8822	0,8226	0,8967	0,825	0,9543	0,6518	0,9709	0,83008	-1,1696463	0,1616931
pipecolate	Amino Acid	1,0504	1,0393	1	1,0618	1,0165	0,9434	0,97	0,8951	1,0813	1,0548	1,0336	0,98892	-1,0451806	0,27717606
pyroglutamine*	Amino Acid	1,1314	0,9956	1,0133	1,015	1,0256	0,9036	1,0185	0,9924	1,1726	0,9552	1,03618	1,00846	-1,0274875	0,60902803
S-adenosylhomocysteine (SAH)	Amino Acid	1,8301	1,0978	1,0552	1,2031	1,1273	1,3721	0,8572	0,9161	1,1742	0,9334	1,2627	1,0506	-1,2018846	0,26099616
taurine	Amino Acid	0,0893	0,0893	0,0893	0,0893	0,0893	0,0893	0,0893	0,0893	0,0893	0,0893	0,0893	0,0893	-1	2
threonine	Amino Acid	1,3126	1,2661	1,1474	1,2233	1,2764	1,094	1,1903	1,1534	1,2544	1,1367	1,24516	1,16576	-1,0681101	0,07695586
trans-4-hydroxyproline	Amino Acid	0,9686	0,9201	1,0077	1,0258	0,975	0,8219	0,8974	0,8724	0,9923	1,0896	0,97944	0,93472	-1,0478432	0,4191927
valine	Amino Acid	1,2502	1,9833	1,1377	1,1379	1,1671	1,0592	1,1019	1,0696	1,1327	1,2006	1,33524	1,1128	-1,1998922	0,24652702
xanthurenate	Amino Acid	1,0011	0,7499	0,9823	0,7477	0,6868	0,8383	0,8728	0,7067	0,7431	0,7816	0,83356	0,7885	-1,0571465	0,55739379
4-imidazoleacetate	Amino Acid	1,0122	0,9682	0,8716	0,9881	0,9737	1,0564	1,0432	0,905	1,1204	0,9533	0,96276	1,01566	1,0549462	0,28283795
alanine	Amino Acid	1,033	1,0419	0,9645	0,9371	1,0272	1,034	1,0226	1,0404	1,0608	1,1352	1,00074	1,0586	1,05781722	0,08180066
alpha-hydroxyisocaproate	Amino Acid	1,4456	0,9708	0,8753	0,8119	0,871	1,2138	0,8471	1,0014	1,1525	0,9961	0,99492	1,04218	1,04750131	0,73272191
aspartate	Amino Acid	1,0586	0,9894	0,9506	0,9624	1,0115	1,0297	1,0841	1,0106	1,1181	1,0749	0,9945	1,06348	1,06936149	0,03521152
ethylmalonate	Amino Acid	0,7807	0,7392	0,8047	0,7392	1,3356	0,8859	0,7392	0,7398	1,1967	0,9705	0,87988	0,90642	1,0301632	0,8574675
glutamate	Amino Acid	0,9563	0,9885	0,7233	1,0058	0,9942	1,1712	1,247	1,1943	1,4677	1,3506	0,93362	1,28616	1,37760545	0,00173601
glycine	Amino Acid	1,3081	1,127	1,2494	1,2628	1,1822	1,1231	1,2027	1,1427	1,4415	1,2703	1,2259	1,23606	1,00828779	0,8819727
guanidinoacetate	Amino Acid	1,0972	0,6146	1,0934	1,3844	0,6831	1,1046	1	0,9058	0,7254	1,3776	0,97454	1,02268	1,04939766	0,79621322
isoleucine	Amino Acid	1,2648	1,1238	1,1452	1,0742	1,202	1,2208	1,1671	1,1304	1,2382	1,1821	1,162	1,18772	1,02213425	0,52289333
kynurenate	Amino Acid	0,8664	0,6308	0,8748	0,7749	0,7909	0,8555	0,8988	0,81	1,0272	0,7934	0,78756	0,87698	1,11354056	0,17864716
methionine	Amino Acid	1,0182	0,9693	0,9272	0,9818	1,0621	1,1629	1,0982	1,0992	1,1786	1,2042	0,99172	1,14862	1,15820998	0,00104888
N-acetylalanine	Amino Acid	0,9658	1,1091	0,9235	0,94	1,0957	1,0572	1,0562	1,3974	1,2363	1,2544	1,00682	1,2003	1,1921694	0,04033587
N-acetylarginine	Amino Acid	0,3485	0,2798	0,2798	0,2798	0,2798	0,4054	0,6587	0,5008	0,7395	0,5657	0,29354	0,57402	1,95550862	0,00738758
N-acetylasparagine	Amino Acid	1,0085	1,0644	1,0962	0,9287	1,2155	1,1956	1,2274	1,1242	1,253	0,9377	1,06266	1,14758	1,07991267	0,2857394
N-acetylaspartate (NAA)	Amino Acid	0,3949	0,3998	0,467	0,4612	0,4146	7,3352	8,2812	12,3127	12,0894	10,5231	0,4275	10,10832	23,645193	0,000635
N-acetylglutamate	Amino Acid	0,8785	0,7962	0,7353	0,8743	0,816	1,4849	1,585	1,7843	2,1916	1,6108	0,82006	1,73132	2,11121137	0,00145244
N-acetylglutamine	Amino Acid	0,2742	0,3003	0,3644	0,4042	0,3024	1,6617	1,9639	2,7624	2,2177	1,7411	0,3291	2,06936	6,2879368	0,00084106
N-acetylhistidine	Amino Acid	0,5149	0,3183	0,5836	0,3183	0,3183	1,1369	1,1205	1,3972	1,2086	1,0886	0,41068	1,19036	2,89850979	1,03E-05
N-acetylleucine	Amino Acid	1,1655	0,8828	1,2131	0,8811	1,0749	1,367	1,3074	1,0511	1,5741	0,9287	1,04348	1,24566	1,19375551	0,17904377
N-acetylmethionine	Amino Acid	0,8415	0,5484	0,825	0,7222	0,7306	1,2018	1,2086	1,1557	1,4926	0,9947	0,73354	1,21068	1,65046214	0,00169883
N-acetylmethionine sulfoxide	Amino Acid	0,8126	0,6495	0,8693	0,7369	0,6781	1,404	1,3291	1,2726	1,4526	1,3576	0,74928	1,36318	1,81931988	4,02E-06
N-acetylphenylalanine	Amino Acid	1,0778	0,7442	0,9095	0,829	0,9385	1,1166	1,2441	1,1609	1,1314	1,0727	0,8998	1,14514	1,27266059	0,00802764
N-acetylproline	Amino Acid	1,1479	1,1241	0,9511	0,9948	1,003	1,0197	1,0381	1,0346	1,2274	1,0652	1,04418	1,077	1,03143136	0,56336781
N-acetylputrescine	Amino Acid	0,9809	0,7866	0,9323	0,9213	1,1367	0,9437	0,9476	0,9347	1,0191	0,9573	0,95156	0,96048	1,00937408	0,885101
N-acetylthreonine	Amino Acid	0,4678	0,4678	0,4678	0,648	0,4678	1,0007	0,8654	1,1921	1,0541	0,9993	0,50384	1,02232	2,02905684	7,80E-05
N-acetyltyrosine	Amino Acid	0,8873	0,3601	0,654	0,457	0,4815	1,5428	1,5231	1,4744	1,8088	1,2527	0,56798	1,52036	2,67678439	7,58E-05
N-acetylvaline	Amino Acid	0,9961	0,7003	0,8994	0,9644	0,9749	1,4683	1,0339	0,9663	1,3429	0,9807	0,90702	1,15842	1,2771714	0,07450521
N-delta-acetylornithine	Amino Acid	1,1848	0,6875	0,8556	1,2311	1,1832	0,8897	1,2133	0,6378	1,0483	1,5393	1,02844	1,06568	1,03621018	0,84726539
N-formylanthranilic acid	Amino Acid	0,983	1,1072	1,0148	0,924	1,0293	1,1139	0,9942	0,8559	1,0893	1,1716	1,01166	1,04498	1,03293597	0,61461533
N-monomethylarginine	Amino Acid	1,1686	1,0081	0,9461	1,0118	1,0534	0,9883	0,9919	1,0337	1,1198	1,1	1,0376	1,04674	1,00880879	0,84747212
N6-acetyllysine	Amino Acid	0,184	0,184	0,184	0,184	0,184	0,8411	0,8439	0,8888	1,0152	0,79	0,184	0,8758	4,75978261	5,47E-05
phenylalanine	Amino Acid	1,124	1,0201	1,0432	1,0384	1,0589	1,0193	1,0431	1,031	1,088	1,1161	1,05692	1,0595	1,00244106	0,92219507
proline	Amino Acid	1,0615	1,0505	1,0001	1,0158	0,9949	0,9927	0,9999	1,0063	1,0716	1,0944	1,02456	1,03298	1,00821816	0,74427001
S-methylmethionine	Amino Acid	1,0005	1,0085	0,8215	0,9995	1,4104	1,2299	1,1038	0,9911	1,1847	1,2055	1,04808	1,143	1,09056561	0,40959418
saccharopine	Amino Acid	1,0321	0,9788	1,0154	0,9846	1,0822	1,0672	1,1009	0,9571	1,1848	1,0465	1,01862	1,0713	1,05171703	0,25176614
serine	Amino Acid	1,0959	0,9533	0,9828	1,0125	0,9961	1,0287	1,0537	0,9981	1,1644	1,1113	1,00812	1,07124	1,06261159	0,13924948
tryptophan	Amino Acid	1,0552	0,9964	0,9678	0,9698	1,053	1,0055	1,0108	1,0087	1,0702	1,1418	1,00844	1,0474	1,03863393	0,27171396
tyramine	Amino Acid	0,7952	0,8528	0,6251	0,9176	0,842	0,6562	0,9307	0,6472	0,9732	0,8582	0,80654	0,8131	1,00813351	0,94013007
tyrosine	Amino Acid	1,2294	1,026	1,001	0,999	0,9302	1,1007	1,1563	1,0081	1,3702	1,1222	1,03712	1,1515	1,11028618	0,18406264
arabonate/xylonate	Carbohydrate	1,1729	0,8812	1,0507	1,0245	1,0817	0,7683	0,9928	1,0072	0,9207	1,1181	1,0422	0,96142	-1,0840216	0,3120413
erythronate*	Carbohydrate	1,1881	1,0539	1,0952	1,115	1,1419	0,9559	1,017	1,0002	1,1275	1,1078	1,11882	1,04168	-1,0740535	0,09268504
fructose	Carbohydrate	0,1146	1,7312	0,0257	1,2054	0,0257	0,2468	0,2192	0,1921	0,1343	0,3085	0,62052	0,22018	-2,8182396	0,3247124
galactitol (dulcitol)	Carbohydrate	1,4706	0,0325	1	1,2755	1,0425	0,6709	1,1254	1,3727	0,0325	1,2692	0,96422	0,89414	-1,078377	0,84612051
galactonate	Carbohydrate	1,1779	0,8372	1,105	1,0001	1,1789	0,6414	0,8904	0,9952	0,8707	1,0157	1,05982	0,88268	-1,2006843	0,09259813
glucose	Carbohydrate	0,1298	1,1057	0,1075	0,7517	0,1075	0,1075	0,1457	0,2443	0,1493	0,3803	0,44044	0,20542	-2,144095	0,32560781
lactate	Carbohydrate	1,1775	1,0848	1,2105	1,1281	1,1801	0,9122	0,9262	1,0074	1,07	0,9872	1,1562	0,9806	-1,179074	0,00151445
maltopentaose	Carbohydrate	0,0119	0,0119	0,0119	0,0123	0,0119	0,0119	0,0119	0,0119	0,0119	0,0119	0,01198	0,0119	-1,0067227	0,37390097
maltotriose	Carbohydrate	0,2632	0,2632	0,2632	0,2632	0,2632	0,2632	0,2632	0,2632	0,2632	0,2632	0,2632	0,2632	-1	2
pyruvate	Carbohydrate	1,1706	1,2522	1,3282	1,0995	1,2212	1,2048	1,1487	1,0007	1,1219	1,0506	1,21434	1,10534	-1,0986122	0,07254645
arabitol/xylitol	Carbohydrate	1,228	0,6427	0,9701	0,6427	0,9222	0,9658	0,9058	1,2533	1	1,3077	0,88114	1,08652	1,23308441	0,17539072

fructose 1,6-diphosphate/glucose 1,6-diphosphate/myo-inositol diphosphates	Carbohydrate	1	0,1986	0,6404	0,4824	0,9056	0,4214	1,2822	1,5068	0,9927	1,3021	0,6454	1,10104	1,70598079	0,09413044
glucuronate	Carbohydrate	1,0083	0,9586	1,0626	0,9994	1,0006	0,9902	0,9733	1,0118	1,054	1,0378	1,0059	1,01342	1,00747589	0,7444315
glycerate	Carbohydrate	1,1554	0,8964	1,011	1,0019	0,9733	1,1051	1,2756	1,1966	1,1782	1,1625	1,0076	1,1836	1,17467249	0,0102688
maltose	Carbohydrate	0,424	0,4707	0,2404	0,5574	0,2891	0,4465	0,3341	0,3768	0,5675	0,3597	0,39632	0,41692	1,0519782	0,78243403
maltotetraose	Carbohydrate	0,6031	0,3501	0,386	0,522	0,3543	0,6664	0,3571	0,1609	0,9833	0,3809	0,4431	0,50972	1,15034981	0,67947593
mannitol/sorbitol	Carbohydrate	1,0454	0,9449	1,0109	1,0218	1,0368	1,0776	0,9846	0,983	1,2238	1,0544	1,01196	1,06468	1,05209692	0,31448366
raffinose	Carbohydrate	1,787	1,0459	0,9251	0,9623	0,9895	1,4937	1,0067	0,9487	1,5413	1,0487	1,14196	1,20782	1,05767277	0,75850796
ribitol	Carbohydrate	1,0072	0,7497	0,981	0,7497	0,9604	0,9928	1,0928	1,3484	1,1192	1,268	0,8896	1,16424	1,30872302	0,01282779
ribonate	Carbohydrate	1,0111	0,8465	0,9566	0,963	1,0209	0,945	0,9169	0,9668	1,0529	1,1199	0,95962	1,0003	1,04239178	0,42859886
ribose	Carbohydrate	1,0794	0,96	1,04	0,7772	0,852	1,1784	1,0733	1,1743	1,0844	1,3415	0,94172	1,17038	1,24281103	0,01560515
sedoheptulose	Carbohydrate	1,066	0,7179	0,4877	0,6589	0,8642	1,1795	1,3365	1,1112	0,9764	1,69	0,75894	1,25872	1,65852373	0,01360922
sucrose	Carbohydrate	2,0338	0,9788	0,0253	0,6534	0,0434	6,5318	5,8872	4,5691	5,181	6,1905	0,74694	5,67192	7,59354165	1,15E-05
gamma-tocotrienol	ofactors and Vitami	1,6364	1,1621	1,1783	1,0528	1,1718	0,8595	0,9642	0,8903	1,1714	0,9676	1,24028	0,9706	-1,2778488	0,05711716
gulonate*	ofactors and Vitami	1,0381	0,8561	0,9255	0,9128	1,0744	0,6496	0,6301	0,9934	0,9178	1,0366	0,96138	0,8455	-1,137055	0,2720135
nicotinamide	ofactors and Vitami	1,1212	1,1445	1,398	0,8727	0,8451	0,8313	1,0781	0,7317	0,9554	0,9534	1,0763	0,90998	-1,1827732	0,20271386
nicotinamide ribonucleotide (NMN)	ofactors and Vitami	0,327	0,327	0,327	0,327	0,327	0,327	0,327	0,327	0,327	0,327	0,327	0,327	-1	2
nicotinamide riboside	ofactors and Vitami	0,4988	0,4988	0,4988	0,4988	0,4988	0,4988	0,4988	0,4988	0,4988	0,4988	0,4988	0,4988	-1	2
nicotinate ribonucleoside	ofactors and Vitami	1,0806	1,0296	0,9746	1,0193	1,0786	1,0081	0,9919	0,8783	1,122	1,0515	1,03654	1,01036	-1,0259116	0,57932692
pyridoxamine	ofactors and Vitami	1,2385	1,0785	0,9965	0,8538	1,0035	0,7849	1,0713	0,7742	0,8701	1,1494	1,03416	0,92998	-1,1120239	0,3240835
pyridoxate	ofactors and Vitami	1,1611	0,9077	1,0767	1,0462	1,0544	0,9773	1,1042	1,0398	0,9996	1,0004	1,04922	1,02426	-1,0243688	0,61054433
pyridoxine (Vitamin B6)	ofactors and Vitami	1,4825	0,7224	1,1405	0,9329	1,0664	1,0607	0,9502	0,3911	0,9809	1,1891	1,06894	0,9144	-1,169007	0,43009484
quinolinate	ofactors and Vitami	1,2692	1,1077	1,264	0,8951	1,2154	0,8772	0,8958	0,9653	0,9502	1,221	1,15028	0,9819	-1,1714839	0,11016278
trigonelline (N'-methylnicotinate)	ofactors and Vitami	1,095	1	0,9826	1,0263	1,0209	0,9804	1,0179	1	1,0647	1,0573	1,02496	1,02406	-1,0008789	0,97232082
gamma-tocopherol/beta-tocopherol	ofactors and Vitami	1,3028	0,8128	1,0116	0,6261	0,9317	0,5552	1,0277	1,2233	1,1538	0,8501	0,937	0,96202	1,02670224	0,88264191
nicotinamide adenine dinucleotide (NAD+)	ofactors and Vitami	2,2908	0,9508	1,4376	1	1,1665	2,6687	1,463	1,3185	1,617	1,2599	1,36914	1,66542	1,21639862	0,43003351
nicotinate	ofactors and Vitami	0,9089	1,0053	0,8693	0,8467	0,9217	0,9639	0,9947	0,8521	0,9866	1,1259	0,91038	0,98464	1,08157033	0,19390318
oxalate (ethanedioate)	ofactors and Vitami	1,2328	0,8164	0,9956	0,7418	1,0428	0,8049	1,1148	1,0233	1,0259	0,9478	0,96588	0,98334	1,01807678	0,86810468
pantothenate	ofactors and Vitami	1,1371	1,0358	1,0629	0,8487	0,9318	1,1225	1,1015	0,9423	1,002	1,1028	1,00326	1,05422	1,05079441	0,43540455
pyridoxal	ofactors and Vitami	1,0105	0,9965	0,9611	1,0433	1,1131	0,9854	0,9832	0,9928	1,1269	1,0662	1,0249	1,0309	1,00585423	0,87968752
thiamin (Vitamin B1)	ofactors and Vitami	1,1079	0,9583	1,0133	1,055	1,0055	0,9943	0,9946	1,0558	1,0054	1,1185	1,028	1,03372	1,0055642	0,8736155
threonate	ofactors and Vitami	1,036	0,964	1,0485	1,0798	1,0259	0,6945	1,1149	0,9218	1,171	1,2703	1,03084	1,0345	1,0035505	0,97350284
alpha-ketoglutarate	Energy	0,8859	1,0048	0,813	0,998	1,002	0,8518	0,842	0,8028	0,9086	1,0898	0,94074	0,899	-1,0464294	0,53315182
phosphate	Energy	1,1785	0,7914	1,0379	0,729	0,9406	0,8382	1,0097	0,9379	0,9381	0,9272	0,93548	0,93022	-1,0056546	0,95364638
succinate	Energy	1,1276	1,0151	0,9707	0,9776	0,9698	1,0037	0,9811	0,9338	1,0233	1,0467	1,01216	0,99772	-1,014473	0,69826066
aconitate [cis or trans]	Energy	1,2215	0,7849	0,7948	0,7857	0,8235	1,1791	0,8497	0,818	1,1082	0,8432	0,88208	0,95964	1,08792853	0,51650657
citrate	Energy	1,4244	0,248	0,4935	0,3962	1,4821	0,2859	1,4428	1,2766	0,5082	0,8862	0,80884	0,87994	1,08790366	0,84209122
fumarate	Energy	1,0156	0,9991	0,9225	0,9732	0,8461	0,9073	1,0009	0,9689	1,0738	1,1249	0,9513	1,01516	1,06712919	0,2314736
malate	Energy	0,8309	0,4631	0,6008	0,6554	0,8684	0,4335	1,0588	1,1074	0,7883	1,1289	0,68372	0,90338	1,32127187	0,19641065
1-linoleoyl-GPC (18:2)	Lipid	1,0154	1,2285	1,0796	1,1615	0,7716	0,8374	0,81	0,9132	1,1372	1,0171	1,05132	0,94298	-1,1148911	0,3086021
1-linoleoyl-GPE (18:2)*	Lipid	1,0057	1,185	1,0825	1,0351	0,7924	0,8042	0,8301	0,9027	1,079	0,9943	1,02014	0,92206	-1,1063705	0,26996727
1-linoleoyl-GPG (18:2)*	Lipid	1,4088	1,1435	0,7473	1,0282	0,7066	0,9763	0,7889	0,8927	1,3475	0,8691	1,00688	0,9749	-1,0328034	0,84946594
1-linoleoyl-GPI (18:2)*	Lipid	1,3583	1,1308	0,7971	0,9983	0,8062	0,9311	0,6984	0,927	1,2655	0,8817	1,01814	0,94074	-1,0822757	0,59508047
1-oleoyl-2-linoleoyl-GPC (18:1/18:2)*	Lipid	1,0404	0,9694	1,2703	0,9786	0,9883	0,7482	0,9043	0,8795	1,0347	1,0474	1,0494	0,92282	-1,1371665	0,14772059
1-oleoyl-GPC (18:1)	Lipid	1,0355	1,1452	1,0706	1,0398	0,7256	0,7797	0,8152	0,8982	1,1176	0,9597	1,00334	0,91408	-1,0976501	0,36979093
1-palmitoleoyl-GPC (16:1)*	Lipid	0,9708	1,197	1,0876	1,2011	0,6817	0,7398	0,811	0,8293	1,089	0,8675	1,02764	0,86732	-1,1848453	0,20105339
1-palmitoyl-2-linoleoyl-GPE (16:0/18:2)	Lipid	0,9685	0,9412	1,2939	0,9146	0,7912	0,8706	0,7081	0,9006	0,8837	1,025	0,98188	0,8776	-1,1188241	0,32371488
1-palmitoyl-2-oleoyl-GPC (16:0/18:1)	Lipid	1,0166	1,0403	1,1046	0,9773	0,9766	0,6886	0,8423	0,9591	1,1415	1,0928	1,02308	0,94486	-1,0827848	0,40810552
1-palmitoyl-2-oleoyl-GPE (16:0/18:1)	Lipid	0,336	0,336	0,336	0,336	0,336	0,336	0,336	0,336	0,336	0,336	0,336	0,336	-1	2
1-palmitoyl-GPC (16:0)	Lipid	1,005	1,192	1,0421	1,0404	0,7365	0,796	0,8137	0,8809	1,1352	0,999	1,0032	0,92496	-1,0845874	0,44620244
1-palmitoyl-GPE (16:0)	Lipid	1,0648	1,1267	1,041	1,05	0,8109	0,8069	0,8909	0,9034	1,1083	0,9727	1,01868	0,93644	-1,087822	0,29828253
1-stearoyl-GPC (18:0)	Lipid	1,0489	1,2245	1,0876	1,0037	0,7223	0,8561	0,7821	0,9109	1,1798	1,0682	1,0174	0,95942	-1,0604323	0,611907
1,2-dilinoleoyl-GPC (18:2/18:2)	Lipid	1,061	0,997	1,1533	0,9876	0,8246	0,7763	0,8738	0,8332	1,0876	1,0043	1,0047	0,91504	-1,0979848	0,28686595
1,2-dioleoyl-GPC (18:1/18:1)	Lipid	1,1354	0,9967	1,3872	0,8983	1,0645	0,8356	0,9151	1,0764	1,2334	1,0792	1,09642	1,02794	-1,0666187	0,54416015
2-hydroxyadipate	Lipid	0,884	0,9057	0,9847	1,0961	1,1187	0,8467	1,1178	0,8698	1,1503	0,9731	0,99784	0,99154	-1,0063538	0,93811244
2-hydroxyglutarate	Lipid	1,0464	0,9113	1,0105	0,9752	0,9732	0,8337	0,8955	0,8713	0,9454	0,9895	0,98332	0,90708	-1,0840499	0,06503983
2-hydroxypalmitate	Lipid	0,8529	1,1518	0,6102	1,1902	1,0422	0,8352	0,8306	1,1008	0,8353	1,1156	0,96946	0,9435	-1,0275146	0,84357342
2-linoleoylglycerol (18:2)	Lipid	0,8877	1,7588	0,6084	0,7073	0,748	0,9437	0,3418	0,8456	0,9936	0,7643	0,94204	0,7778	-1,2111597	0,51675818
3-hydroxy-3-methylglutarate	Lipid	1,2583	0,9048	0,8378	0,9161	0,9768	0,887	0,8894	0,9365	0,9915	0,9365	0,97876	0,92818	-1,0544937	0,53670202
9,10-DiHOME	Lipid	0,9963	1,0057	1,0164	1,0495	1,0037	0,9372	1,0553	0,8305	0,9557	1,0475	1,01432	0,96524	-1,0508475	0,30410442
caprate (10:0)	Lipid	0,635	1,803	0,771	1,8676	1,2245	0,6859	1,8517	0,3524	1,0551	1,0494	1,26022	0,9989	-1,2616078	0,48465203
choline	Lipid	1,085	1,0048	1,0101	1,0352	1,0086	0,9541	0,9915	0,9807	1,0665	1,0447	1,02874	1,0075	-1,0210819	0,43502174
choline phosphate	Lipid	0,8083	0,761	0,7817	0,8776	0,8726	0,7827	0,7773	0,7939	0,8005	0,8848	0,82024	0,80784	-1,0153496	0,69761704
dihomo-linoleate (20:2n6)	Lipid	1,1897	1,1242	1,319	0,9152	0,8411	0,9366	0,893	0,9727	1,2744	0,9824	1,07784	1,01182	-1,0652488	0,56953
glutarate (pentanedioate)	Lipid	1,0092	1,1987	1,4373	1,398	1,1073	0,8737	1,0195	1,1352	1,1699	1,1742	1,2301	1,0745	-1,1448115	0,16467306
glycerol 3-phosphate	Lipid	1,0894	1,1119	1,0508	1,1241	1,2032	0,9252	1,007	1,1496	1,1673	0,993	1,11588	1,04842	-1,0643444	0,25237566
glycerophosphoethanolamine	Lipid	1,3415	1,1455	1,3653	1,1018	1,4908	1,4485	1,1876	1,2484	0,951	1,0091	1,28898	1,16892	-1,1027102	0,3267353
glycerophosphoglycerol	Lipid	1,1182	0,9434	1,1166	1,0049	1,0437	1,0561	0,9976	1,0141	1,0095	1,0068	1,04536	1,01682	-1,0280679	0,45379637
glycerophosphorylcholine (GPC)	Lipid	1,2288	1,1294	1,2289	1,07	1,2458	1,2494	1,1373	1,207	1,0933	1,133	1,18058	1,164	-1,014244	0,71941729
glycosyl ceramide (d18:2/24:1, d18:1/24:2)*	Lipid	0,8749	1,7386	1,2833	1,2808	0,9389	1,3177	0,7717	0,9207	1,4415	0,7903	1,2233	1,04838	-1,1668479	0,42399987
hexadecadienoate (16:2n6)	Lipid	1,0346	0,9168	0,7534	0,9589	0,8337	0,7532	0,8002	0,8545	0,9774	0,9087	0,89948	0,8588	-1,0473684	0,53615184
linoleoyl-linolenoyl-glycerol (18:2/18:3) [1]*	Lipid	1,2222	0,9996	1,0321	0,8965	0,9298	0,8511	0,8053	0,8665	1,3175	0,9867	1,01604	0,96542	-1,0524331	0,65725471
linoleoyl-linolenoyl-glycerol (18:2/18:3) [2]*	Lipid	1,1421	1,0108	1,0157	0,8615	0,9076	0,7377	0,7606	0,8125	1,1851	0,95	0,98754	0,88918	-1,1106188	0,34203418
linoleoyl-linoleoyl-glycerol (18:2/18:2) [1]*	Lipid	1,2995	1,0001	1,0869	0,9526	0,9999	0,916	0,8976	0,8833	1,3108	0,9594	1,0678	0,99342	-1,0748727	0,48557195
malonate	Lipid	1,0256	0,8002	1,0547	0,7537	0,8158	0,7667	0,8458	0,8289	0,9611	0,8679	0,89	0,85408	-1,042057	0,625782
methylmalonate (MMA)	Lipid	0,9369	0,714	0,7216	0,3709	0,5458	0,3709	1,0074	0,3709	0,3709	0,9682	0,65784	0,61766	-1,065052	0,82861291
myo-inositol	Lipid	1,0677	0,9805	1,0605	1,0333	1,0217	0,9901	0,9653	1,028	1,0748	1,0589	1,03274	1,02342	-1,0091067	0,72734005
N-palmitoyl-sphinganine (d18:0/16:0)	Lipid	1,0407	0,9752	1,4975	0,5457	0,9524	0,7878	0,8401	0,9904	1,4934	0,8946	1,0023	1,00126	-1,0010387	0,99594022
oleoyl-linolenoyl-glycerol (18:1/18:3) [2]*	Lipid	1,3351	1,2157	1,1812	0,8611	0,8442	0,8096	0,7462	0,8527	1,6093	1,0798	1,08746	1,01952	-1,0666392	0,7266958
oleoyl-linoleoyl-glycerol (18:1/18:2) [1]	Lipid	1,2511	1,0023	1,0888	0,9302	0,9977	0,9179	0,8714	0,8485	1,3279	0,9932	1,05402	0,99178	-1,0627559	0,56762049
oleoyl-linoleoyl-glycerol (18:1/18:2) [2]	Lipid	1,1919	1,0402	1,0572	0,8643	0,9494	0,8276	0,8803	0,8482	1,2367	0,9718	1,0206	0,95292	-1,0710238	0,48985713
oleoyl-oleoyl-glycerol (18:1/18:1) [1]*	Lipid	1,2874	0,9775	1,1538	1,0007	1,0861	0,9993	0,8741	0,8428	1,4572	0,612	1,1011	0,95708	-1,1504785	0,38098034
oleoyl-oleoyl-glycerol (18:1/18:1) [2]*	Lipid	1,1551	1,0481	1,4351	0,8664	0,9229	0,9178	0,9655	0,8657	1,2908	0,7629	1,08552	0,96054	-1,1301143	0,38039732
oleoyl ethanolamide	Lipid	1,0158	1,1971	0,9984	1,1052	0,8448	0,9519	0,8822	0,8846	1,2616	1,0016	1,03226	0,99638	-1,0360104	0,70507124
palmitoyl-linoleoyl-glycerol (16:0/18:2) [1]*	Lipid	1,2098	0,9661	1,0819	0,91	1,0207	0,9035	0,8827	0,8517	1,2838	0,9793	1,0377	0,9802	-1,0586615	0,56103911
palmitoyl-linoleoyl-glycerol (16:0/18:2) [2]*	Lipid	1,1462	1,0383	1,0669	0,8903	0,9308	0,8328	0,866	0,8642	1,1903	0,965	1,0145	0,94366	-1,0750694	0,40622207
palmitoyl-oleoyl-glycerol (16:0/18:1) [1]*	Lipid	1,2036	0,9529	1,0714	0,9531	1,0897	0,9435	0,9076	0,8343	1,3906	0,9267	1,05414	1,00054	-1,0535711	0,64384692
palmitoyl-oleoyl-glycerol (16:0/18:1) [2]*	Lipid	1,1378	1,0717	1,1185	0,9298	0,9852	0,8848	0,9679	0,8469	1,2859	0,9934	1,0486	0,99578	-1,0530438	0,56556983
palmitoyl-palmitoyl-glycerol (16:0/16:0) [2]*	Lipid	1,0503	1,076	1,1684	0,8574	0,8434	0,838	1,158	0,9257	0,933	0,951	0,9991	0,96114	-1,0394948	0,65976985
phytosphingosine	Lipid	1,142	1,6092	1,1178	1,2147	0,8373	0,8272	0,8667	0,8661	1,3171	1,0576	1,1842	0,98694	-1,1998703	0,24011356
sphingadienine*	Lipid	1,0348	1,1066	1,0353	1,096	0,8346	0,8677	0,8582	0,9684	1,0537	1,0337	1,02146	0,95634	-1,0680929	0,33764096
sphinganine	Lipid	1,0914	1,1646	1,0625	1,0007	0,8239	0,8489	0,8476	0,9163	1,1611	0,9705	1,02862	0,94888	-1,0840359	0,35694886
sphingosine	Lipid	1,0333	1,0752	1,0686	1,0295	0,8002	0,7534	0,8614	0,9051	1,0147	0,8922	1,00136	0,88536	-1,1310201	0,11882471
tetradecanedioate	Lipid	1,1139	1,1155	1,3669	0,5802	1,3302	1,0942	0,9287	1,2659	0,5802	0,5802	1,10134	0,88984	-1,2376832	0,31289956
linolenate [alpha or gamma; (18:3n3 or 6)]	Lipid	1,2186	0,9955	0,8318	0,9744	0,8486	0,9892	0,8792	0,9623	1,0418	1,028	0,97378	0,9801	1,00649017	0,93602846
1-linoleoylglycerol (18:2)	Lipid	1,5419	0,9281	0,7158	0,8987	0,8996	1,0043	0,8036	0,7122	1,7251	0,7906	0,99682	1,00716	1,01037299	0,96584347
1-oleoyl-GPE (18:1)	Lipid	1,5217	1,2579	0,5207	0,8298	0,9921	0,7543	1,1124	0,9067	1,6794	0,9414	1,02444	1,07884	1,05310218	0,82321335
1-oleoyl-GPG (18:1)*	Lipid	1,6638	1,4181	0,7546	0,8868	0,759	1,2409	1	1,1178	1,9856	0,9363	1,09646	1,25612	1,14561407	0,56554719

1-oleoylglycerol (18:1)	Lipid	0,8558	1,0093	0,7619	0,6636	0,7992	0,8443	1,1191	0,7637	0,9907	1,9098	0,81796	1,12552	1,37600861	0,21329515
1-palmitoyl-GPG (16:0)*	Lipid	1,5448	1,2734	0,7997	1,0023	0,8391	1,243	0,8587	0,9223	1,5908	0,8957	1,09186	1,1021	1,00937849	0,96012739
1-palmitoyl-GPI (16:0)	Lipid	1,4135	1,1587	0,7175	0,8409	0,9174	1,3177	0,8671	0,6537	1,5915	0,9055	1,0096	1,0671	1,05695325	0,7918413
1-palmitoylglycerol (16:0)	Lipid	0,9799	0,986	0,6992	0,6751	0,6734	0,7747	1,014	0,7512	0,9139	1,551	0,80272	1,00096	1,24696033	0,27061432
12,13-DiHOME	Lipid	0,9855	1,0015	0,9985	1,1403	1,0438	1,0674	1,0964	0,8646	1,0108	1,1927	1,03392	1,04638	1,01205122	0,84517444
13-HODE + 9-HODE	Lipid	1,006	1,034	0,9699	1,0326	1,0039	0,9719	1,0555	0,982	0,9961	1,1162	1,00928	1,02434	1,01492153	0,63059816
13-HpODE/9-HpODE	Lipid	1,1845	1,1682	0,9436	0,9157	1,0243	1,1942	1,1651	1,0174	1,1823	1,0752	1,04726	1,12684	1,07598877	0,26553353
2-hydroxybehenate	Lipid	1,3927	0,7421	0,8439	0,699	0,8355	0,9946	0,8537	0,8771	1,3826	1,0002	0,90264	1,02164	1,1318355	0,47304379
2-hydroxystearate	Lipid	1,0463	1,0205	0,8631	0,8446	0,9165	1,1219	0,9651	0,9337	1,2183	0,8366	0,9382	1,01512	1,08198678	0,36882708
2-oleoylglycerol (18:1)	Lipid	0,7083	0,5907	0,2939	0,2939	0,2939	0,3591	1,6547	0,5691	0,4182	1,7945	0,43614	0,95912	2,19911038	0,17573925
2-palmitoyl-GPC (16:0)*	Lipid	1,5046	1,005	0,824	0,92	0,8154	1,3793	0,995	0,8918	1,529	0,8624	1,0138	1,1315	1,11609785	0,54491521
3-hydroxyoctanoate	Lipid	1,3034	0,9157	0,9882	1,0106	0,9237	1,1223	0,8845	0,7486	1,4643	0,9894	1,02832	1,04182	1,01312821	0,92682386
3-methylglutarate/2-methylglutarate	Lipid	0,9745	1,0181	0,9483	0,9819	1,1196	1,1173	0,7955	1,1108	1,6087	1,2672	1,00848	1,1799	1,16997858	0,26779498
acetylcholine	Lipid	0,9264	0,8267	0,9682	0,8299	0,8382	0,9528	1,0038	1	1,0587	0,9569	0,87788	0,99444	1,13277441	0,0126683
azelate (nonanedioate)	Lipid	1,0589	0,9931	0,9872	1,0688	1,1152	1,2421	0,9041	0,9805	1,0726	1,0612	1,04464	1,0521	1,00714122	0,90764289
carnitine	Lipid	0,9137	0,8481	1,0407	0,9578	0,9207	0,9584	1,0269	0,8946	1,0618	0,9148	0,9362	0,9713	1,03749199	0,45741064
deoxycarnitine	Lipid	1,0946	0,9204	0,8229	1,3453	1,0687	1,116	1,1937	1,0345	1,3059	1,478	1,05038	1,22562	1,16683486	0,1759277
diacylglycerol (16:1/18:2 [2], 16:0/18:3 [1])*	Lipid	1,1867	0,9282	1,1258	0,8913	0,8623	0,8322	0,9318	0,8848	1,3677	1,0771	0,99886	1,01872	1,01988267	0,8695684
eicosenoate (20:1)	Lipid	1,4003	1,0386	0,678	0,9253	0,923	1,1652	0,871	0,991	1,2617	0,8612	0,99304	1,03002	1,03723918	0,80215158
glycerol	Lipid	0,9733	0,5898	0,6015	0,4697	0,5649	1,9144	1,1819	1,1781	1,5947	1,644	0,63984	1,50262	2,34843086	0,00154734
glycerophosphoinositol*	Lipid	1,1017	1,1008	1,0822	0,8944	0,9838	1,0508	1,024	1,1099	1,0514	1,0162	1,03258	1,05046	1,01731585	0,70067249
linoleate (18:2n6)	Lipid	1,123	1,0108	0,8061	1,002	0,8409	0,942	0,8765	0,9751	1,1166	0,993	0,95656	0,98064	1,02517354	0,74311042
linoleoyl ethanolamide	Lipid	1,1593	0,9716	0,7752	0,9237	0,8979	1,0785	1,0641	0,7966	1,1905	1,021	0,94554	1,03014	1,08947268	0,374715
maleate	Lipid	1,0717	1,1405	1,0578	0,907	0,9363	0,9864	0,8725	1,1304	1,1901	1,377	1,02266	1,11128	1,08665637	0,39656363
myristoleate (14:1n5)	Lipid	1,1114	0,7568	0,9059	0,8108	0,5958	0,7364	0,656	1,0086	0,7502	1,3115	0,83614	0,89254	1,06745282	0,71314868
oleate/vaccenate (18:1)	Lipid	1,2396	1,0098	0,8351	0,9649	0,8306	0,9611	0,8938	0,9722	1,2921	0,9132	0,976	1,00648	1,03122951	0,77773876
palmitate (16:0)	Lipid	1,0067	0,9854	0,8655	0,9933	0,8952	1,0572	0,8954	0,894	1,138	0,9295	0,94922	0,98282	1,03539748	0,57410771
palmitoleate (16:1n7)	Lipid	1,065	1,0493	0,9028	0,9932	0,8567	0,979	0,9213	0,9451	1,0903	0,9646	0,9734	0,98006	1,006842	0,89787184
palmitoyl ethanolamide	Lipid	0,3116	0,5534	0,8068	1,4032	0,7873	1,2936	0,3116	0,3116	1,7916	0,5093	0,77246	0,84354	1,09201771	0,84482406
pelargonate (9:0)	Lipid	0,9774	0,6742	1,4341	0,6742	1,273	1,0699	1,4521	1,737	0,9742	1	1,00658	1,24664	1,23849073	0,29662346
stearoyl-linoleoyl-glycerol (18:0/18:2) [2]*	Lipid	1,2779	0,9843	0,4587	0,8684	1,0157	0,8325	0,779	0,8214	1,1742	1,0332	0,921	0,92806	1,00766558	0,96473201
trans-nonadecenoate (tr 19:1)*	Lipid	0,8166	0,5832	0,7147	0,6037	0,4538	0,8168	0,8087	0,6045	1	0,5993	0,6344	0,76586	1,20721942	0,21448365
2'-deoxyadenosine	Nucleotide	1,1888	1,259	0,9446	1,226	0,9806	1,0766	0,8486	0,8545	1,0905	1,0931	1,1198	0,99266	-1,1280801	0,18346321
2'-deoxyguanosine	Nucleotide	1,0057	0,4119	0,7496	0,8819	0,7655	0,8498	0,6086	0,5465	0,5033	0,5971	0,76292	0,62106	-1,2284159	0,26311952
2'-deoxyinosine	Nucleotide	0,426	0,426	0,426	0,426	0,426	0,426	0,426	0,426	0,426	0,426	0,426	0,426	-1	2
2'-O-methyluridine	Nucleotide	1,4288	0,9251	1,0831	1,1242	1,0399	0,6919	1,006	0,7004	1,0615	0,8311	1,12022	0,85818	-1,3053439	0,05006147
3-ureidopropionate	Nucleotide	0,0335	0,0335	0,0335	0,0335	0,0335	0,0335	0,0335	0,0335	0,0335	0,0335	0,0335	0,0335	-1	2
7-methylguanine	Nucleotide	1,0708	0,9734	0,9151	1,0928	1,0213	1,0171	0,9275	0,9543	1,019	1,1388	1,01468	1,01134	-1,0033025	0,94708572
adenosine	Nucleotide	0,729	1,0861	0,5689	0,7963	0,4846	0,3474	0,3408	0,3308	0,4293	0,3871	0,73298	0,36708	-1,9967854	0,02352945
adenosine 5'-monophosphate (AMP)	Nucleotide	1,6924	1,4091	1,4674	1,7111	1,4112	1,1274	1,2557	1,301	1,3956	1,337	1,53824	1,28334	-1,1986223	0,01659363
allantoin	Nucleotide	0,8591	1,0072	1,0246	1,0654	0,9746	0,7077	0,7021	1,224	0,9964	1,2169	0,98618	0,96942	-1,0172887	0,89525564
cytidine	Nucleotide	1,2768	0,8204	1,0522	1,1129	0,8845	0,4527	0,7507	0,9049	0,9283	0,8741	1,02936	0,78214	-1,3160815	0,07343996
cytidine 2',3'-cyclic monophosphate	Nucleotide	1,3462	1,1368	1,2724	1,287	1,2023	1,5157	1,0746	1,0478	1,1324	1,0567	1,24894	1,16544	-1,0716468	0,42159462
cytosine	Nucleotide	1,1013	0,9714	1,0704	0,9148	0,9865	0,9183	0,9336	0,9772	1,0135	0,9211	1,00888	0,95274	-1,0589248	0,1954908
dihydroorotate	Nucleotide	1,4386	1,0584	1,599	1,4373	0,9977	1,0974	1	0,9263	0,9718	1,0367	1,3062	1,00644	-1,2978419	0,06199096
guanine	Nucleotide	1,3007	1,2677	1,2661	1,1753	1,3389	1,3579	1,2204	1,1808	1,3449	1,2415	1,26974	1,2691	-1,0005043	0,98884766
guanosine	Nucleotide	1,4825	0,8601	1,1353	1,181	0,9165	0,8598	0,9506	0,9266	1,02	1,0203	1,11508	0,95546	-1,1670609	0,22717968
guanosine-2',3'-cyclic monophosphate	Nucleotide	1,792	0,8475	1,1433	1,1097	0,9655	1,5631	1,1603	0,9581	1,2053	0,9568	1,1716	1,16872	-1,0024642	0,98879313
guanosine 3'-monophosphate (3'-GMP)	Nucleotide	1,5843	1,079	0,9463	1,3672	1,1226	1,082	1,1693	0,9497	1,2366	1,1951	1,21988	1,12654	-1,0828555	0,48438683
hypoxanthine	Nucleotide	1,0822	0,9441	1,0027	1,0128	0,9973	0,886	0,831	0,8386	0,9263	0,9412	1,00782	0,88462	-1,1392688	0,00437762
inosine	Nucleotide	0,5806	0,44	0,6309	0,7353	0,5952	0,2299	0,4311	0,4983	0,5639	0,4126	0,5964	0,42716	-1,3961981	0,05115105
N6-succinyladenosine	Nucleotide	1,5519	0,9477	1,0411	1,1632	1,1617	1,3104	1,0443	1,1572	1,3457	0,9517	1,17312	1,16186	-1,0096914	0,93206237
orotate	Nucleotide	1,1181	0,9612	0,9846	1,0384	1,0248	1,037	0,9845	0,9535	1,0801	0,9727	1,02542	1,00556	-1,0197502	0,59238686
uridine	Nucleotide	1,2536	1,0676	0,9312	0,8632	0,7015	0,3801	0,7278	0,7004	0,8253	0,7542	0,96342	0,67756	-1,4218962	0,04720149
uridine 5'-monophosphate (UMP)	Nucleotide	1,3452	0,7887	1,32	1,0956	1,1044	1,3893	1	0,7359	0,8617	0,6192	1,13078	0,92122	-1,2274809	0,24653935
1-methyladenine	Nucleotide	1,1726	0,9715	1,0172	1,0067	0,8681	1,0241	0,9933	0,9482	1,0649	1,0478	1,00722	1,01566	1,0083795	0,87978715
adenine	Nucleotide	1,3283	1,2368	1,2068	1,2303	1,2428	1,2373	1,2693	1,2141	1,3179	1,2911	1,249	1,26594	1,01356285	0,5594228
adenosine-2',3'-cyclic monophosphate	Nucleotide	1,359	0,6233	1,0425	1,1309	0,8835	1,8886	1,0687	0,9501	1,1333	0,8328	1,00784	1,1747	1,16556199	0,47852441
adenosine 3'-monophosphate (3'-AMP)	Nucleotide	1,516	1,085	0,8319	0,9582	0,912	1,1165	1,1324	1,2053	1,2002	1,0517	1,06062	1,14122	1,07599329	0,54878757
allantoic acid	Nucleotide	1,0487	0,8603	0,6053	1,1138	1,0383	0,9078	0,8062	1,1091	1	1,1039	0,93328	0,9854	1,05584605	0,64756305
beta-alanine	Nucleotide	0,982	0,917	0,9523	0,8903	0,9077	0,8508	0,9137	0,9306	1,018	0,9427	0,92986	0,93116	1,00139806	0,96832251
pseudouridine	Nucleotide	1,1112	1,1262	1,0027	0,9192	0,9536	0,8999	1,4777	1,2734	0,9973	1,1733	1,02258	1,16432	1,13861018	0,25141284
uracil	Nucleotide	2,9752	2,9363	2,5617	2,5172	2,9212	3,272	3,1914	2,7828	3,1426	2,8939	2,78232	3,05654	1,09855804	0,07955209
urate	Nucleotide	0,8974	0,8549	0,6849	0,7435	0,7148	0,5169	0,8376	0,7877	0,9582	1,0418	0,7791	0,82844	1,06332948	0,63641045
uridine-2',3'-cyclic monophosphate	Nucleotide	1,5094	0,9842	1,0309	1,1329	1,0158	1,1845	1,2681	1,2447	1,1143	1,1006	1,13464	1,18244	1,0421279	0,66108158
xanthine	Nucleotide	0,9085	0,9223	0,9667	0,9931	0,9054	0,9911	0,9807	0,941	1,0408	1,043	0,9392	0,99932	1,06401193	0,04956226
gamma-glutamylleucine	Peptide	1,2246	0,8274	1,1882	1,0318	1,0783	1,0921	1,0018	1,128	1,0512	0,9895	1,07006	1,05252	-1,0166648	0,82384899
gamma-glutamylphenylalanine	Peptide	1,5524	0,7864	1,0201	0,9629	1,1383	0,9556	1,0213	1,0661	1,1322	0,9056	1,09202	1,01616	-1,0746536	0,59795099
gamma-glutamylalanine	Peptide	1,0801	1,0689	0,9283	0,9862	1,126	0,9595	1,0586	1,0439	1,1365	1,0451	1,0379	1,04872	1,0104249	0,8174162
gamma-glutamyltyrosine	Peptide	1,7456	0,8704	0,8446	0,6599	0,9662	1,0892	1,1463	1,0338	1,1885	1,2191	1,01734	1,13538	1,11602807	0,5694003
gamma-glutamylvaline	Peptide	1,0354	1,1092	0,8446	1,098	1,3462	0,9694	1,0245	0,7986	1,4257	1,4036	1,08668	1,12436	1,03467442	0,8065167
4-hydroxyhippurate	Xenobiotics	0,1977	0,1977	0,1977	0,1977	0,1977	0,1977	0,1977	0,1977	0,1977	0,1977	0,1977	0,1977	-1	2
carotene diol (1)	Xenobiotics	0,9326	1,1278	1,0847	0,9745	0,9002	0,7413	0,8974	0,892	1,0436	1,0044	1,00396	0,91574	-1,0963374	0,23553706
carotene diol (3)	Xenobiotics	0,9277	1,0283	1,0858	0,9901	0,8052	0,6156	0,9256	1,0191	0,8315	1,022	0,96742	0,88276	-1,0959038	0,3762776
diaminopimelate	Xenobiotics	0,9301	1,0576	0,9163	1,0399	1,4326	0,7743	0,6763	0,8273	1	1,0556	1,0753	0,8667	-1,2406831	0,11618712
N-propionylmethionine	Xenobiotics	1,3064	0,9681	1,4861	1,1378	1,1758	0,1405	0,0826	0,1324	0,1066	0,1427	1,21484	0,12096	-10,04332	0,00019124
O-sulfo-L-tyrosine	Xenobiotics	1,1441	1	1,1127	1,0722	1,0199	0,8702	1,0021	1,0644	1,2075	0,9741	1,06978	1,02366	-1,045054	0,48537384
stachydrine	Xenobiotics	1,1315	1,0429	0,9871	1,0339	1,0385	0,9986	0,9929	0,963	1,191	1,0353	1,04678	1,03616	-1,0102494	0,82713955
theanine	Xenobiotics	1,0519	0,9977	0,9517	1,0328	1,0023	0,9314	1,017	0,9299	1,1012	1,0451	1,00728	1,00492	-1,0023484	0,9516864
thioproline	Xenobiotics	1,1296	0,9181	0,8971	1,0819	1,0503	0,9733	0,9949	1,0051	1,0481	1,0541	1,0154	1,0151	-1,0002955	0,99530625
2-oxindole-3-acetate	Xenobiotics	0,9988	1,065	0,9255	1,003	1,0207	0,9707	1,028	1,0012	1,1225	1,0898	1,0026	1,04244	1,03973668	0,30174442
2,3-dihydroxyisovalerate	Xenobiotics	0,9842	0,7748	0,9836	1,1137	0,9129	0,8611	0,725	0,9919	1,1598	1,0946	0,95384	0,96648	1,0132517	0,89903467
3-deoxyoctulosonate	Xenobiotics	1,0296	1,0415	0,9484	0,8506	0,9819	1,0596	0,9972	0,9257	1,0028	1,0117	0,9704	0,9994	1,02988458	0,49774824
4-hydroxybenzoate	Xenobiotics	1,2845	0,9506	0,8983	0,9184	0,9567	1,2211	0,9564	0,9473	1,2668	1,0153	1,0017	1,08138	1,07954477	0,44208154
4-hydroxycinnamate	Xenobiotics	1,6693	1,1014	1,033	0,9174	0,9854	1,3734	1,1651	1,0146	1,2822	0,9589	1,1413	1,15884	1,01536844	0,91408933
beta-cryptoxanthin	Xenobiotics	1,0212	0,8316	0,4959	0,4549	0,838	0,5463	1,3002	1,2362	0,7314	0,9788	0,72832	0,95858	1,31615224	0,24089934
beta-guanidinopropanoate	Xenobiotics	1,5519	0,9748	0,9454	1,1276	0,5911	0,6596	1,0988	0,9166	1,3572	1,2439	1,03816	1,05522	1,01643292	0,93376308
carotene diol (2)	Xenobiotics	0,8213	1,0121	0,9476	0,8309	0,8961	0,6405	1,007	0,9062	0,9991	1,0521	0,9016	0,92098	1,02149512	0,82189823
epsilon-caprolactam	Xenobiotics	1,2192	0,9169	0,8828	1,0815	0,8137	0,9153	1,0274	0,9048	0,8008	1,4264	0,98282	1,01494	1,03268147	0,81403352
ergothioneine	Xenobiotics	1,107	1,1005	0,7356	0,8685	0,948	0,9522	1,1173	1,0183	0,7472	0,9796	0,95192	0,96292	1,01155559	0,90902045
erythritol	Xenobiotics	1,0344	1,059	1,0619	1,1411	1,1086	0,9839	1,1072	1,1069	1,0161	1,3049	1,081	1,1038	1,02109158	0,71585995
gluconate	Xenobiotics	1,0658	0,2772	0,3517	0,7111	0,3998	0,9342	1,1957	1,2488	1,0699	1,8398	0,56112	1,25768	2,24137439	0,01150106
methyl-4-hydroxybenzoate	Xenobiotics	1,0434	1,0441	0,9735	1,0005	0,9749	1,0311	0,9995	0,9781	1,0281	1,0924	1,00728	1,02584	1,01842586	0,47706856
quinate	Xenobiotics	1,0048	0,9867	1,018	1,0545	1,0213	0,944	0,9952	0,9403	1,15	1,0647	1,01706	1,01884	1,00175014	0,96742627
salicylate	Xenobiotics	1,1754	0,5037	1,0116	0,3088	0,6482	1,1692	0,9695	1,024	1,1379	0,6339	0,72954	0,9869	1,35277024	0,21293494
sulfate*	Xenobiotics	1,0906	0,9854	0,9877	0,8575	0,8698	1,0922	0,9944	0,9068	1,0555	0,8764	0,9582	0,98506	1,02803173	0,66532104

Table S3

Table S4. Primers, Related to Figures 1, 2, 4, 5. List of DNA oligonucleotide primers used in this study.

Name	DNA sequence (5'-3')	Annealing t°	Reference
ackA_F	TAAGACGCAAGATACCCGTG	62	This study
acka_R	ACGCACAATCATCAGCTCTT	62	This study
int1_F	TTTAAAACATCGGCTACGGAAG	63	This study
int1_R	TTATTTATCGCCCGCCAAGA	62	This study
cheY_F	CTCGCTCGTGATGTCTTACT	59	This study
cheY_R	TAACAGCACTAGCCACGTTC	60	This study
adhE_F	GGCTCCCTTAATTCACAAAGG	62	This study
adhE_R	ATCCTTGAAAGCTAACCGGG	63	This study
int2_F	AGCGATATCCTCCTGTGAAC	60	This study
int2_R	CGCGTTGTGCTAGCTAATTT	61	This study
lp_0055_F	GCCATGTGTGTAAACGTGTC	61	This study
lp_0055_R	GTGATCCAAGGGGTCCAAAT	62	This study
pstB_F	AAGACAATTAAGGACGGTTCAC	60	This study
pstB_R	TGGTCGATAAGCCACATTCTT	62	This study
lp_0797_F	ATTTTCCAAAGTGTGATTCGGT	63	This study
lp_0797_R	ACTTTCGATCATTCGTTCAGC	63	This study
lp_1258_F	GGCGTTAACGGATGAATCTAA	62	This study
lp_1258_R	GACCTTGTTCTCCGCAGT	60	This study
int3_F	TTCTTCACACTTGGTTTTTCGT	62	This study
int3_R	GCGAATGTCATAGTCGGAGA	62	This study
int4_F	GACGATTAGACTAGTCGCGG	61	This study
int4_R	CATTCAAGCTGATATTGTCGGT	62	This study
lp_0197_F	CCGCCATGTTGACATTGATT	63	This study
lp_0197_R	CGTTGTGCTAGATGATTGGG	63	This study
ackA2_F	GTGAAATCACTGGGGTTGGT	63	This study
ackA2_R	ACCATGATCAAAAGCCGTGA	65	This study
int5_F	CAACGCAGAAGTTACATGCT	60	This study
int5_R	GCAATCCTGCGTTCATCATC	62	This study
int6_F	GTTCGACGTTATTTCACGGAT	62	This study
int6_R	CATCACGAATAGGTGCCAAA	63	This study
16S_UniF	GTGSTGCAYGGYTGTCGTCA	70	(Packey et al., 2013)
16S_UniR	ACGTCRTCCMCACCTTCCTC	68	(Packey et al., 2013)
ackA_NIZO	CGAACGTGTCACTAAAGCCTT	63	This study
ackA_FlyG2	GCGAACGTGTCACTAAAGTAGG	62	This study
ackA_R_RT	CACGCACAATCATCAGCTCT	63	This study

Table S4

Table S5. Plasmids used in this work, Related to Figure 3. List of plasmids used to engineer *Lp*^{NIZO2877}with CRISPR-Cas9.

Plasmid	Description	Resistance	Source	Stock
pJP005	RecT protein under a nisin-inducible promoter, without nisR and nisK genes	Cm	(Van Pijkeren and Britton, 2012)	CB651
pMSP3545	Gram-positive bacterial shuttle vector for nisin-controlled inducible expression	EmR	Addgene CN#46888	pCB574
pCas9	Plasmid containing Streptococcus pyogenes Cas9 and its tracrRNA	Amp	Addgene CN# 42876	pCB339
p3545Cas9	Shuttle vector containing S. pyogenes Cas9 and its tracrRNA	EmR	This work	pCB577
p3545Cas9+RSR	Shuttle vector containing S. pyogenes Cas9, tracrRNA, and a repeat-spacer-repeat array for targeting	EmR	This work	pCB578
p3545Cas9+ackA_G2 target	Cas9 shuttle vector targeting the acetate kinase gene in NIZO.G2	EmR	This work	pCB579
PJP005_NIZO ackA	pJP005 vector with repair template for the ackA target	Cm	This work	CB711

Table S5

Table S6. Oligonucleotides used to engineer *Lp*^{NIZO2877} with CRISPR-Cas9, Related to Figure 3.

Shorthand	Name	Sequence
oRL1	pCas9.Gibson.fwd	GATGATAAGCTGTCCAAACATGAGAATTCCTTACGAAATCATCCTGTGGAGCTTAG
oRL2	pCas9.Gibson.rev	ATTTTTAGGATAACTTCTGCCCCACCTTTTTCAGTCACCTCCTAGCTGACTC
oRL3	pMSP3545.Gibson.fwd	ATTGATTTGAGTCAGCTAGGAGGTGACTGAAAAAGGTGGGGCAGAAGTTATCCTAA
oRL4	pMSP3545.Gibson.rev	CCTACTAAGCTCCACAGGATGATTTCGTAAGGAATTCTCATGTTTGGACAGCTTATCATCG
oRL5	gBlockRSR.Gibson.fwd	TTGGTTCAAAGAAAGCTTGAGCTCTCGAGTCAGGGGTACCGATCA
oRL6	gBlockRSR.Gibson.rev	GGAGGCACTCACCATGGGTACTGCAAATGTCTGCAATGAGTTGATCGC
oRL7	Acet.Kin.pJP005.f	ATTTACTAGTGTTTTTTTCATCATGATCGCCTC
oRL8	Acet.Kin.pJP005.r	TCGCGAGCTCACAACGCATCTATCAGGAAG
oRL9	pJP005.seq.rev	TGATTGTTCTATCGAAAGCGAA
oRL10	pJP005.seq.fwd	AATTGCTAGAAGGATTTCAAAAGTC
oRL11	AcetKin.Outer.fwd	GGAGGAGGACAGCAAAGCC
oRL12	AcetKin.Outer.rev	TGCGCGTCAAAACGTTTGTTGTT
oRL13	G2.Reversion.sgRNA.fwd	CCACCGCGAACGTGTCACTAAAGTGTTTTAGAGCTATGCTGTTTTGAATGGTCCCAAAACATCGATCGAAGC
oRL14	G2.Reversion.sgRNA.rev	GGCCGCTTCGATCGATGTTTTGGGACCATTCAAAACAGCATAGCTCTAAAACACTTTAGTGACACGTTCGCGGTGGAT

Table S6